INSTITUTO DE CIENCIAS E INNOVACIÓN EN MEDICINA
Facultad de Medicina
Clínica Alemana - Universidad del Desarrollo

SACCHAROMYCES CEREVISIAE AS A MODEL FOR THE IDENTIFICATION OF MODIFIER GENES OF PARAQUAT TOXICITY

BY: JUAN CARLOS RUBILAR ESPINOZA

Thesis submitted to the Faculty of Medicine at Universidad del Desarrollo for the Academic Degree of Doctor of Science and Innovation in Medicine

THESIS ADVISORS:

ANDRÉS DAVID KLEIN POSTERNACK, PhD.

FRANCISCO ALBERTO CUBILLOS RIFFO, PhD.

September, 2024

SANTIAGO

INSTITUTO DE CIENCIAS E INNOVACIÓN EN MEDICINA
Facultad de Medicina
Clínica Alemana - Universidad del Desarrollo

DEDICATION

I dedicate this thesis to my parents, whose unwavering support has been the cornerstone of my academic journey

To my father Juan Carlos and my mother Rosa

ACKNOWLEDGEMENTS

This thesis has been a complex journey filled with uncertainty, triumphs, and challenges. I am deeply grateful to those who have supported me along the way.

First, I would like to sincerely thank Dr. Andrés Klein and Dr. Francisco Cubillos for their exceptional mentorship and unwavering support. Their guidance and encouragement were invaluable throughout this process.

I am also indebted to the members of my thesis committee, Drs. Eduardo Pérez, Gonzalo Olivares, and Juan Francisco Calderón, for their insightful feedback and constructive criticism. I would like to thank Dr. Juan Francisco Calderón for his invaluable advice, support, and unwavering belief in my work.

I extend my heartfelt thanks to Professor Gianni Liti for welcoming me into his lab and providing me with invaluable advice and insights. I am also grateful to Professor Jonas Warringer for providing the yeast strains necessary for my research. I would like to express my sincere gratitude to Dr. Michela Deleidi and Federo Bertoli for their invaluable contributions to my project on dopaminergic neurons from Parkinson's patients.

I would like to acknowledge the exceptional mentorship of Dr Christina Schuh, who instilled in me the confidence to explore my ideas and express myself freely.

I am grateful to my lab team, Vale, Benja, Anyelo, and Maca, for their friendship, teamwork, and positive working environment. I would also like to thank my colleagues at the Genetics and Genomics Center and the Immunology Department, including Dani, José, Cony, MaJo, Javi de la Cruz, Naty and Liss, for their support, friendship, and for sharing laughs and conversations during this stressful process. I am especially grateful to Mrs. Maria Elena for her unwavering encouragement and wise advice.

A special thanks to my PhD colleague and friend, Javi Carrasco, for her unwavering support, friendship, and shared experiences. I am also grateful to my colleague and friend, Nixa, for her understanding and support.

I would like to express my gratitude to Sakshi, Federica, Xanita, Nicoló, Lorenzo, Mila, and Matteo for their friendship and support during my internship in Nice.

I am deeply grateful to my friends, who have been a constant source of support and encouragement. I would like to thank Fray for his unwavering belief in me, patience, and motivation, Axa for her friendship, our podcasts daily, for her trust, good vibes, and wishes, Nani and Evy for their constant support, Cata Muñoz Nico Koplow, Marilaura and Carlos for their friendship, companionship and

laughs, Vale Jaramillo for our insightful conversations, and all my other friends who have been there for me.

Finally, I would like to express my deepest gratitude to my parents, Juan Carlos and Rosita, my sister Kathy, and my nephews Agustín and Javier for their unconditional love and support. Their belief in me has been a constant source of motivation. They trusted me from the beginning and the fruit I grow today is fully shared with them. I would like to express my gratitude to my beloved kitty, Blanqui, who was my constant companion during my first year of online classes.

I would also like to thank the PhD Program in Science and Innovation in Medicine - Faculty of Medicine for providing me with scholarships and funding during this process. I am grateful to the PhD Program for the opportunity to complete an internship abroad and to the Vice-Rector's Office for additional scholarship support. I am grateful to DCIM and the Fondecyt Regular Project No. 1230317 of Dr. Andrés Klein for their funding of this thesis.

LIST OF CONTENTS

LIST OF FIGURES

LIST OF TABLES

LIST OF ABBREVIATIONS

µMax	Specific growth rate
ATP	Adenosine triphosphate
CAT	Catalase
CTSB	Chitobiase
DCFH-DA	2',7'-dichlorofluorescein diacetate
DHE	Dihydroethidium
FaST-LMM	Factored Spectrally Transformed Linear Mixed Models
FWER	Family-wise error rate
GBA1	Glucosylceramidase beta 1
GCase	β-Glucocerebrosidase
GSH	Glutathione
GWAS	Genome-wide association studies
Gyp8p	GTPase activator protein
H_2O_2	Hydrogen peroxide
$HO^{-\cdot}$	Hydroxyl radicals
iPD	Idiopathic Parkinson's disease
iPSC	Induced pluripotent stem cells
LOD	Log of odds score

MAF	Minor allele frequency
mPTP	Mitochondrial permeability transition pore
NA	North American
NAD^+	Nicotinamide adenine dinucleotide
NADPH	Nicotinamide adenine dinucleotide phosphate
nm	Nanometre
NR	Nicotinamide riboside
$O_2^{-\cdot}$	Superoxide anion
OD	Optical density
OXPHOS	Oxidative phosphorylation
PBS	Phosphate buffered saline
PD	Parkinson's Disease
PQ	Paraquat
Prx5	Peroxiredoxin 5
QTL	Quantitative trait locus
ROS	Reactive oxygen species
SA	Sake
SIFT	Sorting intolerant from tolerant
SIRT1	Sirtuin 1

SNCA	Alpha synuclein
SNPs	Single-nucleotide Polymorphism
SOD1	Superoxide dismutase 1
TDP-43	TAR DNA-binding protein 43
VCF	Variant Call Format
WA	West African
WE	Wine/European
YNB	Yeast Nitrogen Base
YPD	Yeast extract peptone dextrose

ABSTRACT

Paraquat (PQ) is a potent herbicide that induces oxidative stress and mitochondrial dysfunction. In humans, it is highly toxic, and it can induce Parkinson's Disease (PD). PD is a chronic and progressive neurodegenerative disease, with a worldwide prevalence of 315 per 100,000 people of all ages. Recent studies have revealed that neurons from PD patients exhibit stress responses, mitochondrial dysfunction, and metabolic deficits involving ATP and nicotinamide adenine dinucleotide (NAD^+). While studies have demonstrated the potential of nicotinamide riboside (NR) to mitigate age- and disease-related metabolic decline in PD, the specific effects of NR on PD induced by pesticide exposure, such as paraquat, have not been extensively explored. *Saccharomyces cerevisiae* is a model organism that has allowed the study of relevant biological processes over time. It exhibits remarkable genetic diversity, making it an ideal model for studying the genetic basis of phenotypic variation. In this study, we hypothesized that genetically diverse *Saccharomyces cerevisiae* strains exposed to paraquat exhibit cellular and molecular responses that reveal potential modifier genes associated with its toxicity. We treated 1,011 isolates and 96 segregants from the cross of the SA x WE *Saccharomyces cerevisiae* strains with PQ (75 µg/mL). We measured their growth curves and calculated the specific growth rate (µMax), used as a phenotypic trait for the genome-wide association studies (GWAS) and quantitative trait loci (QTL) mapping. We performed mixed-model association analysis using FaST-LMM for GWAS and linkage analysis using R/qtl

software, calculating LOD scores with a nonparametric model. We used diploid strains (603 isolates) for GWAS and 96 segregants for QTL mapping, identifying variants and markers that exceeded the significance threshold. Using these variants and markers, we identified candidate genes for validation. We validated *NRT1* in a yeast mutant and showed that NR treatment protected significantly against PQ-induced damage in both the S288C laboratory yeast strain and iPSC-derived dopaminergic neurons from GBA-PD patients. In conclusion, this study provides valuable insights into the genetic and metabolic factors underlying PQ resistance in *S. cerevisiae*. The findings highlight the importance of NAD^+ metabolism and mitochondrial function in mitigating the toxic effects of PQ. The identification of *Nrt1* as a key transporter of NR, suggests potential therapeutic targets for interventions aimed at preventing or treating PQ-induced toxicity in PD.

Keywords: *Paraquat, Saccharomyces cerevisiae, Parkinson's disease, herbicides, NAD^+ metabolism*

1. INTRODUCTION

1.1. Human health risk from pesticides

Pesticides and herbicides are frequently employed to eradicate insect and plant pests and harmful organisms that cause substantial damage to crops (Tudi et al., 2021). Approximately 3.5 million tons of pesticides are applied by farmers worldwide each year (Pretty & Bharucha, 2015). Herbicide poisoning causes ~20,000 deaths yearly, making it a significant global public health concern (Ball et al., 2019; D. R. Sharma et al., 2012). In the USA, herbicides have been used since the 60's, while in Chile their use has grown rapidly, due to rising exports (Coria & Elgueta, 2022; Paul et al., 2024). This has allowed identifying these molecules as relevant risk factors, affecting people at geographical and occupational levels (Pouchieu et al., 2018).

1.2. Paraquat mechanisms and Parkinson's risk

Paraquat (PQ) is a potent herbicide that induces oxidative stress and mitochondrial dysfunction (Elkholy et al., 2023; Ossowska et al., 2006; Prasad et al., 2007). In humans, it is highly toxic (Sukumar et al., 2019). It can be absorbed through the gastrointestinal tract, skin contact, or inhalation (Hsieh et al., 2013; L. Shi et al., 2022; M. Shi et al., 2023), and it can induce lung fibrosis, liver tumors,

and Parkinson Disease (PD) (Donaher & Van den Hurk, 2023a; Kumar et al., 2021; P. Sharma & Mittal, 2024).

PQ is classified as an inhibitor of the mitochondrial complex I, increasing reactive oxygen species (ROS) levels (Berry et al., 2010; Romero-Aguilar et al., 2022; Tanner et al., 2011; Torres-Rojas et al., 2020). Enzymatically, PQ is reduced by NADH-cytochrome b5 and NADH-ubiquinone oxidoreductases, forming superoxide anion ($O_2^{\cdot-}$) and hydrogen peroxide (H_2O_2). PQ induces the opening of the mitochondrial permeability transition pore (mPTP), reducing calcium retention capacity inside the mitochondria and exacerbating oxidative stress (Akhter et al., 2017; X. Liu et al., 2022; See et al., 2022; Tiên Nguyên-nhu & Knoops, 2003). Mitochondrial damage directly impacts the lysosomal pathway through membrane contact sites, which results in reduced lysosomal enzyme activity, impaired sphingolipids breakdown and autophagy blockage (D. Li et al., 2020; Rubilar et al., 2024). These disruptions lead to α-synuclein (α-syn) aggregation, dopaminergic neuron death (Klein & Mazzulli, 2018; McCormack et al., 2002; Ossowska et al., 2006; Zhang et al., 2016), which in turn causes motor deficits (Blesa et al., 2022; Islam et al., 2021; LeWitt & Chaudhuri, 2020). These cellular and molecular processes contribute to PD pathogenesis by causing damage to dopaminergic neurons in the brain (Dinis-Oliveira et al., 2006; See et al., 2022). Idiopathic Parkinson's disease (iPD) has been linked to PQ as an etiological factor (Tanner et al., 2011; Zhang et al., 2016). Actually, a California

case-control study conclusively linked PQ exposure to an increased risk of PD (Paul et al., 2024).

1.3. Paraquat in Parkinson's disease models

Model organisms are relevant for developing new therapies and unveiling disease mechanisms. Rats, mice, and even yeast have been employed in PD models (Domínguez-Oliva et al., 2023). Recently, using rat models exposed to PQ at low doses, showed progressive neurodegeneration in the nigrostriatal region with loss of motor function. A decrease in dopamine levels, an increase in α-syn aggregation, and oxidative stress were observed (Cicchetti et al., 2005; Cristóvão et al., 2020; Uversky, 2004). The damage in the dopaminergic mechanisms is due to PQ, which can cross the blood-brain barrier (Bastías-Candia et al., 2019). In the substantia nigra pars compacta (SNpc) of mice exposed to PQ, oxidized glutathione (GSSG) and NADPH oxidase levels were increased, causing a depletion of these antioxidant factors with elevated oxidative stress in the system. These suggest the major role of PQ in inducing oxidative stress and mitochondrial dysfunction (Cicchetti et al., 2005; Kang et al., 2009).

1.4. Parkinson's disease: A genetic and environment overview

PD is a progressive neurodegenerative disease, which is mediated by genetic and environmental factors (See et al., 2024). PD has a prevalence of 315 per 100,000 people of all ages (Han et al., 2019), and it is the second most common neurological disorder in the population (Ou et al., 2021). The progressive loss of dopaminergic neurons in the SNpc is an essential characteristic of PD. This loss mostly results in motor and cognitive function impairments (Gupta et al., 2023).

Recently, PD patients exhibited diverse hallmarks, which are oxidative stress response, mitochondrial dysfunction, and metabolic deficits of ATP and nicotinamide adenine dinucleotide (NAD^+) (Mischley et al., 2023; Schöndorf et al., 2018). NAD^+ is a crucial coenzyme in cellular energy processes like glycolysis, fatty acid beta-oxidation, the Krebs cycle, and oxidative phosphorylation (OXPHOS) (P. Belenky, Bogan, et al., 2007; Gaare et al., 2023). Given the potential of NAD^+ precursors to mitigate age- and disease-related metabolic decline, researchers investigated the effects of nicotinamide riboside (NR) on mitochondrial function in PD neurons. The supplementation with NR in dopaminergic neurons derived from induced pluripotent stem cells (iPSC) from *GBA*-PD patients and fly models of *GBA*-PD prevented the loss of neurons and motor impairment (Schöndorf et al., 2018).

Reports indicate a strong interaction between genetic and environmental factors and their association with increased risk of PD (Burbulla & Krüger, 2011; Dardiotis

et al., 2013). This gene-environment interaction plays a relevant role in the heterogeneity of the disease. This diversity is characterized by different ages of disease onset, variety in motor and cognitive symptoms, and genetic mutations that affect PD. While individual factors may have a limited influence, their combined effect can contribute to the development of PD (Cannon & Greenamyre, 2013; Dardiotis et al., 2013; Gao & Hong, 2011). PD is influenced by genetic factors. In familial and sporadic forms of PD different genetic variations in *SNCA*, *LRRK2*, *PINK1*, *PARK2*, and *PARK7* genes have been observed (Singleton et al., 2013). Although monogenic causes only explain 10% of cases (de Lau & Breteler, 2006), family studies and twin studies indicate a genetic influence, specifically in early-onset PD (Marder et al., 2003; Tanner et al., 1999).

The pathogenesis of PD seems to be modulated by mitochondria, which is associated with oxidative stress (Pan-Montojo et al., 2010; Pereira et al., 2015; Zhu et al., 2003) and lysosomal dysfunction (Klein & Mazzulli, 2018). Genetic studies have identified a strong association between variants in mitochondrial and lysosomal genes, including *GBA1*, and the risk of developing iPD (Blauwendraat, Nalls, et al., 2020; Goker-Alpan et al., 2004). Notably, *GBA1* encodes for lysosomal β-glucocerebrosidase (GCase). *GBA1* variants are a major genetic risk factor for developing PD (Blauwendraat, Nalls, et al., 2020; Sidransky et al., 2009). Remarkably, GCase plays roles in both organelles: in the lysosome it degrades certain ceramides, while in mitochondria it promotes complex I stability (Blauwendraat, Nalls, et al., 2020; Brooker et al., 2024; Klein & Outeiro, 2023;

Rubilar et al., 2024). Since pesticides target mitochondria, a recent study identified enrichment in genomic variants in 26 genes associated with lysosomal function. These results support that impaired lysosomal and mitochondria dysfunction are necessary to develop PD (Ngo et al., 2024). However, identified genes explain a limited portion of the disease's heritability, indicating the existence of undiscovered genetic factors. Estimates suggest that approximately 40% of the variation in disease susceptibility is due to these unidentified genes (Hamza & Payami, 2010).

1.5. Parkinson's variability and modifier genes

The heterogeneity in PD patients is characterized by different ranges of symptom severity and is due to the interaction between parietal-premotor compensation and basal ganglia dysfunction. Although parietal-premotor areas attempt to compensate for the loss of dopaminergic neurons and the resulting basal ganglia dysfunction, this compensatory mechanism is insufficient (Johansson et al., 2024). The genetic factors only can explain a proportion of individual differences in patients' PD symptom severity, suggesting other genetic elements. The modifier genes may influence the phenotypic expression of the causal or primary variation, contributing to the common heterogeneity in PD patients (Kearney & Jorge, 2012; Nadeau, 2001).

Modifier genes are not causative, but can affect the phenotypic expression or severity, and have been described for various genetic diseases and disorders

(Marian, 2002). The expression of modifier genes affects and changes the phenotypes of the disease; although these intermediating genes do not directly contribute to the disease causality, they could initiate or delay the onset of symptoms and severity (Haldane, 1941; Rahit & Tarailo-Graovac, 2020). Modifier genes also provide options for exploring disease pathogenesis mechanisms and the underlying biology (Nadeau, 2001).

1.6. Strategies to uncover modifier genes

Genome-wide association studies (GWAS) are an efficient and successful tool for the identification of modifier genes in complex diseases. GWAS are categorized as unbiased approaches because they can study the whole genome through associations between genotype and phenotype, in search for disease risk and uncover unexpected genetic markers or SNPs (Nalls et al., 2019; Satake et al., 2009). Despite all efforts, GWAS cannot fully explain the missing heritability of complex traits. However, they are a valuable tool for uncovering novel disease-associated loci. For example, a study in 2017 identified 17 new susceptibility loci for PD (Chang et al., 2017), and revealed 90 significant independent genome-wide risk signals associated with human diseases (Nalls et al., 2019). Another GWAS was performed to investigate the genetic determinants of GBA risk and age at onset in PD. They were able to identify common genetic variants near *SNCA* and *CTSB* (encoding cathepsin B). These elements are modifier genes for

GBA risk and age at onset. The interplay between *GBA* and *CTBS* has implications for lysosomal dysfunction in PD (Blauwendraat, Reed, et al., 2020). On the other hand, linkage analysis has proven to be another powerful technique in identifying genetic modifiers, as exemplified by the discovery of *SNCA* (encoding α-syn), as a major modifier of age at onset in PD. A nonsense mutation (A53T) in the *SNCA* gene was identified using a large Italian family and three Greek families in 1996 (Polymeropoulos et al., 1997). Additionally, other studies have identified mutations in the SNCA gene, such as A30P and E64K confirming *SNCA* as an essential gene in PD (Brockmann et al., 2013; Hyun et al., 2013). Other studies focused on identifying genes associated with heterogeneity in the onset and progression of PD (Ross & Rademakers, 2016). The success in finding modifier genes was corroborated with genome-wide linkage analysis on 113 individuals with leucine-rich repeat kinase 2 (*LRRK2*) mutations to identify genetic modifiers influencing the age of onset of PD. This analysis led to the identification of two novel genomic regions that may harbor modifiers of *LRRK2*-related PD onset or penetrance (Latourelle et al., 2011).

1.7. Genetic panels and diseases

In humans, the studies of neurodegenerative diseases are limited many times by insufficient sample sizes making it impossible to perform GWAS and Linkage analyses. Although several studies have reported risk loci associated with these diseases, GWAS usually requires large sample sizes and Linkage analysis is

challenging due to the difficulty in finding large families with multiple affected individuals. To address this limitation, panels of model organisms are an invaluable source for these genetic analyses. The sequencing of gene panels in flies, rats, mice, and yeast represents a valuable strategy for studying a spectrum of phenotypes, enhancing our understanding of genetic diseases (Aitman et al., 2011).

In addition, using these sequenced panels of model organisms facilitates the understanding of the variability in a large cohort of individuals and a deep exploration of the correlation between phenotypic severity and genetic variants (Olivares et al., 2019). Bloom and colleagues used a panel of yeast segregants harboring genotypic and phenotypic variability and measured the heritable components of 46 quantitative trait loci (QTLs), enabling the identification of underlying loci and deeper missing heritability (Bloom et al., 2013).

1.8. *Saccharomyces cerevisiae* as a model for identifying modified genes

Saccharomyces cerevisiae is a model organism that has allowed the study of relevant biological processes over time (Bai et al., 2022a; Karathia et al., 2011a; Oftadeh et al., 2021a). Yeast has been a key organism in elucidating signal transduction, vesicle trafficking, and protein exchange (Menezes et al., 2015). Sharing 2,564 orthologous genes with humans (O'Brien et al., 2005), which constitutes one-third of its genome (Kachroo et al., 2015), makes it a valuable model organism. Despite a billion years of evolutionary divergence, yeast and

human genes retain remarkable functional similarity in cellular and metabolic processes associated with human diseases (W. Liu et al., 2017). Yeast has been widely employed to identify novel therapeutic targets for PD by elucidating the molecular mechanisms underlying α-synuclein toxicity and enabling high-throughput screening of potential drug candidates (Outeiro & Lindquist, 2003; Tenreiro et al., 2017).

Whole-genome screens in yeast identified 52 genes linked to mutant huntingtin toxicity and 86 genes associated with α-syn toxicity. Huntingtin-responsive genes were primarily involved in stress response, protein folding, and ubiquitination, while α-syn modifiers were enriched in lipid metabolism and vesicular transport (Willingham et al., 2003). In another study, a yeast model was employed to investigate the mechanisms underlying TAR-DNA-binding protein 43 (TDP-43) aggregation and toxicity. The yeast cells exhibited TDP-43 overexpression, forming cytoplasmic aggregation and cell toxicity, recapitulating key pathological features of TDP-43-related neurodegenerative diseases (Johnson et al., 2008). Finally, a yeast-based study identified genes that modify α-syn toxicity. Expression of human α-syn in *S. cerevisiae* disrupted endoplasmic reticulum-to-Golgi trafficking. The GTPase Rab (Ypt1p) was found to be associated with α-syn inclusions, while Gyp8p (a GTPase activator protein) enhanced α-syn toxicity (Cooper et al., 2006).

1.9. Yeast as a tool to study paraquat-induced responses

S. cerevisiae exhibits extensive genetic diversity, representing an ideal biological system for studying the genetic basis of phenotypic variation. To identify the genetic bases of phenotypic differences among the strains, a strategy is to use QTLs, because QTL mapping can uncover how the genetic diversity in *S. cerevisiae* is responsible for a wide range of phenotypic traits. These traits include variations in energy metabolism, stress response, and cellular morphology (Cubillos et al., 2011; Warringer et al., 2011). Thus, the yeast has allowed dissection of the underlying genetic and molecular mechanisms of PD pathogenesis due to their high degree of conservation with humans (W. Liu et al., 2017), rapid growth rate and generation time, availability of panels of strains bearing genotypic variability and the capacity for rapid characterization and implementation of large-scale studies using yeast strains with single gene deletions (Mülleder et al., 2012; Winzeler et al., 1999).

Human peroxiredoxin 5 (Prx5) is crucial for protecting the cells when they are exposed to stressors, such PQ. In yeast, Prx5 was found to prevent oxidative stress inside the cell, specifically in the mitochondria and cytosol. These results indicate that a redox imbalance and cellular alterations are caused by PQ exposure (Tiên Nguyên-nhu & Knoops, 2003). Additionally, PQ-treated cells exhibited altered metabolism, including an inability to metabolize ethanol (Hansson & Häggström, 1986) and a decreased growth rate in susceptible strains (Cubillos et al., 2013). Most PQ studies in *S. cerevisiae* have been performed in one strain, revealing reduced replicative lifespan (Jarolim et al., 2004a;

Nestelbacher et al., 2000a), and mitochondrial damage (Y. Li et al., 2021; Stenberg et al., 2022; Tiên Nguyên-nhu & Knoops, 2003). However, the genomic variations between yeast strains have not been harnessed in depth to study the cellular and molecular adaptive strategies to PQ.

This thesis seeks to unravel the genetic foundations of genotype-by-environment interactions using *S. cerevisiae* as a model organism. By exposing yeast strains to PQ, we will investigate cellular and molecular responses to this herbicide. To identify potential modifier genes, we will employ GWAS and QTL mapping, leveraging the natural genetic variation within yeast populations. By focusing on biochemical, cellular, and physiological phenotypes, we aim to uncover combinations of genetic variants that contribute to susceptibility or resistance to PQ. This approach offers a more comprehensive understanding of complex traits compared to traditional methods that rely on single-gene mutants. Understanding the biology of the resistant strains is crucial for designing new strategies to prevent pesticide-induced PD, followed by validations in animal models and human cells.

2. HYPOTHESIS

Genetically diverse *Saccharomyces cerevisiae* strains exposed to paraquat exhibit cellular and molecular responses that reveal potential modifier genes associated with its toxicity.

3. MAIN OBJECTIVE

To identify paraquat toxicity modifier genes in a genetically diverse collection of *Saccharomyces cerevisiae* strains.

3.1. SPECIFIC AIMS

3.1.1. To characterize the cellular and molecular response in four genetically diverse strains of *Saccharomyces cerevisiae* exposed to paraquat.

3.1.2. To identify modifier genes responsible for differences in susceptibility/resistance to paraquat in genetically diverse strains of *Saccharomyces cerevisiae* through GWAS and QTL mapping.

3.1.3. To validate candidate modifier genes of the paraquat susceptibility/resistance phenotype in yeast strains with pre-existing targeted gene deletions.

4. **Chapter 1:** To characterize the cellular and molecular response in four genetically diverse strains of *Saccharomyces cerevisiae* exposed to paraquat.

Strain-dependent oxidative stress and vacuolar adaptations to paraquat in *Saccharomyces cerevisiae*

Juan Carlos Rubilar[1], Francisco A. Cubillos[2,3,4], Andrés. D. Klein[1]

*Correspondence to: Andrés D. Klein, andresklein@udd.cl

[1]Centro de Genética y Genómica, Facultad de Medicina, Clínica Alemana Universidad del Desarrollo, Santiago 7780272, Chile.

[2]Departamento de Biología, Facultad de Química y Biología, Universidad de Santiago de Chile, Santiago, Chile.

[3]Millennium Institute for Integrative Biology (iBio), Santiago, Chile.

[4]Millenium Nucleus of Patagonian Limit of Life (LiLi), Santiago, Chile.

Running title: *Differential responses to Paraquat in yeast*

Keywords: *Paraquat, Saccharomyces cerevisiae, Parkinson's disease, herbicide, pollution.*

Abstract

Paraquat (PQ) is an herbicide that increases Parkinson's disease (PD) risk in humans. *Saccharomyces cerevisiae* represents an ideal system for studying PQ toxicity/resistance due to its evolutionary conservation with mammals and strain-specific responses to PQ. However, the biological effects of PQ exposure across genetic backgrounds are unknown. To address this, we treated four yeast strains (NA, SA, WA, and WE) with PQ and assessed physiological, molecular and cellular consequences on each genetic background. First, we measured the strain's physiological growth kinetics and calculated the specific growth rate (μMax). PQ significantly reduced μMax in WE and WA, but not in SA and NA. Additionally, PQ increased superoxide and peroxide levels in all strains, but to different extents, being the SA and WE the most affected. PQ also influenced vacuolar morphologies strain-dependently, shifting from one large organelle to small disaggregate vacuoles, with WE being the most susceptible. Surprisingly, we found an inverse association between superoxide levels and the percentage of semi-disaggregate vacuoles. In support of our findings, we observed significant Pearson correlations between non-synonymous gene polymorphisms (*CTT1*, *YHC3*) and vacuolar B phenotype. These genes encode a hydrogen peroxide detoxification enzyme and a vacuolar arginine transporter, respectively. SA carried a deleterious variant in *YHC3*, while NA and WA had deleterious variants in *CTT1*. In conclusion, our findings demonstrate that genetically diverse yeast exhibit distinct cellular and molecular effects to PQ exposure. We speculate that

the most resistant strains may facilitate the development of novel therapeutics for humans exposed to PQ.

Introduction

Paraquat (PQ) is a potent herbicide widely employed globally due to its efficacy in eradicating harmful organisms detrimental to crops (1). Despite its widespread use, with an estimated global consumption of 3.5 million tons annually (2), PQ poisoning causes ~20,000 deaths yearly (3, 4). A clear link between PQ exposure and Parkinson's disease (PD) has been established (5), raising environmental and human health concerns (6).

PD pathogenesis is complex, with the etiology of most cases remaining unknown (7, 8). However, it is well-established that a complex interplay between genetic and environmental factors contributes to its development. Several PD genetic risk factors interact with pesticide and herbicide exposure (9, 10). Nevertheless, the precise molecular mechanisms of gene-environment interaction remain elusive. Elucidating them is essential for achieving early diagnosis, preventative strategies, and translating potential therapeutic interventions (11, 12).

PQ inhibits mitochondrial complex I by reducing NADH-cytochrome b5 and NADH-ubiquinone oxidoreductases, increasing superoxide anion ($O_2^{\cdot -}$), which is further converted into hydrogen peroxide (H_2O_2) and hydroxyl radicals ($HO^{\cdot}$) (13–18). Additionally, PQ induces the opening of the mitochondrial permeability transition pore (mPTP), reducing intra-mitochondrial calcium retention capacity

and decreasing the membrane potential, which also contributes to increasing reactive oxygen species (ROS) levels (19–23). Mitochondrial damage directly impacts the lysosomal pathway via membrane contact sites, leading to decreased lysosomal enzyme activities, impaired sphingolipids degradation and autophagy blockage (24, 25). These disruptions contribute to α-synuclein (α-syn) aggregation, dopaminergic neuron death (26–29), and ultimately motor impairments (30–32).

Yeast models represents a powerful biological tool for dissecting the underlying genetic and molecular mechanisms of PD pathogenesis due to its high degree of conservation with humans (33), rapid growth rate and generation time, availability of panels of strains bearing genotypic variability, and capacity for rapid characterization and implementation of large-scale studies using yeast strains with single gene deletions (34, 35).

In this study, we investigated the biological effects of PQ exposure on four *S. cerevisiae* strains with distinct genetic backgrounds. We employed a multi-tiered approach, examining its consequences at three levels: (i) physiological (growth rates), (ii) molecular (superoxide and hydrogen peroxide levels), and (iii) cellular (vacuolar morphology). Interestingly, PQ treatment displayed strain-specific modulation of all phenotypes. Notably, no correlation was observed between the growth rate (physiological phenotype) and any other measured parameter. This finding implies that additional processes contribute to PQ toxicity and resistance,

potentially reflecting the presence of strain-specific adaptive and compensatory mechanisms.

Results

Paraquat-induced strain-specific growth rates responses

We chose four phylogenetically distinct strains exhibiting extensive genomic variability: Y12 (Sake, SA), YPS128 (North American, NA), DBVPG6044 (West African, WA) and DBVPG6765 (Wine/European, WE). As a proxy of cell health, we measured their growth rates under control and PQ exposure. Initially, we set the lowest PQ concentration, which induced reproducible variation across strains. We tested a range of 12.5 - 125 µg/mL (Supplementary Figure 1) and chose 75 µg/mL to discriminate between strains. Under control conditions (YNB media 2% glucose) all strains exhibited similar growth patterns (Figure 1A). However, upon PQ exposure we identified a lower growth rate in the WE background than untreated cells (susceptibility phenotype) (Figure 1B). This effect was quantified by calculating the Area Under the Curve (AUC) (*P*-value = 0.0013, ANOVA) (Figure 1C). Conversely, SA, NA and WA exhibit the highest tolerance to PQ (resistance phenotype, *P*-value = ns, ANOVA) (Figure 1B and C).

Then, we calculated the specific growth rate (µMax). PQ exposure differentially impacted µMax across the strains. PQ-treated WE exhibited a decrease in µMax compared to NA (*P*-value = 0.0012, ANOVA) (Figure 1D). Notably, the WE strain

exhibited a 40% reduction in μMax compared to SA (*P*-value = 0.0001, ANOVA), with WA showing a 20% decrease when compared to SA (*P*-value = 0.033, ANOVA) (Figure 1D). Furthermore, we found a significant difference between WA and WE (*P*-value = 0.033, ANOVA). These results demonstrate that PQ differentially impacts each strain, with WE and WA exhibiting the most significant susceptibility. Therefore, PQ exposure appears to have a strain-specific impact on yeast reproductive fitness and physiological adaptation.

PQ-induced strain-specific ROS responses.

Since PQ inhibits mitochondrial complex I, we analyzed superoxide anion levels with DHE, under control and PQ treatments (75 μg/mL for 48-hours). PQ treatment significantly increased superoxide levels in SA (*P*-value = 0.007, ANOVA) and WE strains (*P*-value = 0.005, ANOVA) (Supplementary Figure 2). Interestingly, PQ-treated NA and WA strains showed no significant differences in superoxide anion levels (Supplementary Figure 2). Notably, the NA strain, which displayed high PQ resistance in the growth curves (Figure 1B and 1E), exhibited a 30% reduction in superoxide anion production compared to SA (*P*-value = 0.017, ANOVA), and a 35% reduction compared to WE (*P*-value = 0.003, ANOVA) (Figure 2A). In contrast, the WE strain showed increased superoxide anion production compared to the other strains (Figure 2A), despite its greater PQ susceptibility in growth assays.

Complementary to the fluorometric measurement, we analyzed DHE labeling

through confocal microscopy to visualize the spatial distribution of superoxide anion within yeast cells and assess cell viability. Under control conditions, the probe remained in the cytoplasm, emitting a blue signal (Figure 2B). Upon PQ exposure, oxidized DHE binds to DNA, emitting red fluorescence (Figure 2B). All PQ-treated strains exhibited probe oxidation (red fluorescence), confirming cell viability. Furthermore, probe localization shifted from primarily cytoplasmic distribution in the control groups to a predominantly nuclear pattern in PQ-treated cells, correlating with superoxide anion levels (Figure 2C). Interestingly, the NA strain exhibited lower fluorescence intensity compared to SA (*P*-value = 0.001, ANOVA) and WE (*P*-value = 0.0002, ANOVA), suggesting potentially lower oxidative stress levels in this strain when exposed to PQ (Figure 2C).

To assess the impact of PQ on hydrogen peroxide production, another major ROS, we used the 2',7'-dichlorofluorescein diacetate (DCFH-DA) probe. PQ exposure significantly increased hydrogen peroxide levels compared to controls in SA, NA, and WE (*P*-value = 0.035; *P*-value = 0.006; *P*-value = 0.023, respectively; Kruskall Wallis) (Supplementary Figure 3). In contrast, the WA strain showed no significant change (Supplementary Figure 3). Furthermore, the rate of DCF fluorescence (PQ-treated cells normalized to control groups) also exhibited significant differences among strains (*P*-value < 0.05, Kruskal Wallis) (Figure 3A). Consistent with the previous observations, NA and WA displayed lower hydrogen peroxide production, while SA and WE showed higher production. Notably, SA exhibited a significant increase in superoxide levels compared to NA (33.4%, *P*-

value = 0.048, Kruskal Wallis) and WA (42.6%, *P*-value = 0.016, Kruskal Wallis) (Figure 3A).

Confocal microscopy analysis of DCFH-DA labeling corroborated findings on hydrogen peroxide levels (Figure 3B). Strains grown under control conditions displayed weaker fluorescence than PQ-treated strains (Figure 3B and 3C), indicating higher ROS levels upon exposure. These results indicate that PQ differentially impacts the yeast strains superoxide anion and hydrogen peroxide levels.

PQ induced strain-specific vacuolar adaptations

To investigate how yeast strains adapt to PQ exposure, we examined their vacuolar morphology, as changes in vacuole structure often indicate activation of stress response mechanisms (36). Vacuoles are typically classified into three phenotypes: A, up to three large vacuoles per cell; B, multiple small vacuoles with defined borders, and C, highly fragmented vacuoles (Figure 4A and 4B) (37).

We quantified the percentage of each phenotype under control conditions and PQ exposure (75 µg/mL for 48 hours) (Table 1). We observed distinct changes in vacuolar morphology across the four yeast strains. Specifically, phenotype A prevalence significantly decreased in NA (64% control vs. 13% PQ; *P*-value = 0.002, Kruskal Wallis) and WE (79% control vs. 19% PQ; *P*-value = 0.006, Kruskal Wallis) strains upon PQ treatment compared to the control condition (Figure 4C,

4D). In contrast, no significant differences were found for phenotype A in SA (*P*-value = 0.273, Kruskal Wallis) and WA (*P*-value = 0.184, Kruskal Wallis).

Surprisingly, a significant increase in phenotype B, characterized by multiple small vacuoles (51% increase), was observed exclusively in strain NA (32% control to 83% PQ; *P*-value = 0.009, Kruskal Wallis) (Figure 4C, 4D). In contrast, phenotype C, characterized by highly fragmented vacuoles, increased significantly only in strain WA (33% increase; 6% control vs. 0% PQ; *P*-value = 0.016, Kruskal Wallis) (Figure 4C, 4D). Micrographs (Figure 4A, 4B) support these findings, showing a clear decrease in phenotype A and a corresponding increase in phenotype B in PQ-treated WA strain compared to the control (Figure 4C, 4D).

Intriguingly, the WE strain exhibited a striking increase in phenotype C, rising from 4% in the control condition (Figure 4C) to 53% in PQ-exposure cells (Figure 4D) (*P*-value = 0.082, Kruskal Wallis). While this change did not reach statistical significance, a shift in vacuolar morphology is observed (Figure 4A & 4B). Compared to the control condition, the PQ-treated WE strain displays a marked decrease in phenotype A and a dramatic increase in phenotype C. This transition towards a fragmented vacuolar state (phenotype C) in WE upon PQ exposure may represent a stress response mechanism to preserve organelle integrity for survival.

The percentage of phenotype B inversely correlates with ROS levels in PQ-treated yeast.

To elucidate the compensatory mechanism to PQ exposure, we examined the relationships between the different measured traits through correlations. Multiple correlations were performed between μMax fold change, DHE and DCFH-DA probes, and vacuolar morphologies A, B and C. Most traits were not interconnected (Pearson and Spearman correlations) (Supplementary Table 1). However, a significant negative correlation (Pearson correlation: $r = -0.96$, P-value = 0.038) emerged between changes in superoxide anion levels and the change in the percentage of phenotype B (Figure 5A and Figure 5B), suggesting a shared adaptive response to PQ exposure involving intracellular ROS levels and vacuolar morphology.

Genetic determinants of phenotypic responses to PQ exposure.

Genomic variants in genes that participate in oxidative stress response and lysosomal function have been implicated in PD development, including humans exposed to pesticides (38) (Table 2). Given this, we hypothesized that these variants might contribute to PQ responses across different yeast strains (Figure 6). To test this hypothesis, we correlated the number of deleterious variants as predicted by SIFT (Sorting Intolerant From Tolerant) in oxidative stress and vacuolar genes (listed in Table 2) with multiple phenotypes: specific growth rates (μMax), ROS levels (measured using DHE and DCFH-DA probes), and vacuolar phenotype across four yeast strains (Table 2).

Significant Pearson's correlations (P-value < 0.05) emerged between variant

counts in specific genes and these phenotypes. *YEH1* and *DAL5* variants correlated with μMax (Pearson's r = -0.980, P-value = 0.020; r = 0.980, P-value = 0.019, respectively). A significant positive correlation was found between *SSA2* variant count and DHE-measured ROS levels (r = 0.972, P-value = 0.028). Phenotype B was positively correlated with variants in *THI73*, *FEN2*, *ICT1*, and *ATG5*, while a negative correlation was observed with variants in *YHC3* (Table 2). Additionally, vacuolar phenotype B positively correlated with variants in oxidative stress genes *CTT1* and *COX11,* while a negative correlation was observed with variants in *TSA1* (Table 2). However, following adjustment for multiple comparisons (see “Experimental procedures”) these correlations did not remain significant when considering all nonsynonymous and synonymous variants in the gene set. The conservative nature of the Bonferroni correction likely contributed to this outcome. Additionally, we identified one deleterious variant in the *YHC3* gene on chromosome 10 in the SA strain and found three deleterious variants within the *CTT1* gene: two in the NA strain and one in the WA strain. Among the 339 predicted variants in the four strains, 18.3% were nonsynonymous, 81.4% were synonymous, and 0.3% were frameshift deletions (Supplementary Table 2).

Discussion

In humans, PQ is highly toxic (39). It can be absorbed through the gastrointestinal tract, skin contact, or inhalation (40–42). It can induce lung fibrosis, liver tumors, and PD (43–45). PQ disrupts the intracellular redox cycle (43, 46), inducing

mitochondrial fragmentation via ROS and reactive nitrogen species, which, in turn, can trigger apoptosis (47–49). These cellular and molecular events contribute to PD pathogenesis by causing damage to dopaminergic neurons in the brain (20, 50).

While *S. cerevisiae* has served as a valuable model for elucidating PQ toxicity mechanisms (51, 52). Yeast has been enormously helpful in identifying mechanisms that regulate mammalian cellular processes (53, 54), but most studies have been confined to a single strain. Although these studies have revealed important insights, such as reduced replicative lifespan (55, 56), and mitochondrial damage (19, 57, 58), the genomic variations between yeast strains have not been harnessed in depth to study the cellular and molecular adaptive strategies to PQ.

Our findings demonstrate a differential impact of PQ on μMax across four genetically diverse *S. cerevisiae* strains. PQ reduced μMax in WE and WA (PQ-susceptible) while SA and NA presented a higher tolerance to PQ-induced growth inhibition. Under control conditions, μMax is controlled by Gcn4, a transcriptional factor that regulates amino acid biosynthesis, along with other factors as Fil1 and Gcn2 (59–62). Whether changes in Gcn4, Fil1 and Gcn2 with amino acid metabolism relate to the strain-specific variations in μMax upon PQ exposure has to be determined. Our results highlight the significance of genetic background in determining yeast susceptibility to PQ toxicity, which is consistent with previous

findings in other models (52, 63–65).

Genetic studies demonstrate a direct association between various mitochondrial and lysosomal genes and the risk of idiopathic Parkinson disease (iPD) (66, 67). Among them is the *GBA1* gene, which encodes for lysosomal β-glucocerebrosidase (GCase). *GBA1* variants are a major genetic risk factor for developing PD (67, 68). Remarkably, GCase plays roles in both organelles: in the lysosome it degrades certain ceramides, while in mitochondria it promotes complex I stability (24, 67, 69, 70). Since pesticides target mitochondria, a recent study identified enrichment in genomic variants in 26 genes associated with lysosomal function. These results support the idea that impaired lysosomal and mitochondrial dysfunction is necessary to develop PD (38). Similarly, our yeast study shows correlations between the number of missense variants in different genes associated with vacuolar/lysosomal function and PQ-induced phenotypes. For instance, WE, the most susceptible strain to PQ, exhibited more vacuolar variants, including in the *YHC3* gene, the yeast ortholog of human *CLN3* (71). While *CLN3* variants are linked to Batten disease (72), they induce ceramide accumulation and are unable to detoxify oxidative species in tissues (73, 74), like *GBA1* variants, which have also been implicated in PD (75). Ceramide buildup in yeast inhibits cell growth and participates in stress responses (76). This suggests that *YHC3* may play a crucial role in stress-induced phenotypic alterations and that the tested yeast strains are a good proxy for studying PQ susceptibility in humans.

While PQ is a ROS inductor, it was not equal in all strains. SA and WE strains exhibited the highest DHE and DCFH-DA fluorescence levels compared to the others. In contrast, NA showed the lowest superoxide levels. NA also has a high tolerance to oxalic acid (77), a toxic product of ascorbic acid oxidation (78, 79). Similarly to PQ, oxalate exposure impairs mitochondrial metabolism and promotes free radical formation (79). These results suggest that NA likely possesses enhanced antioxidant defenses, which may include increased superoxide dismutase activity (Sod; a superoxide scavenger), catalase (Ctt1; a peroxide scavenger), high glutathione (Gsh) levels, or others (80). In addition, NA and WA strains showed the lowest hydrogen peroxide levels than the other strains. In yeast *Tsa1* (dominant peroxide scavenger) is the major peroxiredoxin, acting as a specific antioxidant to reduce peroxide (81–83). Surprisingly, our SIFT variant analysis revealed that NA and WA strains, unlike SA and WE strains, lack variants in the *TSA1* gene. This finding suggests that NA and WA strains may have higher levels of functional *Tsa1* protein during PQ exposure, enhancing their ability to protect the cell from oxidative stress.

Vacuoles are highly dynamic organelles that adapt to environmental cues, such as oxidative and osmotic stress, by undergoing regulated fusion and fission processes (37, 84). Superoxide anion levels are known activators of cellular adaptations that reduce phenotype B vacuoles (85–87). Upon PQ treatments, WE strain exhibited the largest shift in vacuolar morphology from phenotype B to C, which correlates with high ROS levels, reduced growth rates, indicating a

transition towards fission yeast-like cytokinesis (88, 89). Vacuolar protein sorting 1 (Vps1) and autophagy-related protein 8 (Atg8) tightly regulate vacuole fragmentation (90). Vps1, a key protein involved in intracellular trafficking, is also essential for developing resistance to oxidative stress, while Atg8 stabilizes the vacuole membrane independently of autophagy (90, 91). Double mutants in Vps1 and Atg8 exhibit enhanced sensitivity to PQ, osmotic stress, and Ca^{2+} overload than the single mutations, indicating impaired vacuolar function (90–93). The potential strains-specific role of these proteins in determining each PQ susceptibility has to be determined.

Our study has limitations: i) We used a small number of strains; which makes it difficult to identify significant associations across traits; ii) we focused only on two PD-related phenotypes: ROS and vacuolar adaptations, omitting other like proteostasis that could be involved on PD pathogenesis (94); iii) we used domesticated strains which have been selected by their abilities to tolerate stressors and higher genetic stability, thereby minimizing the risk of spontaneous mutations and related to genotypic and phenotypic variability; iv) this is a phenotypic characterization, lacking mechanistic assays; among other. However, by investigating the cellular and molecular responses underlying resistance and susceptibility to PQ, our study reveals the biological foundation supporting these differences and highlights the fundamental role of genetics in understanding these complex processes.

In conclusion, our work explores cellular and molecular mechanisms underlying PQ toxicity in four different yeast backgrounds, which resulted in good proxies for studying PQ susceptibility/resistance in humans. Understanding the biology of the resistant strains is crucial for designing new strategies to prevent pesticide-induced PD. These can be achieved by gene mapping studies and omics in *S. cerevisiae*, followed by validations in animal models and human cells.

Experimental procedures

Yeast strains and culture conditions

The four haploid (*MAT α* and *MAT a*) *S. cerevisiae* strains used in this study were: North American (NA; YPS128, *MAT α/a, ho: HygMX, ura3::kanMX*), West African (WA; DBVPG6044, *MAT α/a, ho: HygMX, ura3::kanMX*), Sake (SA; Y12, *MAT α/a, ho: HygMX, ura3::kanMX*) and. Wine/European (WE; DBVPG6765, *MAT α/a, ho: HygMX, ura3::kanMX*) (95, 96). These strains were stored in solid media (YPD) at 4°C. Liquid and solid culture media were used depending on the experiments to be performed: YPD media (2% glucose, 2% peptone, 1% yeast extract) and YNB (0.67% YNB base without amino acids, 0.2% uracil, 0.0875% com drop out and 2% glucose).

Growth curves conditions

Yeast cells were pre-cultured in 200 µL of YNB medium supplemented with uracil (0.2% uracil) for 48 h at 28 °C. For the experimental run, the four yeast strains

were inoculated to an optical density (OD) of 0.03-0.1 (wavelength of 620 nm) in 200 µL of medium and incubated without shaking at 28 °C for 48 h (YNB control and Paraquat (Sigma Aldrich-Merck, CAS No. 75365-73-0) at 75 µg/mL) in a Tecan Sunrise absorbance microplate reader (Tecan Trading AG, Männedorf, Switzerland). OD was measured every 30 min using a 620 nm filter. Each experiment was performed in triplicate. Growth rates for each strain were calculated as previously described (97, 98). Briefly, OD measurements as a function of time were fitted to the mathematical model of the re-parameterized Gompertz sigmoid curve describing microbiological temporal growth, previously proposed (99) from which growth rates were obtained. The parameters of each curve were processed in the GrowthRates software to obtain OD max, µmax, and the average time of the lag phase. Finally, the area under the curve (AUC) values of the growth curves were calculated using R commands.

Measurement of levels of Reactive Oxygen Species (ROS)

The yeast strain cultures were incubated for 48 hours at 28°C in 3 ml of YNB medium and centrifuged at 1700 x g at 4 °C for 4 min. Intracellular levels of superoxide anion were detected through the dihydroethidium (DHE) probe (Thermofisher Scientific, NºD1168, U.S.A), and intracellular levels of hydrogen peroxide (H_2O_2) were detected through the 2′,7′-dichlorofluorescein diacetate (DCFH-DA) probe (Sigma Aldrich, NºD6883, U.S.A). The pellet was incubated with the DHE probe at a concentration of 10 µg/mL (100) in 500 µL of PBS (80

mM Na_2HPO_4, 20 mM NaH_2PO_4 and 100 mM NaCl) (101) for 30 min and washed with PBS as previously reported (100, 101). The DCFH-DA probe was used at a concentration of 10 µM (102) in 500 µL of PBS for 1 h and washed with a PBS buffer. Fluorescence intensity was measured using a fluorometer Cytation3 microplate reader (BioTek Instruments, Santa Clara, CA, U.S.A) at 518/605 nm for DHE and 490/530 for DCFH-DA. For microscopic analysis, 4 µL of each incubated strain (DHE and DCFH-DA probe) were taken, added to a slide, and squeezed with a coverslip gently for *in vivo* visualization and observed under a Leica SP8 confocal microscope (Leica Microsystems, Germany), using a 63X objective and 5X magnification. Images were processed in ImageJ (103) and LASX software (Leica Microsystems, Germany).

FM4-64 internalization assay in *S. cerevisiae*: Vacuolar phenotypes

Yeasts were seeded on a plate with YPD medium and 2% agar-agar. Isolations were made from each strain to obtain single colonies previously incubated at 28°C without shaking for 48 hours. Then, inocula were transferred into 500 µL of liquid YPD and incubated with 3 µM of FM4-64 (Ex: 565 nm - Em: 744 nm) (ThermoFisher Scientific, N° F34653, U.S.A) for 24 hours in 48-hour cultures in control condition (104) and with 75 µg/mL Paraquat at 28°C with shaking (150 rpm) in the dark. 4 µL of each incubated strain was added to a slide and squeezed with a coverslip gently for in vivo viewing and observed on Leica SP8 confocal microscope (Leica Microsystems, Germany), using 63X objective and 5X

magnification. Images were processed in ImageJ and LASX software (Leica Microsystems, Germany). The vacuolar characteristics of 110-150 cells per field were analyzed and classified according to their phenotype into "A", "B" or "C", as proposed by Seeley E. et al. (2002) (104). The assay was repeated three times and quantified by three researchers independently for each yeast strain.

Statistical analysis

Growth parameters μMax, ROS level by DHE and DCFH-DA, and percentage of vacuolar phenotypes were used as quantitative variables in the control condition and PQ at a 75 μg/mL concentration. Shapiro Wilk normality test $p>0.05$, parametric ANOVA test $P<0.05$ with multiple comparisons, and non-parametric Kruskal Wallis test p-value < 0.05 with multiple comparisons were used for all measurements. Sample “N” in the experiments was 5 biological replicates and 3 technical replicates per sample for μMax, 6 biological replicates and 3 technical replicates per sample for ROS level by DHE and DCFH-DA probe, and 3 biological replicates with 3 technical replicates per sample for quantification of vacuolar phenotypes. Statistical significance was considered for a value of $P<0.05$. Furthermore, multiple correlations were conducted in this study. Pearson correlations were performed for the fold change of DHE, DCFH, μMax, and vacuolar phenotypes A and B, as the data exhibited normal distribution (Shapiro-Wilk test $P > 0.05$). However, a Spearman correlation was employed for vacuolar phenotype C and its combinations due to their departure from the normality

assumption. The potential effects of variants in each gene of the four yeast strains were determined using SIFT software (Table 2) and the *S. cerevisiae* S288C reference genome (https://www.yeastgenome.org/). The number of variants in oxidative stress and lysosomal genes was correlated with µMáx, ROS levels (DHE and DCFH-DA probes), and phenotype B using Pearson correlations. To adjust for multiple comparisons, we applied the Bonferroni procedure to control for the error rate and establish a corrected statistical significance threshold and adjusted P-value (P_{adj} *a*) based on a significance level of 0.05. Statistical analysis was performed in SPSS software version 20.0 (Illinois, U.S.A) and plotted in GraphPad (California, U.S.A) and RStudio (U.S.A).

References

1. Tudi, M., Daniel Ruan, H., Wang, L., Lyu, J., Sadler, R., Connell, D., Chu, C., and Phung, D. T. (2021) Agriculture Development, Pesticide Application and Its Impact on the Environment. *Int. J. Environ. Res. Public Health*. 10.3390/ijerph18031112

2. Pretty, J., and Bharucha, Z. P. (2015) Integrated Pest Management for Sustainable Intensification of Agriculture in Asia and Africa. *Insects*. **6**, 152–182

3. Ball, N., Teo, W.-P., Chandra, S., and Chapman, J. (2019) Parkinson's Disease and the Environment. *Front. Neurol.* **10**, 218

4. Sharma, D. R., Thapa, R. B., and Manandhar, H. K. (2012) Use of pesticides in Nepal and impacts on human health and environment. *J. Agric. West. Aust.*

5. Paul, K. C., Cockburn, M., Gong, Y., Bronstein, J., and Ritz, B. (2024) Agricultural paraquat dichloride use and Parkinson's disease in California's Central Valley. *Int. J. Epidemiol.* 10.1093/ije/dyae004

6. Coria, J., and Elgueta, S. (2022) Towards safer use of pesticides in Chile. *Environ. Sci. Pollut. Res. Int.* **29**, 22785–22797

7. Ashraf, D., Khan, M. R., Dawson, T. M., and Dawson, V. L. (2024) Protein Translation in the Pathogenesis of Parkinson's Disease. *Int. J. Mol. Sci.* 10.3390/ijms25042393

8. Morris, H. R., Spillantini, M. G., Sue, C. M., and Williams-Gray, C. H. (2024) The pathogenesis of Parkinson's disease. *Lancet*. **403**, 293–304

9. Fleming, S. M. (2017) Mechanisms of Gene-Environment Interactions in Parkinson's Disease. *Curr Environ Health Rep*. **4**, 192–199

10. Prasad, K., Winnik, B., Thiruchelvam, M. J., Buckley, B., Mirochnitchenko, O., and Richfield, E. K. (2007) Prolonged toxicokinetics and toxicodynamics of paraquat in mouse brain. *Environ. Health Perspect.* **115**, 1448–1453

11. Burbulla, L. F., and Krüger, R. (2011) Converging environmental and genetic pathways in the pathogenesis of Parkinson's disease. *J. Neurol. Sci.* **306**, 1–8

12. Dardiotis, E., Xiromerisiou, G., Hadjichristodoulou, C., Tsatsakis, A. M., Wilks, M. F., and Hadjigeorgiou, G. M. (2013) The interplay between environmental and genetic factors in Parkinson's disease susceptibility: the evidence for pesticides. *Toxicology*. **307**, 17–23

13. Tanner, C. M., Kamel, F., Ross, G. W., Hoppin, J. A., Goldman, S. M., Korell, M., Marras, C., Bhudhikanok, G. S., Kasten, M., Chade, A. R., Comyns, K., Richards, M. B., Meng, C., Priestley, B., Fernandez, H. H., Cambi, F., Umbach, D. M., Blair, A., Sandler, D. P., and Langston, J. W. (2011) Rotenone, paraquat, and Parkinson's disease. *Environ. Health Perspect.* **119**, 866–872

14. Torres-Rojas, C., Zhuang, D., Jimenez-Carrion, P., Silva, I., O'Callaghan, J. P., Lu, L., Zhao, W., Mulligan, M. K., Williams, R. W., and Jones, B. C. (2020) Systems Genetics and Systems Biology Analysis of Paraquat Neurotoxicity in BXD Recombinant Inbred Mice. *Toxicol. Sci.* **176**, 137–146

15. Berry, C., La Vecchia, C., and Nicotera, P. (2010) Paraquat and Parkinson's disease. *Cell Death Differ.* **17**, 1115–1125

16. Romero-Aguilar, L., Vázquez-Meza, H., Guerra-Sánchez, G., Luqueño-Bocardo, O. I., and Pardo, J. P. (2022) The Mitochondrial Alternative Oxidase in Is Not Involved in Response to Oxidative Stress Induced by Paraquat. *J Fungi (Basel)*. 10.3390/jof8111221

17. Elkholy, A. R., El-Sheakh, A. R., and Suddek, G. M. (2023) Nilotinib alleviates paraquat-induced hepatic and pulmonary injury in rats via the Nrf2/Nf-kB axis. *Int. Immunopharmacol.* **124**, 110886

18. Hernandez-Baixauli, J., Chomiciute, G., Tracey, H., Mora, I., Cortés-Espinar, A. J., Ávila-Román, J., Abasolo, N., Palacios-Jordan, H., Foguet-Romero,

E., Suñol, D., Galofré, M., Alcaide-Hidalgo, J. M., Baselga-Escudero, L., Del Bas, J. M., and Mulero, M. (2024) Exploring Metabolic and Gut Microbiome Responses to Paraquat Administration in Male Wistar Rats: Implications for Oxidative Stress. *Antioxidants (Basel)*. 10.3390/antiox13010067

19. Tiên Nguyên-nhu, N., and Knoops, B. (2003) Mitochondrial and cytosolic expression of human peroxiredoxin 5 in Saccharomyces cerevisiae protect yeast cells from oxidative stress induced by paraquat. *FEBS Lett.* **544**, 148–152

20. See, W. Z. C., Naidu, R., and Tang, K. S. (2022) Cellular and Molecular Events Leading to Paraquat-Induced Apoptosis: Mechanistic Insights into Parkinson's Disease Pathophysiology. *Mol. Neurobiol.* **59**, 3353–3369

21. Liu, X., Yang, H., and Liu, Z. (2022) Signaling pathways involved in paraquat-induced pulmonary toxicity: Molecular mechanisms and potential therapeutic drugs. *Int. Immunopharmacol.* **113**, 109301

22. Akhter, F., Chen, D., Yan, S. F., and Yan, S. S. (2017) Mitochondrial Perturbation in Alzheimer's Disease and Diabetes. *Prog. Mol. Biol. Transl. Sci.* **146**, 341–361

23. Song, C.-Q., Sun, D.-Z., Xu, Y.-M., Yang, C., Cai, Q., and Dong, X.-S. (2019) Effect of endoplasmic reticulum calcium on paraquat-induced apoptosis of human lung type II alveolar epithelial A549 cells. *Mol. Med. Rep.* **20**, 2419–2425

24. Rubilar, J. C., Outeiro, T. F., and Klein, A. D. (2024) The lysosomal β-glucocerebrosidase strikes mitochondria: implications for Parkinson's therapeutics. *Brain*. 10.1093/brain/awae070

25. Li, D., Mastaglia, F. L., Fletcher, S., and Wilton, S. D. (2020) Progress in the molecular pathogenesis and nucleic acid therapeutics for Parkinson's disease in the precision medicine era. *Med. Res. Rev.* **40**, 2650–2681

26. Ossowska, K., Smiałowska, M., Kuter, K., Wierońska, J., Zieba, B., Wardas, J., Nowak, P., Dabrowska, J., Bortel, A., Biedka, I., Schulze, G., and Rommelspacher, H. (2006) Degeneration of dopaminergic mesocortical neurons and activation of compensatory processes induced by a long-term paraquat administration in rats: implications for Parkinson's disease. *Neuroscience*. **141**, 2155–2165

27. Zhang, X.-F., Thompson, M., and Xu, Y.-H. (2016) Multifactorial theory applied to the neurotoxicity of paraquat and paraquat-induced mechanisms of developing Parkinson's disease. *Lab. Invest.* **96**, 496–507

28. McCormack, A. L., Thiruchelvam, M., Manning-Bog, A. B., Thiffault, C., Langston, J. W., Cory-Slechta, D. A., and Di Monte, D. A. (2002) Environmental risk factors and Parkinson's disease: selective degeneration of nigral dopaminergic neurons caused by the herbicide paraquat. *Neurobiol. Dis.* **10**, 119–

127

29. Klein, A. D., and Mazzulli, J. R. (2018) Is Parkinson's disease a lysosomal disorder? *Brain*. **141**, 2255–2262

30. LeWitt, P. A., and Chaudhuri, K. R. (2020) Unmet needs in Parkinson disease: Motor and non-motor. *Parkinsonism Relat. Disord.* **80 Suppl 1**, S7–S12

31. Blesa, J., Foffani, G., Dehay, B., Bezard, E., and Obeso, J. A. (2022) Motor and non-motor circuit disturbances in early Parkinson disease: which happens first? *Nat. Rev. Neurosci.* **23**, 115–128

32. Islam, M. S., Azim, F., Saju, H., Zargaran, A., Shirzad, M., Kamal, M., Fatema, K., Rehman, S., Azad, M. A. M., and Ebrahimi-Barough, S. (2021) Pesticides and Parkinson's disease: Current and future perspective. *J. Chem. Neuroanat.* **115**, 101966

33. Liu, W., Li, L., Ye, H., Chen, H., Shen, W., Zhong, Y., Tian, T., and He, H. (2017) From Saccharomyces cerevisiae to human: The important gene co-expression modules. *Biomed Rep*. **7**, 153–158

34. Winzeler, E. A., Shoemaker, D. D., Astromoff, A., Liang, H., Anderson, K., Andre, B., Bangham, R., Benito, R., Boeke, J. D., Bussey, H., Chu, A. M., Connelly, C., Davis, K., Dietrich, F., Dow, S. W., El Bakkoury, M., Foury, F., Friend, S. H., Gentalen, E., Giaever, G., Hegemann, J. H., Jones, T., Laub, M., Liao, H., Liebundguth, N., Lockhart, D. J., Lucau-Danila, A., Lussier, M., M'Rabet, N., Menard, P., Mittmann, M., Pai, C., Rebischung, C., Revuelta, J. L., Riles, L., Roberts, C. J., Ross-MacDonald, P., Scherens, B., Snyder, M., Sookhai-Mahadeo, S., Storms, R. K., Véronneau, S., Voet, M., Volckaert, G., Ward, T. R., Wysocki, R., Yen, G. S., Yu, K., Zimmermann, K., Philippsen, P., Johnston, M., and Davis, R. W. (1999) Functional characterization of the S. cerevisiae genome by gene deletion and parallel analysis. *Science*. **285**, 901–906

35. Mülleder, M., Capuano, F., Pir, P., Christen, S., Sauer, U., Oliver, S. G., and Ralser, M. (2012) A prototrophic deletion mutant collection for yeast metabolomics and systems biology. *Nat. Biotechnol.* **30**, 1176–1178

36. Saldaña, C., Villava, C., Ramírez-Villarreal, J., Morales-Tlalpan, V., Campos-Guillen, J., Chávez-Servín, J., and García-Gasca, T. (2021) Rapid and reversible cell volume changes in response to osmotic stress in yeast. *Braz. J. Microbiol.* **52**, 895–903

37. Aufschnaiter, A., and Büttner, S. (2019) The vacuolar shapes of ageing: From function to morphology. *Biochim. Biophys. Acta Mol. Cell Res.* **1866**, 957–970

38. Ngo, K. J., Paul, K. C., Wong, D., Kusters, C. D. J., Bronstein, J. M., Ritz, B., and Fogel, B. L. (2024) Lysosomal genes contribute to Parkinson's disease

near agriculture with high intensity pesticide use. *NPJ Parkinsons Dis*. **10**, 87

39. Sukumar, C. A., Shanbhag, V., and Shastry, A. B. (2019) Paraquat: The Poison Potion. *Indian J. Crit. Care Med.* **23**, S263–S266

40. Shi, L., Yu, G., Li, Y., Zhao, L., Wen, Z., Tao, Y., Wang, W., and Jian, X. (2022) The toxicokinetics of acute paraquat poisoning in specific patients: a case series. *J. Int. Med. Res.* **50**, 3000605221122745

41. Hsieh, Y.-W., Lin, J.-L., Lee, S.-Y., Weng, C.-H., Yang, H.-Y., Liu, S.-H., Wang, I.-K., Liang, C.-C., Chang, C.-T., and Yen, T.-H. (2013) Paraquat poisoning in pediatric patients. *Pediatr. Emerg. Care*. **29**, 487–491

42. Shi, M., Zeng, M., Jian, T., Yu, G., Genjiafu, A., Zhang, X., Guo, L., Shang, R., Zhou, Z., Zhang, T., Jian, X., and Kan, B. (2023) A mass event of paraquat poisoning via inhalation. *Front Public Health*. **11**, 1309708

43. Donaher, S. E., and Van den Hurk, P. (2023) Ecotoxicology of the herbicide paraquat: effects on wildlife and knowledge gaps. *Ecotoxicology*. **32**, 1187–1199

44. Kumar, S., Gupta, S., Bansal, Y. S., Bal, A., Rastogi, P., Muthu, V., and Arora, V. (2021) Pulmonary histopathology in fatal paraquat poisoning. *Autops Case Rep*. **11**, e2021342

45. Sharma, P., and Mittal, P. (2024) Paraquat (herbicide) as a cause of Parkinson's Disease. *Parkinsonism Relat. Disord.* **119**, 105932

46. Houzé, P., Baud, F. J., Mouy, R., Bismuth, C., Bourdon, R., and Scherrmann, J. M. (1990) Toxicokinetics of paraquat in humans. *Hum. Exp. Toxicol.* **9**, 5–12

47. Alural, B., Ozerdem, A., Allmer, J., Genc, K., and Genc, S. (2015) Lithium protects against paraquat neurotoxicity by NRF2 activation and miR-34a inhibition in SH-SY5Y cells. *Front. Cell. Neurosci.* **9**, 209

48. Djukic, M., Jovanovic, M. C., Ninkovic, M., Vasiljevic, I., and Jovanovic, M. (2007) The role of nitric oxide in paraquat-induced oxidative stress in rat striatum. *Ann. Agric. Environ. Med.* **14**, 247–252

49. Xiong, G., Zhao, L., Yan, M., Wang, X., Zhou, Z., and Chang, X. (2019) N-acetylcysteine alleviated paraquat-induced mitochondrial fragmentation and autophagy in primary murine neural progenitor cells. *J. Appl. Toxicol.* **39**, 1557–1567

50. Dinis-Oliveira, R. J., Remião, F., Carmo, H., Duarte, J. A., Navarro, A. S., Bastos, M. L., and Carvalho, F. (2006) Paraquat exposure as an etiological factor of Parkinson's disease. *Neurotoxicology*. **27**, 1110–1122

51. Sillapawattana, P., Gruhlke, M. C. H., Seiler, T.-B., Klungsupya, P., and

Charerntantanakul, W. (2024) Oxidative stress related effect of xenobiotics on eukaryotic model organism, Saccharomyces cerevisiae. *Free Radic. Biol. Med.* **212**, 149–161

52. Olguín, V., Durán, A., Las Heras, M., Rubilar, J. C., Cubillos, F. A., Olguín, P., and Klein, A. D. (2022) Genetic Background Matters: Population-Based Studies in Model Organisms for Translational Research. *Int. J. Mol. Sci.* 10.3390/ijms23147570

53. Oftadeh, O., Salvy, P., Masid, M., Curvat, M., Miskovic, L., and Hatzimanikatis, V. (2021) A genome-scale metabolic model of Saccharomyces cerevisiae that integrates expression constraints and reaction thermodynamics. *Nat. Commun.* **12**, 4790

54. Karathia, H., Vilaprinyo, E., Sorribas, A., and Alves, R. (2011) Saccharomyces cerevisiae as a model organism: a comparative study. *PLoS One*. **6**, e16015

55. Nestelbacher, R., Laun, P., Vondráková, D., Pichová, A., Schüller, C., and Breitenbach, M. (2000) The influence of oxygen toxicity on yeast mother cell-specific aging. *Exp. Gerontol.* **35**, 63–70

56. Jarolim, S., Millen, J., Heeren, G., Laun, P., Goldfarb, D. S., and Breitenbach, M. (2004) A novel assay for replicative lifespan in Saccharomyces cerevisiae. *FEMS Yeast Res.* **5**, 169–177

57. Li, Y., Zhong, X., Ye, J., Guo, H., and Long, Y. (2021) Proteome of Saccharomyces cerevisiae under paraquat stress regulated by therapeutic concentration of copper ions. *Ecotoxicol. Environ. Saf.* **217**, 112245

58. Stenberg, S., Li, J., Gjuvsland, A. B., Persson, K., Demitz-Helin, E., González Peña, C., Yue, J.-X., Gilchrist, C., Ärengård, T., Ghiaci, P., Larsson-Berglund, L., Zackrisson, M., Smits, S., Hallin, J., Höög, J. L., Molin, M., Liti, G., Omholt, S. W., and Warringer, J. (2022) Genetically controlled mtDNA deletions prevent ROS damage by arresting oxidative phosphorylation. *Elife*. 10.7554/eLife.76095

59. Fendt, S.-M., Oliveira, A. P., Christen, S., Picotti, P., Dechant, R. C., and Sauer, U. (2010) Unraveling condition-dependent networks of transcription factors that control metabolic pathway activity in yeast. *Mol. Syst. Biol.* **6**, 432

60. Albrecht, G., Mösch, H. U., Hoffmann, B., Reusser, U., and Braus, G. H. (1998) Monitoring the Gcn4 protein-mediated response in the yeast Saccharomyces cerevisiae. *J. Biol. Chem.* **273**, 12696–12702

61. Duncan, C. D. S., Rodríguez-López, M., Ruis, P., Bähler, J., and Mata, J. (2018) General amino acid control in fission yeast is regulated by a nonconserved transcription factor, with functions analogous to Gcn4/Atf4. *Proc. Natl. Acad. Sci.*

U. S. A. **115**, E1829–E1838

62. Yang, R., Wek, S. A., and Wek, R. C. (2000) Glucose limitation induces GCN4 translation by activation of Gcn2 protein kinase. *Mol. Cell. Biol.* **20**, 2706–2717

63. Lovejoy, P. C., Foley, K. E., Conti, M. M., Meadows, S. M., Bishop, C., and Fiumera, A. C. (2021) Genetic basis of susceptibility to low-dose paraquat and variation between the sexes in Drosophila melanogaster. *Mol. Ecol.* **30**, 2040–2053

64. Yin, L., Lu, L., Prasad, K., Richfield, E. K., Unger, E. L., Xu, J., and Jones, B. C. (2011) Genetic-based, differential susceptibility to paraquat neurotoxicity in mice. *Neurotoxicol. Teratol.* **33**, 415–421

65. Olivares, G. H., Olguín, P., and Klein, A. D. (2019) Modeling Parkinson's Disease Heterogeneity to Accelerate Precision Medicine. *Trends Mol. Med.* **25**, 1052–1055

66. Goker-Alpan, O., Schiffmann, R., LaMarca, M. E., Nussbaum, R. L., McInerney-Leo, A., and Sidransky, E. (2004) Parkinsonism among Gaucher disease carriers. *J. Med. Genet.* **41**, 937–940

67. Blauwendraat, C., Nalls, M. A., and Singleton, A. B. (2020) The genetic architecture of Parkinson's disease. *Lancet Neurol.* **19**, 170–178

68. Sidransky, E., Nalls, M. A., Aasly, J. O., Aharon-Peretz, J., Annesi, G., Barbosa, E. R., Bar-Shira, A., Berg, D., Bras, J., Brice, A., Chen, C.-M., Clark, L. N., Condroyer, C., De Marco, E. V., Dürr, A., Eblan, M. J., Fahn, S., Farrer, M. J., Fung, H.-C., Gan-Or, Z., Gasser, T., Gershoni-Baruch, R., Giladi, N., Griffith, A., Gurevich, T., Januario, C., Kropp, P., Lang, A. E., Lee-Chen, G.-J., Lesage, S., Marder, K., Mata, I. F., Mirelman, A., Mitsui, J., Mizuta, I., Nicoletti, G., Oliveira, C., Ottman, R., Orr-Urtreger, A., Pereira, L. V., Quattrone, A., Rogaeva, E., Rolfs, A., Rosenbaum, H., Rozenberg, R., Samii, A., Samaddar, T., Schulte, C., Sharma, M., Singleton, A., Spitz, M., Tan, E.-K., Tayebi, N., Toda, T., Troiano, A. R., Tsuji, S., Wittstock, M., Wolfsberg, T. G., Wu, Y.-R., Zabetian, C. P., Zhao, Y., and Ziegler, S. G. (2009) Multicenter analysis of glucocerebrosidase mutations in Parkinson's disease. *N. Engl. J. Med.* **361**, 1651–1661

69. Brooker, S. M., Naylor, G. E., and Krainc, D. (2024) Cell biology of Parkinson's disease: Mechanisms of synaptic, lysosomal, and mitochondrial dysfunction. *Curr. Opin. Neurobiol.* **85**, 102841

70. Klein, A. D., and Outeiro, T. F. (2023) Glucocerebrosidase mutations disrupt the lysosome and now the mitochondria. *Nat. Commun.* **14**, 6383

71. Guo, W. X., Mao, C., Obeid, L. M., and Boustany, R. M. (1999) A disrupted homologue of the human CLN3 or juvenile neuronal ceroid lipofuscinosis gene in

Saccharomyces cerevisiae: a model to study Batten disease. *Cell. Mol. Neurobiol.* **19**, 671–680

72. Mole, S., Williams, R., and Goebel, H. (2011) *The Neuronal Ceroid Lipofuscinoses (Batten Disease)*, Oxford University Press

73. El-Sitt, S., Soueid, J., Al Ali, J., Makoukji, J., Makhoul, N. J., Harati, H., and Boustany, R.-M. (2019) Developmental Comparison of Ceramide in Wild-Type and Mouse Brains and Sera. *Front. Neurol.* **10**, 128

74. Tuxworth, R. I., Chen, H., Vivancos, V., Carvajal, N., Huang, X., and Tear, G. (2011) The Batten disease gene CLN3 is required for the response to oxidative stress. *Hum. Mol. Genet.* **20**, 2037–2047

75. Abbott, S. K., Li, H., Muñoz, S. S., Knoch, B., Batterham, M., Murphy, K. E., Halliday, G. M., and Garner, B. (2014) Altered ceramide acyl chain length and ceramide synthase gene expression in Parkinson's disease. *Mov. Disord.* **29**, 518–526

76. Jenkins, G. M., Richards, A., Wahl, T., Mao, C., Obeid, L., and Hannun, Y. (1997) Involvement of yeast sphingolipids in the heat stress response of Saccharomyces cerevisiae. *J. Biol. Chem.* **272**, 32566–32572

77. Warringer, J., Zörgö, E., Cubillos, F. A., Zia, A., Gjuvsland, A., Simpson, J. T., Forsmark, A., Durbin, R., Omholt, S. W., Louis, E. J., Liti, G., Moses, A., and Blomberg, A. (2011) Trait variation in yeast is defined by population history. *PLoS Genet.* **7**, e1002111

78. Hancock, R. D., Galpin, J. R., and Viola, R. (2000) Biosynthesis of L-ascorbic acid (vitamin C) by Saccharomyces cerevisiae. *FEMS Microbiol. Lett.* **186**, 245–250

79. Foster, J., and Nakata, P. A. (2014) An oxalyl-CoA synthetase is important for oxalate metabolism in Saccharomyces cerevisiae. *FEBS Lett.* **588**, 160–166

80. Lushchak, V., Semchyshyn, H., Mandryk, S., and Lushchak, O. (2005) Possible role of superoxide dismutases in the yeast Saccharomyces cerevisiae under respiratory conditions. *Arch. Biochem. Biophys.* **441**, 35–40

81. Weids, A. J., and Grant, C. M. (2014) The yeast peroxiredoxin Tsa1 protects against protein-aggregate-induced oxidative stress. *J. Cell Sci.* **127**, 1327–1335

82. Zimmermann, J., Lang, L., Calabrese, G., Laporte, H., Amponsah, P. S., Michalk, C., Sukmann, T., Oestreicher, J., Tursch, A., Peker, E., Owusu, T. N. E., Weith, M., Roma, L. P., Deponte, M., Riemer, J., and Morgan, B. (2024) Tsa1 is the dominant peroxide scavenger and a source of H_2O_2-dependent GSSG production in yeast. *bioRxiv*. 10.1101/2024.07.03.601836

83. Garrigós, V., Picazo, C., Matallana, E., and Aranda, A. (2020) Wine yeast peroxiredoxin plays a role in growth, stress response and trehalose metabolism in biomass propagation. *Microorganisms*. 10.3390/microorganisms8101537

84. Li, S. C., and Kane, P. M. (2009) The yeast lysosome-like vacuole: endpoint and crossroads. *Biochim. Biophys. Acta*. **1793**, 650–663

85. Mao, X., Yang, L., Liu, Y., Ma, C., Ma, T., Yu, Q., and Li, M. (2021) Vacuole and Mitochondria Patch (vCLAMP) Protein Vam6 Is Involved in Maintenance of Mitochondrial and Vacuolar Functions under Oxidative Stress in. *Antioxidants (Basel)*. 10.3390/antiox10010136

86. Kim, D., Song, M., Do, E., Choi, Y., Kronstad, J. W., and Jung, W. H. (2021) Oxidative Stress Causes Vacuolar Fragmentation in the Human Fungal Pathogen. *J Fungi (Basel)*. 10.3390/jof7070523

87. Corson, L. B., Folmer, J., Strain, J. J., Culotta, V. C., and Cleveland, D. W. (1999) Oxidative stress and iron are implicated in fragmenting vacuoles of Saccharomyces cerevisiae lacking Cu,Zn-superoxide dismutase. *J. Biol. Chem.* **274**, 27590–27596

88. Proctor, S. A., Minc, N., Boudaoud, A., and Chang, F. (2012) Contributions of turgor pressure, the contractile ring, and septum assembly to forces in cytokinesis in fission yeast. *Curr. Biol.* **22**, 1601–1608

89. Pollard, T. D., and Wu, J.-Q. (2010) Understanding cytokinesis: lessons from fission yeast. *Nat. Rev. Mol. Cell Biol.* **11**, 149–155

90. Mikawa, T., Kanoh, J., and Ishikawa, F. (2010) Fission yeast Vps1 and Atg8 contribute to oxidative stress resistance. *Genes Cells*. **15**, 229–242

91. Ishii, A., Kurokawa, K., Hotta, M., Yoshizaki, S., Kurita, M., Koyama, A., Nakano, A., and Kimura, Y. (2019) Role of Atg8 in the regulation of vacuolar membrane invagination. *Sci. Rep.* **9**, 14828

92. Liu, X.-M., Yamasaki, A., Du, X.-M., Coffman, V. C., Ohsumi, Y., Nakatogawa, H., Wu, J.-Q., Noda, N. N., and Du, L.-L. (2018) Lipidation-independent vacuolar functions of Atg8 rely on its noncanonical interaction with a vacuole membrane protein. *Elife*. 10.7554/eLife.41237

93. Xu, D.-D., and Du, L.-L. (2022) Fission Yeast Autophagy Machinery. *Cells*. 10.3390/cells11071086

94. Kulkarni, A., Preeti, K., Tryphena, K. P., Srivastava, S., Singh, S. B., and Khatri, D. K. (2023) Proteostasis in Parkinson's disease: Recent development and possible implication in diagnosis and therapeutics. *Ageing Res. Rev.* **84**, 101816

95. Brice, C., Cubillos, F. A., Dequin, S., Camarasa, C., and Martínez, C. (2018) Adaptability of the Saccharomyces cerevisiae yeasts to wine fermentation

conditions relies on their strong ability to consume nitrogen. *PLoS One*. **13**, e0192383

96. Salinas, F., de Boer, C. G., Abarca, V., García, V., Cuevas, M., Araos, S., Larrondo, L. F., Martínez, C., and Cubillos, F. A. (2016) Natural variation in non-coding regions underlying phenotypic diversity in budding yeast. *Sci. Rep.* **6**, 21849

97. García-Ríos, E., López-Malo, M., and Guillamón, J. M. (2014) Global phenotypic and genomic comparison of two Saccharomyces cerevisiae wine strains reveals a novel role of the sulfur assimilation pathway in adaptation at low temperature fermentations. *BMC Genomics*. **15**, 1059

98. Quispe, X., Tapia, S. M., Villarroel, C., Oporto, C., Abarca, V., García, V., Martínez, C., and Cubillos, F. A. (2017) Genetic basis of mycotoxin susceptibility differences between budding yeast isolates. *Sci. Rep.* **7**, 9173

99. Zwietering, M. H., Jongenburger, I., Rombouts, F. M., and van 't Riet, K. (1990) Modeling of the bacterial growth curve. *Appl. Environ. Microbiol.* **56**, 1875–1881

100. Mendes-Ferreira, A., Sampaio-Marques, B., Barbosa, C., Rodrigues, F., Costa, V., Mendes-Faia, A., Ludovico, P., and Leão, C. (2010) Accumulation of non-superoxide anion reactive oxygen species mediates nitrogen-limited alcoholic fermentation by Saccharomyces cerevisiae. *Appl. Environ. Microbiol.* **76**, 7918–7924

101. Rego, A., Mendes, F., Costa, V., Chaves, S. R., and Côrte-Real, M. (2020) Pkh1p-Ypk1p and Pkh1p-Sch9p Pathways Are Activated by Acetic Acid to Induce a Mitochondrial-Dependent Regulated Cell Death. *Oxid. Med. Cell. Longev.* **2020**, 7095078

102. Chapela, S. P., Burgos, H. I., and Stella, C. A. (2022) N-Acetyl cysteine improves cellular growth in respiratory-deficient yeast. *Braz. J. Microbiol.* **53**, 791–794

103. Schneider, C. A., Rasband, W. S., and Eliceiri, K. W. (2012) NIH Image to ImageJ: 25 years of image analysis. *Nat. Methods*. **9**, 671–675

104. Seeley, E. S., Kato, M., Margolis, N., Wickner, W., and Eitzen, G. (2002) Genomic analysis of homotypic vacuole fusion. *Mol. Biol. Cell*. **13**, 782–794

Figure legends

Figure 1: Reproductive fitness in *S. cerevisiae* parental strains against PQ exposure. (A) Growth curves in four yeast strains in control condition (B) Growth curves in four yeast strains exposed to 75 µg/mL PQ. (C) Area under the curve (AUC) in four yeast strains (D) Fold change of µMax (PQ/mock). N= 5, Shapiro Wilk normality test *P*-value > 0.05, ANOVA test *P*-value < 0.05, post-hoc Holm-Sidak (AUC and fold change). *P*-value ≤ 0.05 (*), *P*-value < 0.01 (**), *P*-value < 0.001 (***), *P*-value < 0.0001 (****), ns = not significant (*P*-value > 0.05). Statistical analysis was performed in SPSS software version 20.0 and plotted in GraphPad.

Figure 2: Cellular response of *S. cerevisiae* to oxidative stress (superoxide anion) induced by PQ exposure. (A) Fold change of DHE signal in four strains after exposure to PQ (75 µg/mL). N=6, Shapiro Wilk normality test *P*-value > 0.05, ANOVA test *P*-value < 0.05, post-hoc Tukey. (B) DHE staining of untreated and paraquat-exposed (75 µg/mL) yeast strains visualized using an EVOS FL epifluorescence microscopy with a 40x objective and 2.6x zoom. White arrows: blue fluorescence in the cytosol indicates unoxidized probe (DHE). Yellow arrows: red fluorescence marks the probe oxidized by reactive molecules (DHEox). (C) Quantification of ROS levels obtained in confocal micrographs. N=3, Shapiro Wilk normality test *P*-value > 0.05, ANOVA test *P*-value < 0.05, post-hoc Tukey. . N =3. *P*-value ≤ 0.05 (*), *P*-value < 0.01 (**), *P*-value < 0.001 (***), *P*-value < 0.0001 (****), ns = not significant (*P*-value > 0.05). Statistical analysis was performed in

SPSS software version 20.0 and plotted in GraphPad and RStudio.

Figure 3: **Cellular response of *S. cerevisiae* to oxidative stress (hydrogen peroxide) induced by PQ exposure**. (A) Fold change of DCFH-DA signal in *S. cerevisiae* parental strains after exposure to PQ (75 µg/mL). N=6, Shapiro Wilk normality test *P*-value > 0.05, Kruskal Wallis test *P*-value <0.05. (B) DCFH-DA staining of untreated and paraquat-exposed (75 µg/mL) yeast strains visualized using an EVOS FL epifluorescence microscopy with a 40x objective and 2.6x zoom. White arrows: green fluorescence in SA and NA strains (control and PQ). Yellow arrows: green fluorescence in WA and WE strains (control and PQ). (C) Quantification of ROS levels obtained in confocal micrographs. N=3, Shapiro Wilk normality test *P*-value > 0.05, ANOVA test *P*-value < 0.05, post-hoc Tukey. N =3. *P*-value ≤ 0.05 (*), *P*-value < 0.01 (**), *P*-value < 0.001 (***), *P*-value < 0.0001 (****), ns = not significant (*P*-value > 0.05). Statistical analysis was performed in SPSS software version 20.0 and plotted in GraphPad.

Figure 4: Cellular response of *S. cerevisiae* to PQ-exposure involving vacuolar changes. (A) Confocal microscopy on four S. cerevisiae strains through FM4-64 probe (control condition and PQ treatment). Yellow arrows: Phenotype A, blue light arrows: Phenotype B and white arrows: Phenotype C. (B) Quantification of vacuolar phenotypes without PQ treatment (top) and 75 µg/mL PQ (bottom). N= 3, Shapiro Wilk normality test *P*-value > 0.05, Kruskal Wallis test *P*-value <0.05. *P*-value ≤ 0.05 (*), *P*-value < 0.01 (**), *P*-value < 0.001 (***), *P*-value <

0.0001 (****), ns = not significant (*P*-value > 0.05). Statistical analysis was performed in SPSS software version 20.0 and plotted in GraphPad.

Figure 5: Interplay between physiological parameters, oxidative stress and vacuolar morphology. (A) Plot of multiple correlations between fold change of μMax, DHE probe, DCFH-DA probe, phenotype A, phenotype B and phenotype C. (B) Pairwise correlations between fold change of μMax, DHE probe, DCFH-DA probe, phenotype A, phenotype B and phenotype C. N=4, Pearson correlation p-value < 0.05 in μMax, DHE probe, DCFH-DA probe, phenotype A and phenotype B. For phenotype C and combinations with other parameters were used Spearman correlation. Shapiro Wilk test *P*-value > 0.05. *P*-value ≤ 0.05 (*), *P*-value < 0.01 (**), *P*-value < 0.001 (***), *P*-value < 0.0001 (****), ns = not significant (*P*-value > 0.05). Statistical analysis was performed in SPSS software version 20.0 and plotted in RStudio.

Figure 6: PQ affect differentially biological processes in four backgrounds of *S. cerevisiae*. The effect of PQ on the four yeast strains is specific. SA and NA strains exhibit resistance to PQ, while WA and WE strains are susceptible, impacting their low specific growth rate. SA and WE strains produce higher levels of ROS, including superoxide anion and hydrogen peroxide, compared to NA and WA strains. Finally, PQ affects vacuolar morphology. The percentage of phenotype C increases in the WE strain, while NA and WA strains show an increase in phenotype B compared to the control condition. Figure created with

BioRender.com

Table 1: Vacuolar morphology in four *Saccharomyces cerevisiae* strains in control and PQ conditions. Vacuolar phenotypes were determined for each strain. The number of cells in each phenotype, expressed as mean ± standard deviation and percentage (%), is presented.

Table 2: Correlations of lysosomal and oxidative stress genes with the number of variants in yeast strains. The potential effects of variants in each gene of the four yeast strains were determined using SIFT. The number of variants in oxidative stress and lysosomal genes was correlated with μMáx, ROS levels (DHE and DCFH-DA probes), and phenotype B using Pearson correlations. To adjust for multiple comparisons, we applied the Bonferroni procedure to control for the error rate and establish a corrected statistical significance threshold and adjusted *P*-value (P_{adj} *a*) based on a significance level of 0.05. Statistical analysis was performed in RStudio.

Supplementary Figure 1: Growth curves in four yeast strains exposed to different PQ concentrations. Growth curves in PQ concentrations of 12.5 μg/mL, 25 μg/mL, 50 μg/mL, 75 μg/mL, 100 μg/mL, and 125 μg/mL to determine the optimal concentration with a differential effect in the four strains yeast.

Supplementary Figure 2: Cellular response of *S. cerevisiae* to superoxide anion induced by PQ exposure. A.F.U (arbitrary fluorescent unity) of DHE signal in S. cerevisiae parental strains in the control condition and after exposure to PQ

(75 µg/mL). N=6, Shapiro Wilk normality test *P*-value > 0.05, ANOVA test *P*-value < 0.05, post-hoc Tukey. *P*-value ≤ 0.05 (*), *P*-value < 0.01 (**), *P*-value < 0.001 (***), *P*-value < 0.0001 (****), ns = not significant (*P*-value > 0.05). Statistical analysis was performed in SPSS software version 20.0 and plotted in GraphPad and RStudio.

Supplementary Figure 3: Cellular response of *S. cerevisiae* to hydrogen peroxide induced by PQ exposure. A.F.U (arbitrary fluorescent unity) of DCFH-DA signal in S. cerevisiae parental strains in the control condition and after exposure to PQ (75 µg/mL). N=6, Shapiro Wilk normality test p-value > 0.05, Kruskal Wallis test *P*-value <0.05. *P*-value ≤ 0.05 (*), *P*-value < 0.01 (**), *P*-value < 0.001 (***), *P*-value < 0.0001 (****), ns = not significant (*P*-value > 0.05). Statistical analysis was performed in SPSS software version 20.0 and plotted in GraphPad.

Supplementary Table 1: Correlations between the different phenotypes studied. Method: Pearson or Spearman, *r* = the correlation coefficient and *P*-value based on a significance level of 0.05. Statistical analysis was performed in RStudio.

Supplementary Table 2: SIFT-predicted variants in vacuolar and oxidative stress genes in the four yeast strains. Ref allele: reference allele, Ref amino acid: reference amino acid.

Figures

Figure 1.

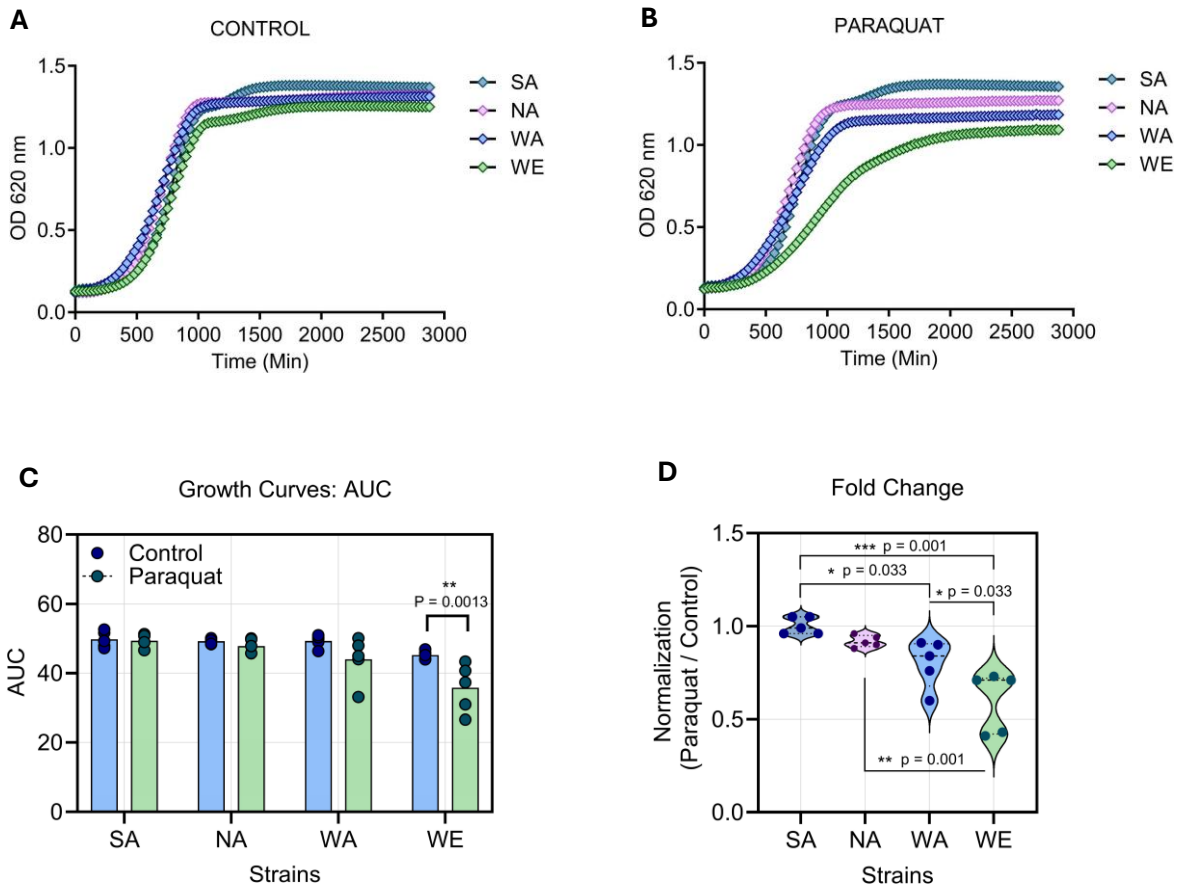

Figure 2.

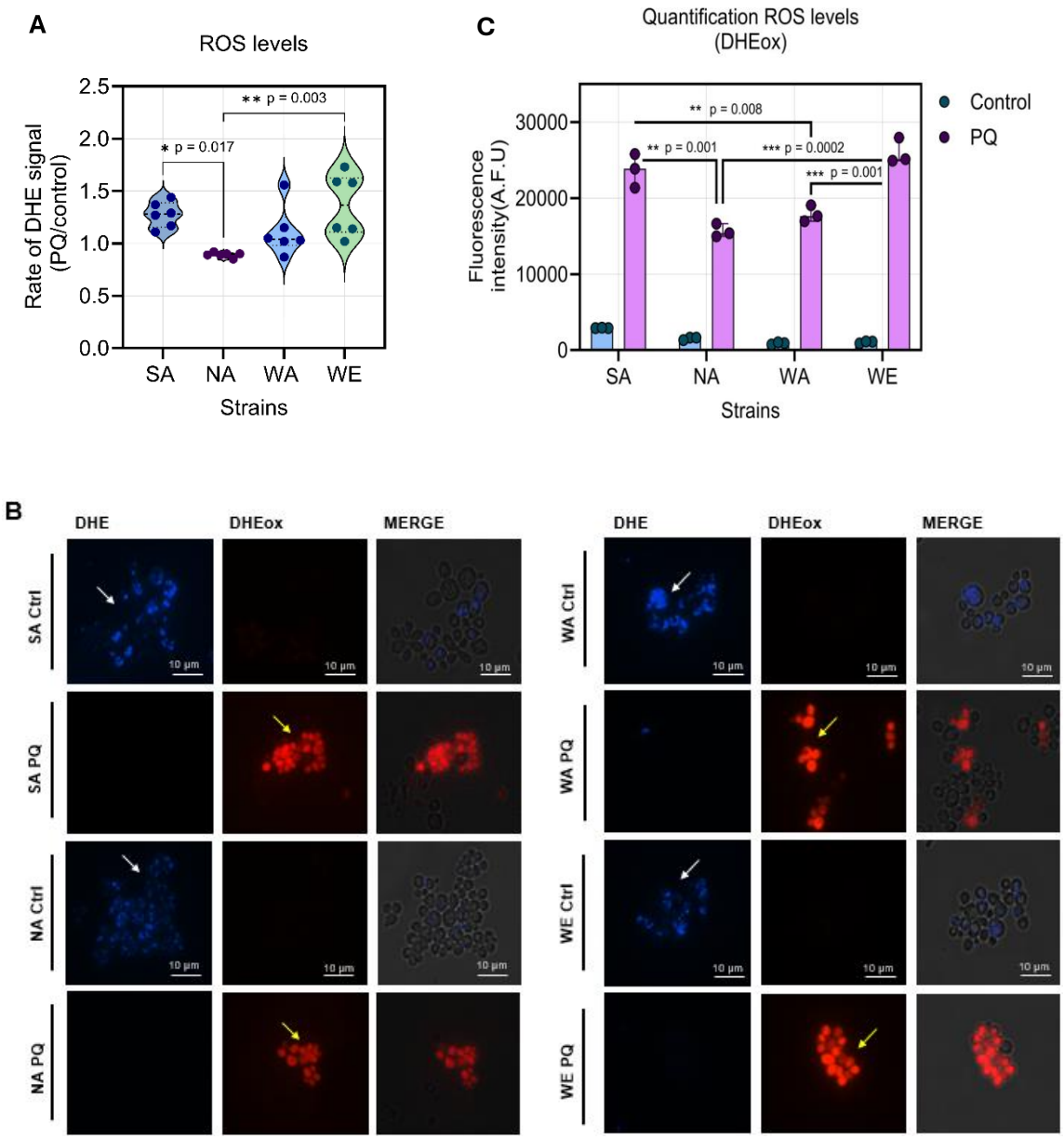
A
ROS levels
Rate of DHE signal (PQ/control)
2.5
2.0
1.5
1.0
0.5
0.0
* p = 0.017
** p = 0.003
SA
NA
WA
WE
Strains
C
Quantification ROS levels (DHEox)
Fluorescence intensity(A.F.U)
30000
20000
10000
0
** p = 0.008
** p = 0.001
*** p = 0.0002
*** p = 0.001
Control
PQ
SA
NA
WA
WE
Strains
B
DHE
DHEox
MERGE
SA Ctrl
SA PQ
NA Ctrl
NA PQ
WA Ctrl
WA PQ
WE Ctrl
WE PQ
10 µm

Figure 3.

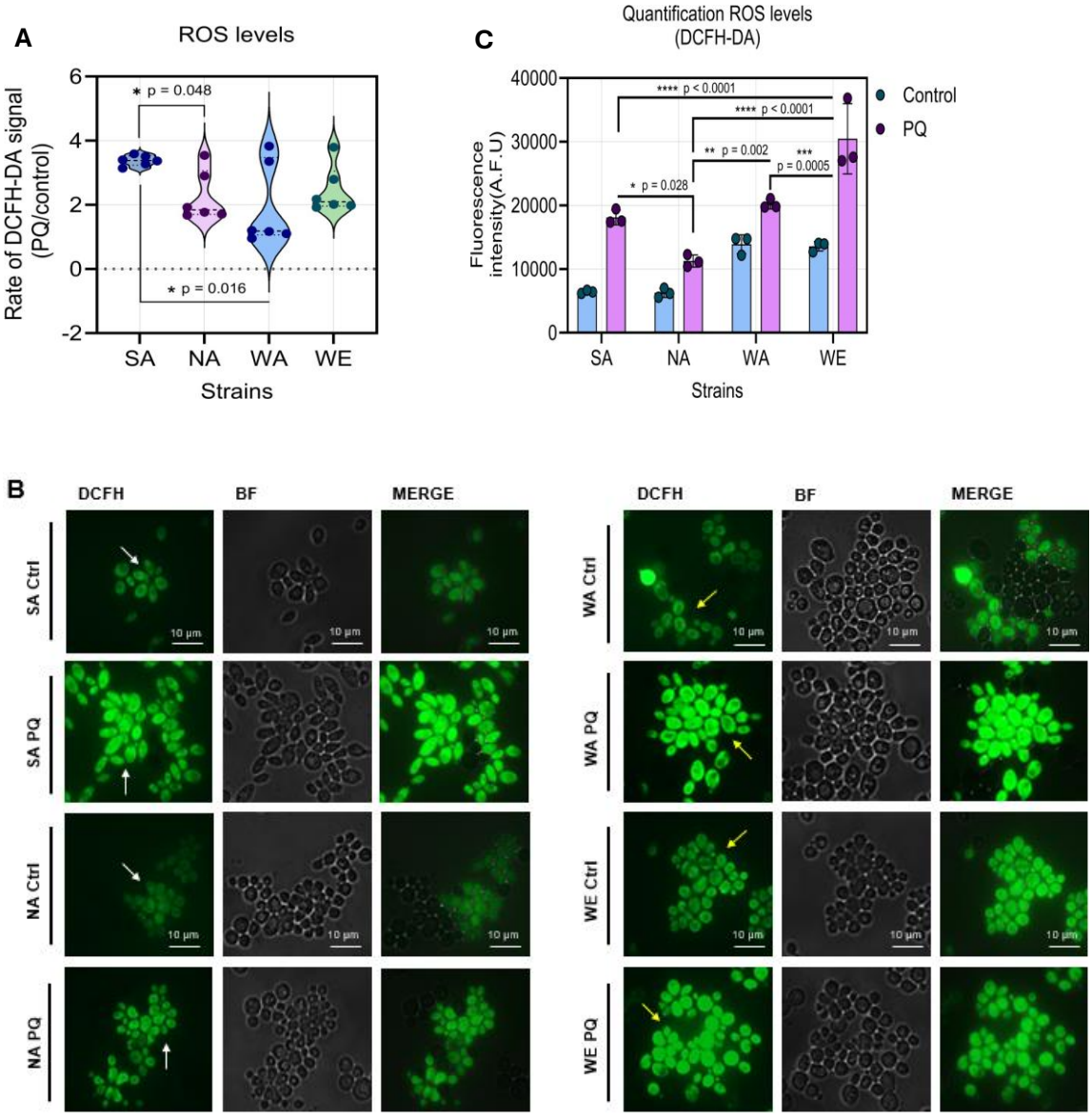
A
ROS levels
Rate of DCFH-DA signal (PQ/control)
* p = 0.048
* p = 0.016
SA
NA
WA
WE
Strains
C
Quantification ROS levels (DCFH-DA)
Fluorescence intensity(A.F.U)
**** p < 0.0001
**** p < 0.0001
** p = 0.002
*** p = 0.0005
* p = 0.028
Control
PQ
Strains
B
DCFH
BF
MERGE
SA Ctrl
SA PQ
NA Ctrl
NA PQ
WA Ctrl
WA PQ
WE Ctrl
WE PQ
10 µm

Figure 4.

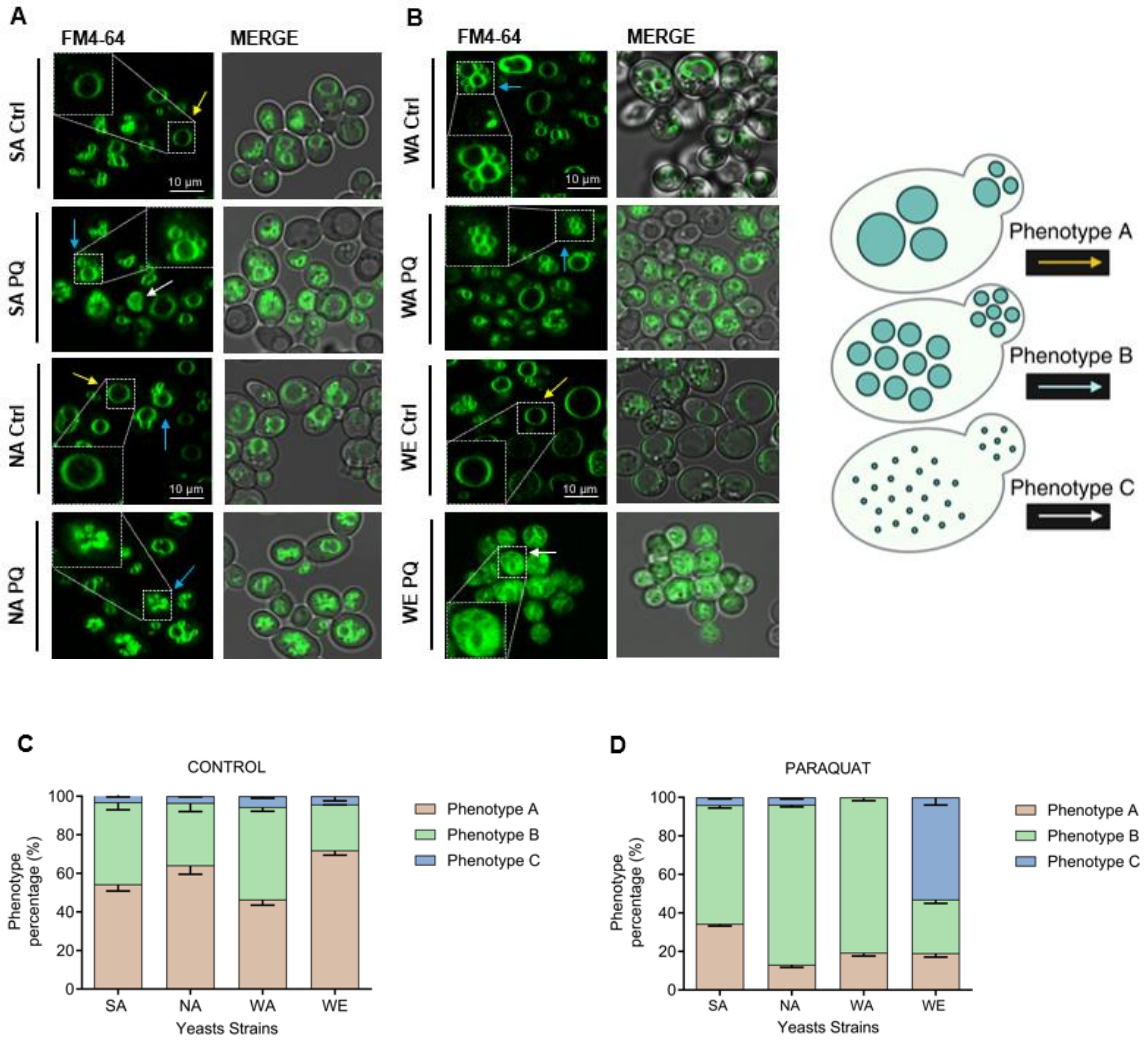
A
FM4-64
MERGE
SA Ctrl
SA PQ
NA Ctrl
NA PQ
10 µm
B
FM4-64
MERGE
WA Ctrl
WA PQ
WE Ctrl
WE PQ
10 µm
Phenotype A
Phenotype B
Phenotype C
C
CONTROL
Phenotype percentage (%)
100
80
60
40
20
0
SA
NA
WA
WE
Yeasts Strains
Phenotype A
Phenotype B
Phenotype C
D
PARAQUAT
Phenotype percentage (%)
100
80
60
40
20
0
SA
NA
WA
WE
Yeasts Strains
Phenotype A
Phenotype B
Phenotype C

Figure 5.

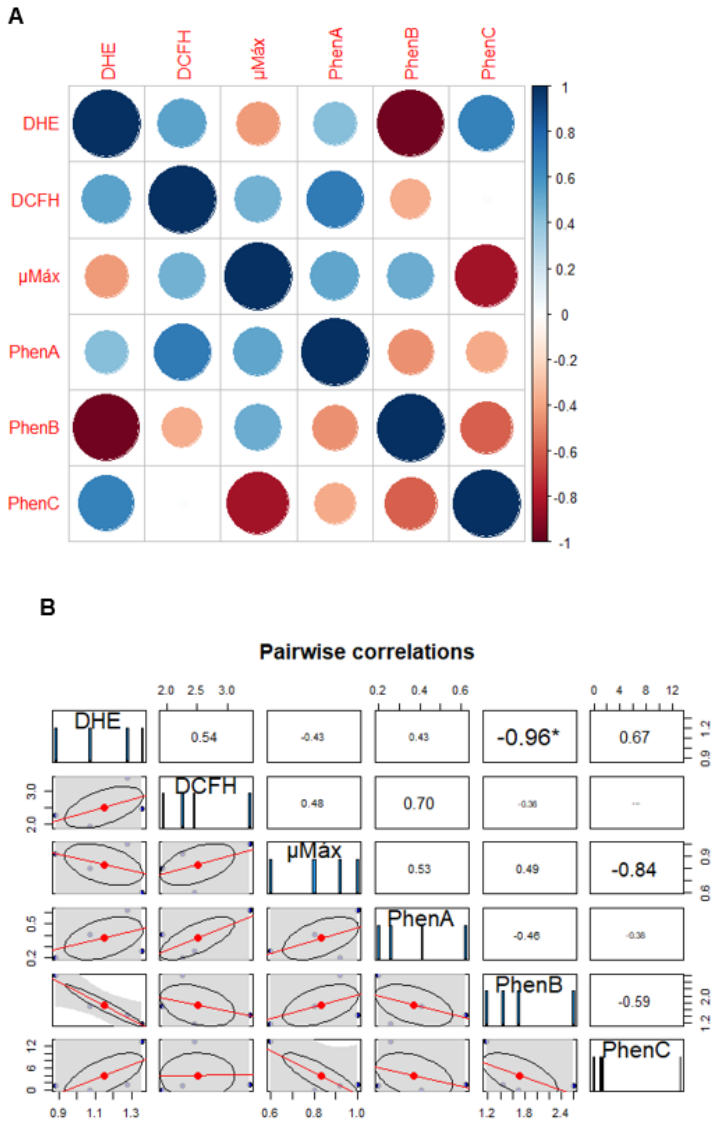
A
DHE
DCFH
µMáx
PhenA
PhenB
PhenC
1
0.8
0.6
0.4
0.2
0
-0.2
-0.4
-0.6
-0.8
-1
B
Pairwise correlations
0.54
-0.43
0.43
-0.96*
0.67
0.48
0.70
0.53
0.49
-0.84
-0.46
-0.59

Figure 6.

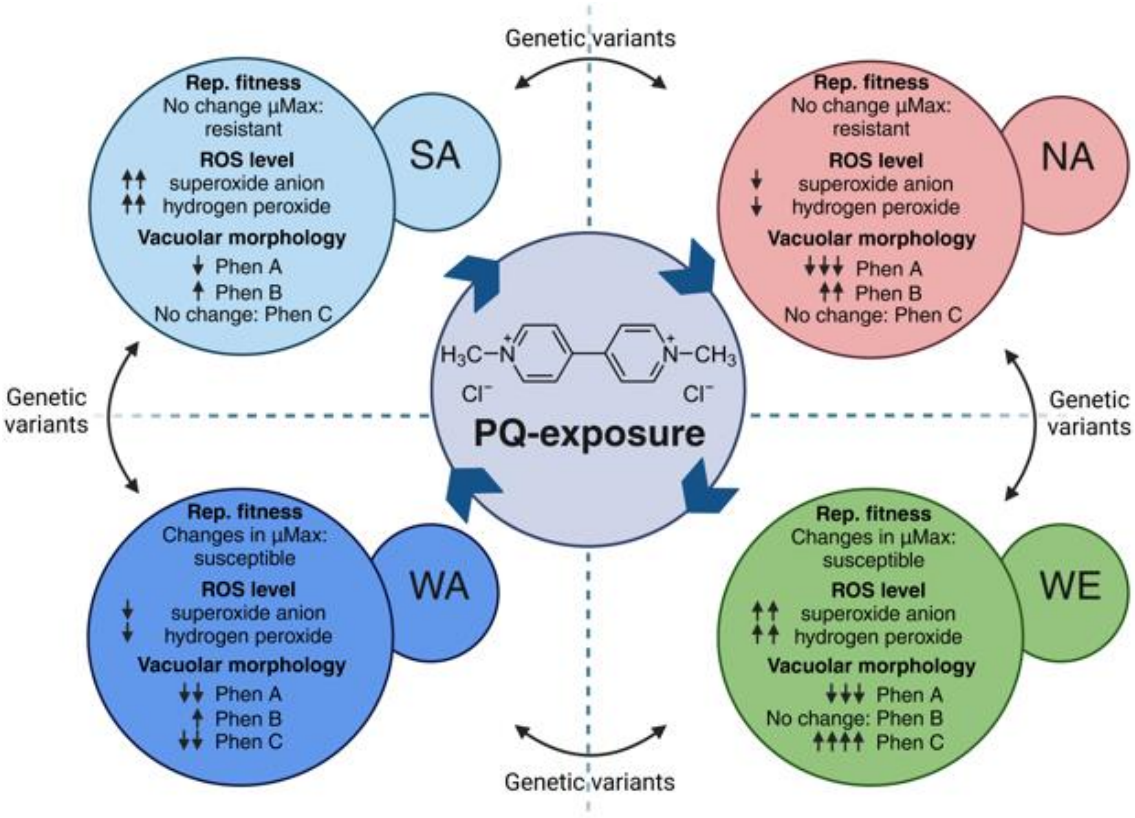
Genetic variants
Rep. fitness
No change µMax: resistant
ROS level
superoxide anion
hydrogen peroxide
Vacuolar morphology
Phen A
Phen B
No change: Phen C
SA
Rep. fitness
No change µMax: resistant
ROS level
superoxide anion
hydrogen peroxide
Vacuolar morphology
Phen A
Phen B
No change: Phen C
NA
Genetic variants
PQ-exposure
Genetic variants
Rep. fitness
Changes in µMax: susceptible
ROS level
superoxide anion
hydrogen peroxide
Vacuolar morphology
Phen A
Phen B
Phen C
WA
Rep. fitness
Changes in µMax: susceptible
ROS level
superoxide anion
hydrogen peroxide
Vacuolar morphology
Phen A
No change: Phen B
Phen C
WE
Genetic variants

Table 1.

	Vacuolar morphology percentage: no. cells ± sd (%)							
	SA control	NA control	WA control	WE control	SA PQ	NA PQ	WA PQ	WE PQ
Phenotype A	78 ± 1.53 (54)	99 ± 9.29 (64)	61 ± 4.73 (46)	100 ± 9.07 (72)	51 ± 4.36 (34)	19 ± 4.73 (13)	30 ± 3.05 (19)	22 ± 3.79 (19)
Phenotype B	63 ± 2.52 (43)	50 ± 9.16 (32)	63 ± 3.60 (48)	34 ± 1.53 (24)	93 ± 2.65 (62)	122 ± 7.81 (83)	130 ± 6.51 (81)	34 ± 4.04 (28)
Phenotype C	4 ± 1.73 (3)	6 ± 1.53 (4)	8 ± 2.52 (6)	6 ± 6.00 (4)	6 ± 1.53 (4)	6 ± 1.53 (4)	0	64 ± 4.73 (53)

Table 2.

		Number of variants				µMax			DHE			DCFH-DA			Phenotype B		
Human lysosomal genes	**Orthologue in *S. cerevisiae***	**SA**	**NA**	**WA**	**WE**	***P-value***	***P_{adj} a***	***r***	***P-value***	***P_{adj} a***	***r***	***P-value***	***P_{adj} a***	***r***	***P-value***	***P_{adj} a***	***r***
CLN3	YHC3	5	4	3	9	0.438	1.000	-0.562	0.489	1.000	0.511	0.690	1.000	0.310	**0.025**	0.300	**-0.975**
LIPA	YEH1	0	3	6	11	**0.020**	0.240	**-0.980**	0.745	1.000	-0.256	0.572	1.000	-0.428	0.368	1.000	-0.633
SLC17A1	DAL5	11	9	5	4	**0.019**	0.228	**0.980**	0.555	1.000	0.445	0.439	1.000	0.561	0.585	1.000	0.415
SLC17A1	THI73	3	4	4	0	0.346	1.000	0.654	0.522	1.000	-0.478	0.714	1.000	-0.286	**0.009**	0.108	**0.991**
SLC17A1	FEN2	6	7	8	1	0.398	1.000	0.601	0.528	1.000	-0.472	0.732	1.000	-0.268	**0.026**	0.312	**0.974**
ABHD5	ICT1	8	10	12	3	0.540	1.000	0.460	0.400	1.000	-0.600	0.593	1.000	-0.407	**0.032**	0.384	**0.968**
ATG5	ATG5	6	7	6	3	0.197	1.000	0.803	0.659	1.000	-0.341	0.835	1.000	-0.165	**0.048**	0.576	**0.952**
HSPA8	SSA2	32	27	27	31	0.965	1.000	0.035	**0.028**	0.336	**0.972**	0.088	1.000	0.912	0.255	1.000	-0.745
Human oxidative stress genes	**Orthologue in *S. cerevisiae***	**SA**	**NA**	**WA**	**WE**	***P-value***	***P_{adj} a***	***r***	***P-value***	***P_{adj} a***	***r***	***P-value***	***P_{adj} a***	***r***	***P-value***	***P_{adj} a***	***r***
CAT	CTT1	13	22	16	1	0.302	1.000	0.698	0.501	1.000	-0.499	0.655	1.000	-0.345	**0.030**	0.360	**0.970**
PRDX4	TSA1	1	0	0	2	0.528	1.000	-0.473	0.312	1.000	0.688	0.475	1.000	0.525	**0.010**	0.120	**-0.990**
COX11	COX11	2	3	4	0	0.595	1.000	0.405	0.357	1.000	-0.643	0.545	1.000	-0.455	**0.041**	0.492	**0.959**
		87	96	91	65	0.273	1.000	0.727	0.565	1.000	-0.436	0.744	1.000	-0.256	**0.018**	0.216	**0.982**
Paraquat: µMáx (OD/h)		**0.257**	**0.238**	**0.180**	**0.142**												
Paraquat: DHE (A.F.U)		**8214**	**5644**	**5258**	**7039**												
Paraquat: DCFH-DA (A.F. U)		**29473**	**10410**	**9663**	**17217**												
Paraquat: Phenotype B (%)		**61.67**	**83.07**	**80.60**	**27.80**												

Supplementary Figure 1.

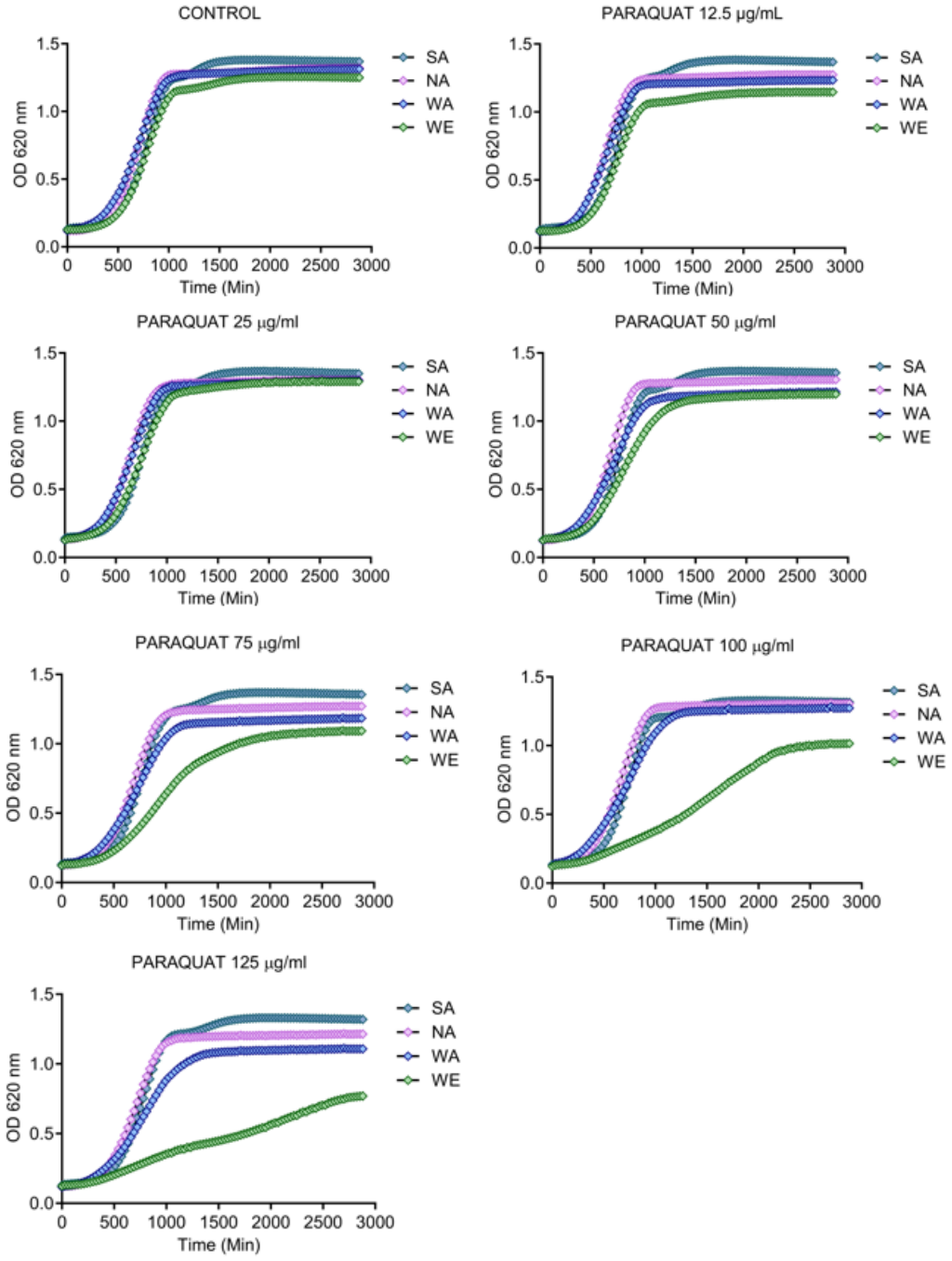

Supplementary Figure 2.

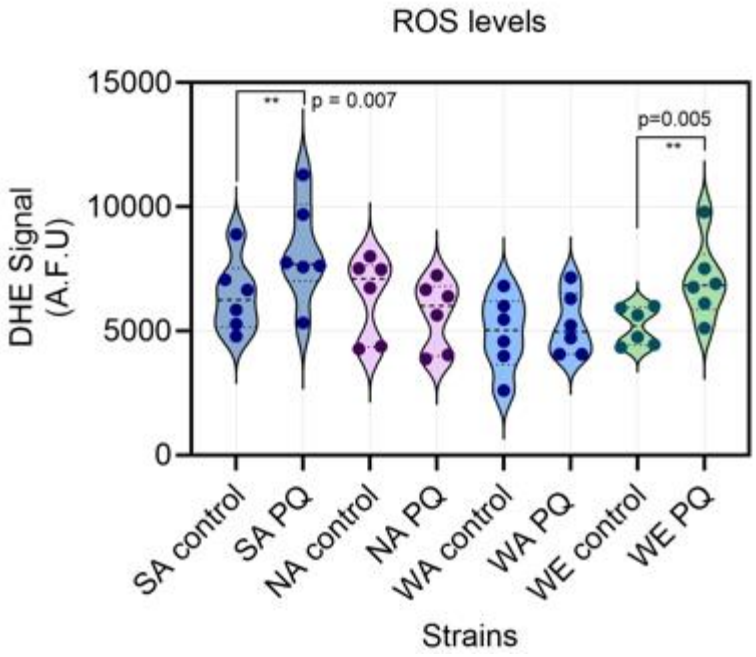

Supplementary Figure 3.

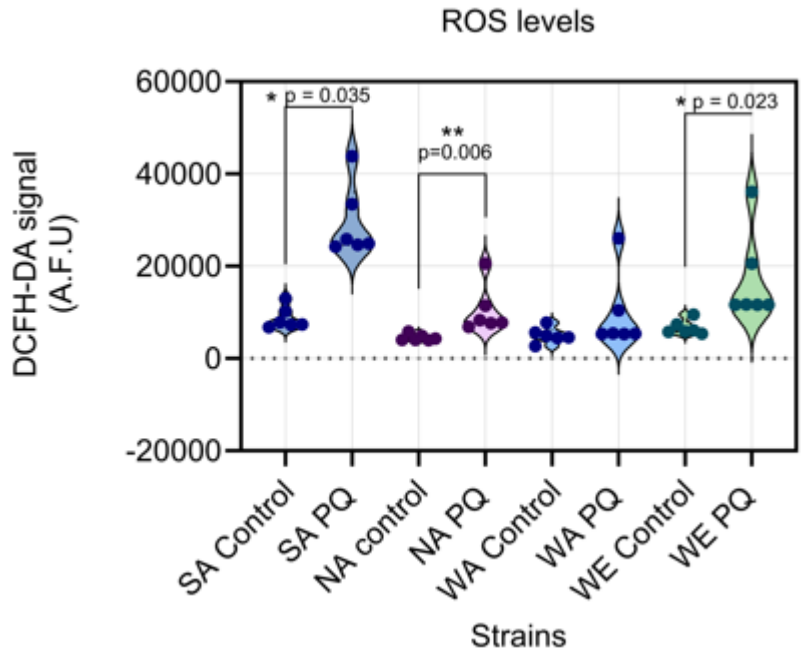

Supplementary Table 1.

Correlations between phenotypes			
	Method	*r*	*P*-value
DHE probe - DCFH probe	Pearson	0.537	0.463
DHE probe - Phenotype A	Pearson	0.429	0.571
DHE probe - Phenotype B	Pearson	-0.962	0.038
DHE probe - Phenotype C	Spearman	0.800	0.200
DHE probe - µMáx	Pearson	-0.426	0.574
DCFH probe - Phenotype A	Pearson	0.700	0.299
DCFH probe - Phenotype B	Pearson	-0.364	0.636
DCFH probe - Phenotype C	Pearson	0.800	0.200
DCFH probe - µMáx	Pearson	0.479	0.521
Phenotype A - Phenotype B	Pearson	-0.459	0.541
Phenotype A - Phenotype C	Spearman	0.000	1.000
Phenotype A - µMáx	Pearson	0.525	0.475
Phenotype B - Phenotype C	Spearman	-0.800	0.200
Phenotype B - µMáx	Pearson	0.491	0.508
Phenotype C - µMáx	Spearman	-0.200	0.800

5. **Chapter 2**: To identify modifier genes responsible for differences in susceptibility/resistance to paraquat in genetically diverse strains of *Saccharomyces cerevisiae* through GWAS and QTL mapping.

6. EXPERIMENTAL PROCEDURES: Chapter 2

6.1. Yeast strains and culture conditions

The four haploid (*MAT α* and *MAT a*) *S. cerevisiae* strains used in this study were: North American (NA; YPS128, *MAT α/a, ho: HygMX, ura3::kanMX*), West African (WA; DBVPG6044, *MAT α/a, ho: HygMX, ura3::kanMX*), Sake (SA; Y12, *MAT α/a, ho: HygMX, ura3::kanMX*) and Wine/European (WE; DBVPG6765, *MAT α/a, ho: HygMX, ura3::kanMX*) (Brice et al., 2018; Salinas et al., 2016).

The segregating strains used were provided by Professor Francisco Cubillos previously generated, through crosses between four haploid strains with opposite mating types (*MAT α* and *MAT a*) in YPD media (Cubillos et al., 2009). 96 segregants were obtained from the SA x WE cross. All segregants were SNP-genotyped for the same 171 markers placed every approximately 70 kb (genotyping covers 88.9% of the genome using the S288c strain as reference). The only region of the genome not covered was the subtelomeric containing the repetitive multicopy gene families (Cubillos et al., 2011).

The 1,011 *S. cerevisiae* isolates used in this study and their corresponding genome sequences were described previously (Peter et al., 2018). These strains were stored in solid media (YPD) at 4°C. Liquid and solid culture media were used depending on the experiments to be performed: YPD media (2% glucose, 2% peptone, 1% yeast extract) and YNB (0.67% YNB base without amino acids, 0.2% uracil, 0.0875% com drop out and 2% glucose).

6.2. Growth curves conditions: phenotyping

Yeast cells were pre-cultured in 200 µL of YNB medium supplemented with uracil (0.2% uracil) for 48 h at 28 °C. For the experimental run, the four yeast strains were inoculated to an optical density (OD) of 0.03-0.1 (wavelength of 620 nm) in 200 µL of medium and incubated without shaking at 28 °C for 48 h in different conditions, i) control (YNB media, 2% glucose) and PQ (Sigma Aldrich-Merck, CAS No. 75365-73-0) at 75 µg/mL (dissolved in distilled water) for the phenotyping of 1,011 isolates; ii) control (YNB media, 2% glucose), PQ 200 µg/mL, nicotinamide riboside chloride (NR), dissolved in distilled water (Cayman Chemicals, CAS No. 23111-00-4) at 20 µM and co-treatment PQ 200 µg/mL and NR 20 µM for the validation assays in a Tecan Sunrise absorbance microplate reader (Tecan Trading AG, Männedorf, Switzerland). OD was measured every 30 min using a 620 nm filter. Each experiment was performed in triplicate. Growth rates for each strain were calculated as previously described (García-Ríos et al., 2014; Quispe et al., 2017). Briefly, OD measurements as a function of time were

fitted to the mathematical model of the re-parameterized Gompertz sigmoid curve describing microbiological temporal growth, previously proposed (Zwietering et al., 1990) from which growth rates were obtained. The parameters of each curve were processed in the GrowthRates software to obtain OD max, μmax, and the average time of the lag phase.

6.3. Genome-wide association study (GWAS) analysis

6.3.1. Genotype files

We conducted mixed-model association analysis using FaST-LMM v.2.07 software (Lippert et al., 2011; Peter et al., 2018). We converted the VCF (Variant Call Format) file to MAP and BED formats using PLINK to prepare the data. Binary genotype files were then transformed into ASCII plain text files. The resulting files were ".map" and ".ped". The ".map" file is a tab-separated matrix containing all SNPs. The ".ped" file contains individual genotypes coded as 0 (NA), 1 (first allele), and 2 (second allele). Rows represent individuals, and columns represent variants (in the same order as the ".map" file). Each variant has two columns due to the diploid nature of yeast. The PLINK command used for the VCF conversion was: *plink --vcf ALLECOLIBAM/ECOLI20200319.rehead.vcf --maf 0.05 --geno 0.1 --recode12 --allow-extra-chr --noweb --list-duplicate-vars suppress-first --double-id --out ECOLI20200319.maf0.05.geno0.1.r12.*

6.3.2. Phenotype files

The raw phenotype file, containing µMax measurements for 1,011 isolates in three biological replicates, was organized as a three-column file with “sample ID”, “family ID”, and “phenotype value”. The phenotype value was calculated for the control condition, PQ treatment, and fold change (PQ/control), depending on the specific analysis. The sample ID and family ID were identical and matched those in the genotype data. To normalize the phenotype values, we applied a quantile transformation using the *qqnorm* function in Rstudio v4.3.1. This transformation orders the values into a normal distribution ranging from -3 to 3. Any NA values were replaced with -9 in the final file.

6.3.3. Running a GWAS

We selected genetic markers with a minor allele frequency (MAF) greater than 5% and excluded variants with missing genotypes labeled as "fs." We decided to apply an arbitrary threshold and remove variants present in fewer than 1,000 individuals. The GWAS analysis was conducted using the following command: *fastlmmc -file Genotype_filename -maxThreads 22 -pheno pehnotype_filename -mpheno 1 -fileSim Genotype_filename -verboseOutput -out GWAS_output_filename.out > GWAS_output_filename.err.* To estimate the trait-specific *P*-value threshold, we conducted 100 permutations of the phenotypic values between individuals. The command to go over 100 files was: *for f in*

{1..100};do echo "fastlmmc -file Genotype_filename -maxThreads 22 -pheno shuffled_phenotypes_filename_"$f".txt -mpheno 1 -fileSim Genotype_filename -verboseOutput -out Shuffled_GWAS_output_"$f".out 2> Shuffled_"$f".err">> autoindex_shuffled.sh;done. In addition, we used a 5% family-wise error rate (FWER) threshold, determined by the 5% quantile (the 5th lowest *P*-value from the permutations). The commands used were: i) *for i in shuffled_phenotypes_filename_*.out;do head -2 $i | tail -1 >> phenotype.heads ;done* ii) *awk '{print $6}' phenotype.heads | sort | head -6 | tail -1 >> file.out*. Finally, to quantify the extent of volume inflation and excessive false positive rate (FDR), we calculated the genomic inflation factor, λ, for each condition in Rstudio v4.3.1. We used Rstudio v.4.3.1 with the *qqnorm* package to create a Q-Q plot, visualizing the correlation between a given sample and the normal distribution. Additionally, we employed the *qqman* package to generate a Manhattan plot.

6.4. Quantitative trait loci (QTL) mapping

QTL mapping was performed with R/qtl software where LOD scores were calculated using a nonparametric model (Cubillos et al., 2011). The significance of a QTL was determined from permutations. For each phenotypic trait (μMax) and cross (SA x WE), we permuted the phenotype values within the intervals 1000 times, recording the maximum LOD score each time. A significant QTL is recognized when the LOD score is greater than the 0.05 tail of the 1000 LOD scores obtained. The phenotypic variance score explained for a QTL is calculated

using Formula 1, where 'n' represents the sample size. Formula 1: Percentage of variance explained = 100(1–10(−2LOD/n)) (Cubillos et al., 2011).

6.5. Analysis and selection of candidate modifier genes

6.5.1. QTL mapping.

To identify and prioritize candidate modifier genes, all genomic regions located 40 kb upstream and downstream of the markers identified in the QTL mapping peaks were analyzed. The selection of these genes was based on the following criteria: i) matching with results from GWAS; ii) presence of human orthologs in databases such as Alliance of Genome Resources and Saccharomyces Genome Database; and iii) association with NAD+, mitochondrial or lysosomal metabolism. In addition, the SIFT software was used to identify non-synonymous variants in these genes, comparing the sequences of the four strains (SA, NA, WA, and WE) with the reference genome S288C (https://www.yeastgenome.org/). The number of variants in *NRT1* and *YOR072W* genes was correlated with μMax.

6.5.2. GWAS analysis

We identified variants that crossed the significance threshold. We were able to locate these variants within the reference genome (https://www.yeastgenome.org/) and determine their location relative to genes (genic or intergenic). Notably, most variants associated with the trait (μMax) were

found to be genic regions. Once these candidate genes were obtained, we prioritized them based on: i) their association with NAD+ metabolism and ii) their known biological functions.

7. RESULTS: Chapter 2

7.1. Phenotypic diversity in specific growth rates (μMax) between species

1,011 isolates of *S. cerevisiae* strains were selected for this thesis (Peter et al., 2018). These strains were isolated from diverse geographical locations and were chosen for their extensive genomic variability. They belong to distinct clades and dispersed across different branches of the phylogenetic tree (Figure 1).

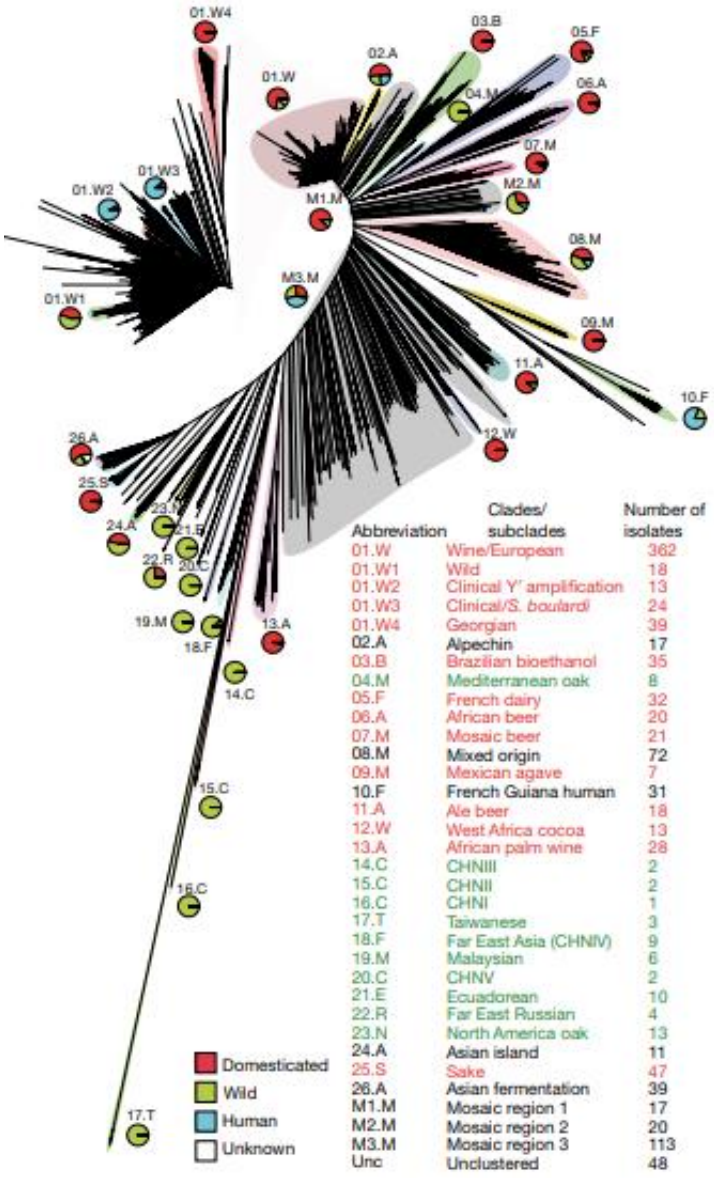

Abbreviation	Clades/ subclades	Number of isolates
01.W	Wine/European	362
01.W1	Wild	18
01.W2	Clinical Y' amplification	13
01.W3	Clinical/*S. boulardi*	24
01.W4	Georgian	39
02.A	Alpechin	17
03.B	Brazilian bioethanol	35
04.M	Mediterranean oak	8
05.F	French dairy	32
06.A	African beer	20
07.M	Mosaic beer	21
08.M	Mixed origin	72
09.M	Mexican agave	7
10.F	French Guiana human	31
11.A	Ale beer	18
12.W	West Africa cocoa	13
13.A	African palm wine	28
14.C	CHNIII	2
15.C	CHNII	2
16.C	CHNI	1
17.T	Taiwanese	3
18.F	Far East Asia (CHNIV)	9
19.M	Malaysian	6
20.C	CHNV	2
21.E	Ecuadorean	10
22.R	Far East Russian	4
23.N	North America oak	13
24.A	Asian island	11
25.S	Sake	47
26.A	Asian fermentation	39
M1.M	Mosaic region 1	17
M2.M	Mosaic region 2	20
M3.M	Mosaic region 3	113
Unc	Unclustered	48

Figure 1. Neighbor-joining tree constructed with the biallelic SNPs. Twenty-six clades and three mosaic groups (M1 to M3) were identified. Colors represent the ecological origins of the clade: domesticated (red), wild (green), and human (cyan). Figure obtained from Peter. J., et al. 2018 (Peter et al., 2018).

To analyze the phenotypic diversity of the 1,011 isolates of *S. cerevisiae*, we evaluated the distribution of their specific growth rates (μMax) through scatter and frequency plots. Under control conditions, our results show that the majority of isolates (55%) exhibit μMax between 0.28 and 0.30 OD/h. In contrast, only 2% of the isolates showed very low μMax, between 0.08 and 0.18 OD/h (Figure 2A). These data suggest a wide variability in growth rate among the different *S. cerevisiae* isolates. For PQ exposure (75 μg/mL), we found that 49% of the isolates show a μMax between 0.28 and 0.30 and 8% between 0.04 and 0.18 (Figure 2B), indicating that a higher proportion of the isolates are susceptible to PQ. However, we found 29 strains (5%) with μMax between 0.32 and 0.34, being resistant to PQ (Figure 2B). Finally, we calculated the fold change and observed that 446 isolates (74%) exhibited no change against PQ exposure, while 124 of them (25%) showed a decrease in growth in PQ treatment. Surprisingly, we found that 6 of the isolates (1%) showed an increased growth rate against PQ (Figure 2C).

A

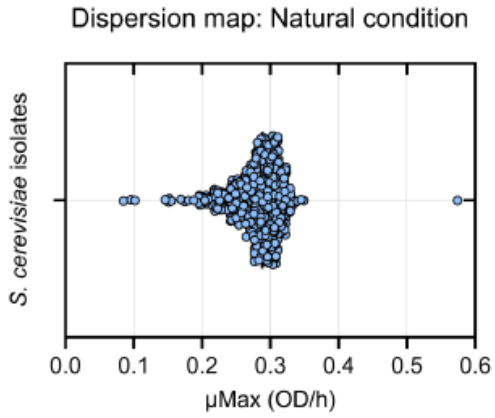
Dispersion map: Natural condition
S. cerevisiae isolates
0.0 0.1 0.2 0.3 0.4 0.5 0.6
µMax (OD/h)

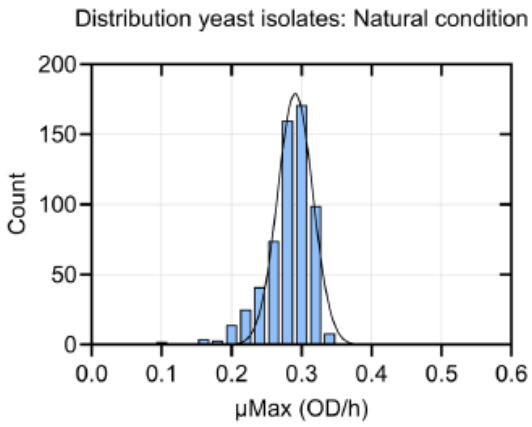
Distribution yeast isolates: Natural condition
Count
0 50 100 150 200
0.0 0.1 0.2 0.3 0.4 0.5 0.6
µMax (OD/h)

B

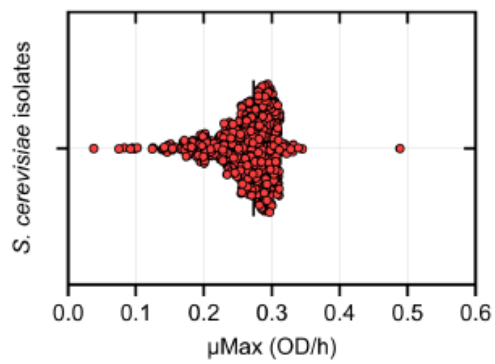
Dispersion map: Paraquat
S. cerevisiae isolates
0.0 0.1 0.2 0.3 0.4 0.5 0.6
µMax (OD/h)

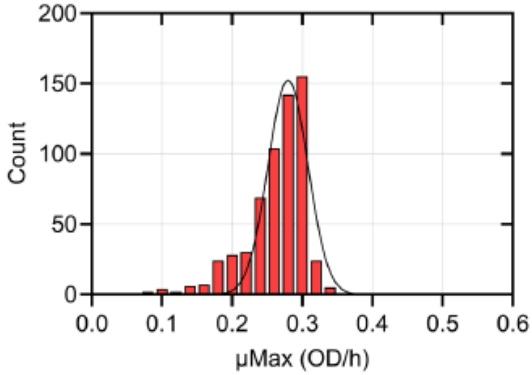
Distribution yeast isolates: Paraquat
Count
0 50 100 150 200
0.0 0.1 0.2 0.3 0.4 0.5 0.6
µMax (OD/h)

C

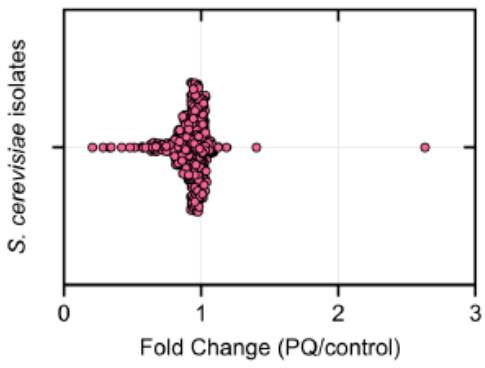
Dispersion map: Fold Change
S. cerevisiae isolates
0 1 2 3
Fold Change (PQ/control)

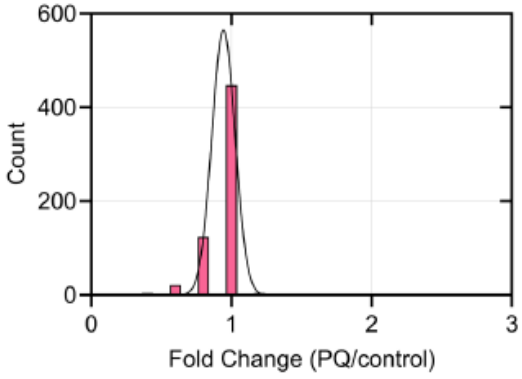
Distribution yeast isolates: Fold Change
Count
0 200 400 600
0 1 2 3
Fold Change (PQ/control)

Figure 2. Characterization and distribution of Saccharomyces cerevisiae isolates in natural environments, PQ exposure, and fold change (PQ/control) according to their growth parameters. (A) Dispersion map using µMax as a growth parameter in control (left) and Distribution of the yeast isolates according to their µMax in the control condition (right) (B) Dispersion map using µMax as a growth parameter in PQ treatment (left) and Distribution of the yeast isolates according to their µMax in PQ treatment (right). (C) Dispersion map using µMax as a growth parameter in fold change (left) and Distribution of the yeast isolates according to their µMax in fold change (right). N sample = 603 isolates of S. cerevisiae. Non-linear Histogram function in µMax using GraphPad. Statistical analysis was performed and plotted in GraphPad.

7.2. Association analysis between SNPs and µMax in isolates.

We used PLINK to filter SNPs with low allele frequency (MAF < 5%) and create the input files for FaST-LMM. We used FaST-LMM software to fit the mixed models in GWAS, allowing us to control for population structure. The final data used for the GWAS studies contained 101,635 SNPs genotyped in 603 *S. cerevisiae* isolates. We tested the 101,635 SNPs for associations with the phenotype data, which contained the µMax data from the 603 diploid isolates. To maintain population structure and accurately identify genetic associations, GWAS analyses were restricted to diploid isolates.

We generated Manhattan plots for the control condition, which is the natural variability, PQ exposure (to see the effect) and Fold change (PQ/control), to see the gene-environment interaction (Figure 3A, B and C, respectively). Under control conditions, we identified seven SNPs that were significantly associated with the phenotype analyzed ($-\log_{10}$(*P*-value*)* >5) (Figure 3A). These variants surpassed the permutation-based significance threshold, demonstrating strong associations (*P*-value = 1.17×10^{-5}). The significance threshold was determined by permuting phenotypic values 100 times, creating a null distribution. The 5th percentile of this null distribution served as the threshold, controlling the family-wise error rate (FWER) at 5%, thus minimizing false positives. In addition, we found one SNP that surpassed an even more stringent threshold, with a $-\log_{10}$(*P*-value*)* >8. This indicates a very strong association (Figure 3A). After identifying the positions of these variants, we mapped them to the reference genome (https://www.yeastgenome.org/). This revealed that some variants resided within gene regions, while others were located upstream or downstream of genes (Table 1).

In PQ exposure, we identified six SNPs that surpassed the permutation-based significance threshold, demonstrating strong associations (*P*-value = 1.08×10^{-5}). These variants allowed us to map associated genes (Figure 3B and Table 2). In our association analysis using fold change (PQ/control), we identified four SNPs on chromosome 15 that exceeded the significance threshold (*P*-value = 1.13×10^{-5}). Two of these variants were located near the *YOR072W* gene (sv86664 =107

bp and sv86663 =91 bp upstream, respectively), while the others were within the *NRT1* gene (Figure 3C and Table 3). Among the candidate genes identified, *NRT1* stood out as a particularly interesting one. It is a high-affinity nicotinamide riboside (NR) transporter associated with rescuing Parkinson's phenotypes in flies (P. A. Belenky et al., 2008; Schöndorf et al., 2018).

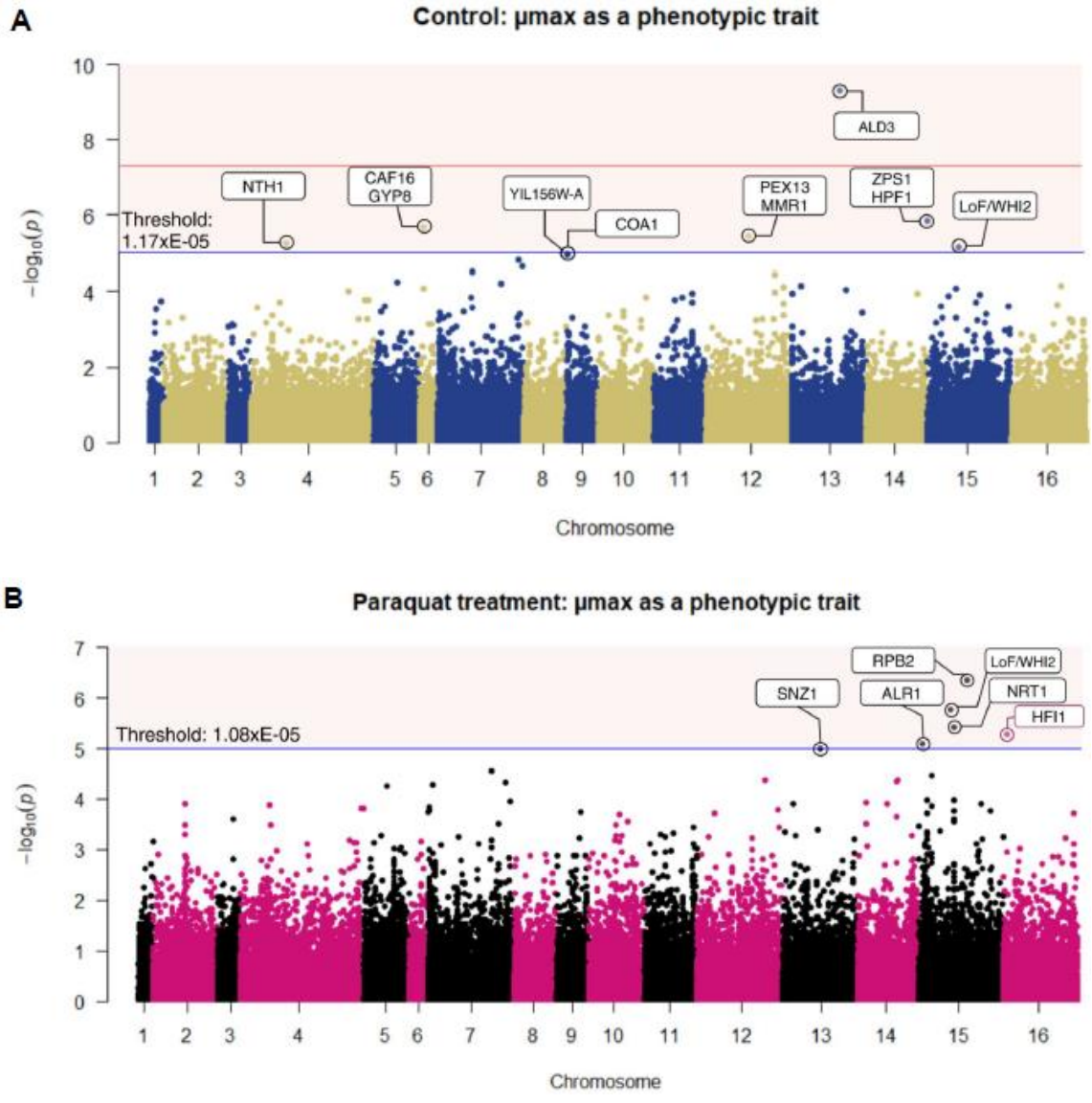

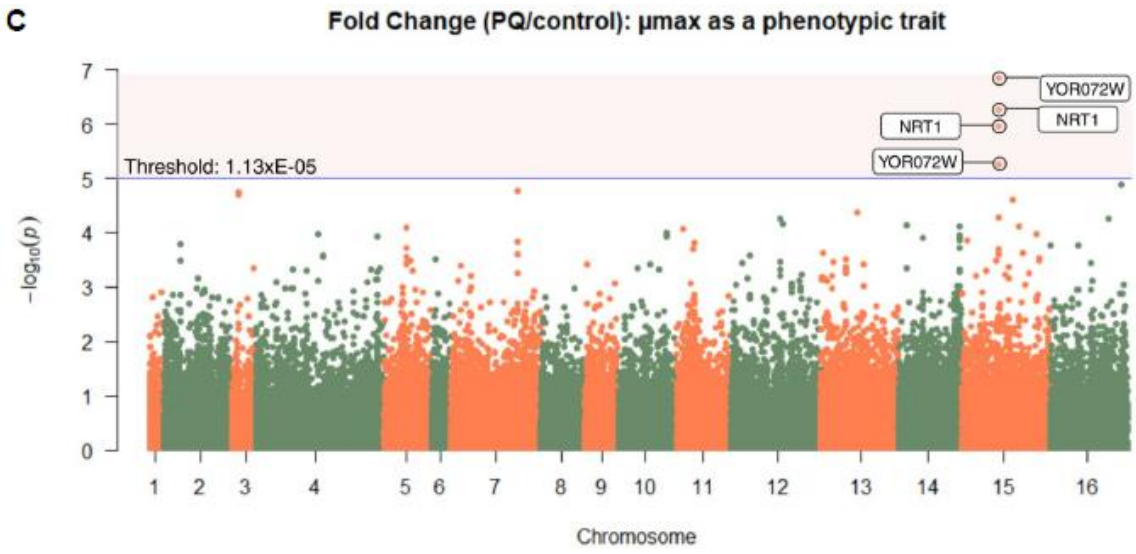

Figure 3. Genome-wide association studies (GWAS) in a collection of S. cerevisiae in PQ treatment through growth parameters. (A) Manhattan plot with significant SNVs and markers identified using GWAS with a threshold of 1.17x10E-5 using µMax as a phenotypic trait. These markers were found in a biological sample of 3 (603 isolates analyzed). (B) Manhattan plot with significant SNVs and markers identified using GWAS with a threshold of 1.08x10E-5 using µMax as a phenotypic trait. These markers were found in a biological sample of 3 (603 isolates analyzed) (C) Manhattan plot with significant SNVs and markers identified using GWAS with a threshold of 1.08x10E-5 using µMax as a phenotypic trait. These markers were found in a biological sample of 3 (603 isolates analyzed). Mixed-model association analysis was performed using FaST-LMM v.2.07 and we used the markers showing a minor allele frequency (MAF) >5%.

We estimated a trait-specific *P*-value threshold for each condition by permuting phenotypic values between individuals 100 times. The significance threshold was the 5% quantile (the 5th lowest *P*-value from the permutations). N sample: 603 isolates. Plotted in Rstudio v4.3.1.

Table 1. List of genes found across GWAS μMax variants in the control condition

Control Condition								
Variant	**Position**	**Chromosome**	**p-value**	**Gene**	**Human orthologue**	**Gene position**	**Length**	**Function**
PA560	599352 - 600872	13	4.80E-10	*ALD3*	*ALDH1L1*	599352 - 600872	1,521 bp	Cytoplasmic aldehyde dehydrogenase; involved in beta-alanine synthesis; uses NAD+ as the preferred coenzyme; expression is induced by stress and repressed by glucose.
				ZPS1	-	34658 - 35407	750 bp	Putative GPI-anchored protein; transcription is induced under low-zinc conditions, as mediated by the Zap1p transcription factor, and at alkaline pH.
sv82553	33671	15	2.10E-05	*HPF1*	-	28703 - 31606	2,904 bp	Haze-protective mannoprotein; reduces particle size of aggregated proteins in white wines, thereby decreasing turbidity; intragenic repeat expansion controls chronological aging; expansion of intragenic tandem repeats within N-terminus sufficient to cause pronounced life span shortening.
				CAF16	-	79344 - 80213	870 bp	Part of evolutionarily-conserved CCR4-NOT regulatory complex; contains single ABC-type ATPase domain but no transmembrane domain.
sv28182	80290	6	2.15E-06	*GYP8*	*TBC1D20*	80419 - 81912	1,494 bp	GTPase-activating protein for yeast Rab family members; Ypt1p is the preferred in vitro substrate but also acts on Sec4p, Ypt31p and Ypt32p; involved in the regulation of ER to Golgi vesicle transport.
				PEX13	*PEX13*	537272 - 538432	1,161 bp	Peroxisomal importomer complex component; integral peroxisomal membrane protein required for docking and translocation of peroxisomal matrix proteins.
sv63320	537230	12	3.58E-06	*MMR1*	-	535214 - 536689	1,476 bp	Phosphorylated protein of the mitochondrial outer membrane; localizes only to mitochondria of the bud; interacts with Myo2p to mediate mitochondrial distribution to buds.
sv14394	451706	4	5.57E-06	*NTH1*	*TREH*	450220 - 452475	2,256 bp	Neutral trehalase, degrades trehalose; required for thermotolerance and may mediate resistance to other cellular stresses.
LoF_WHI2	410870 - 412330	15	6.88E-06	*WHI2*	*GPATCH1*	410870 - 412330	1,461 bp	Negative regulator of TORC1 in response to limiting leucine; suppresses TORC1 activity with binding partners Psr1p/Psr2p, acting in parallel with SEACIT; regulates cell cycle arrest in stationary phase; inhibits Ras-cAMP-PKA regulation of apoptosis during nutrient depletion.
LoF_YIL156	47292 - 47693	9	1.06E-05	*YIL156W-A*	-	47292 - 47693	402 bp	Dubious open reading frame; unlikely to encode a functional protein, based on available experimental and comparative sequence data; overlaps ORF COA1/YIL157C
sv43415	47525	9	1.11E-05	*COA1*	-	46949 - 47542	594 bp	Mitochondrial inner membrane protein; required for assembly of the cytochrome c oxidase complex (complex IV); interacts with complex IV assembly factor Shy1p during the early stages of assembly

Table 2. List of genes found across GWAS µMax variants in PQ-exposure

Paraquat								
Variant	**Position**	**Chromosome**	**p-value**	**Gene**	**Human orthologue**	**Gene position**	**Length**	**Function**
sv88076	614674	15	4.36E-07	*RPB2*	*POLR2B*	612997 - 616671	3,675 bp	RNA polymerase II second largest subunit B150; part of central core; similar to bacterial beta subunit
LoF_WHI2	410870 - 412330	15	6.88E-06	*WHI2*	*GPATCH1*	410870 - 412330	1,461 bp	Negative regulator of TORC1 in response to limiting leucine; suppresses TORC1 activity with binding partners Psr1p/Psr2p, acting in parallel with SEACIT; regulates cell cycle arrest in stationary phase; inhibits Ras-cAMP-PKA regulation of apoptosis during nutrient depletion.
sv86657	461014	15	3.86E-06	*NRT1*	-	459480 - 461276	1,797 bp	High-affinity nicotinamide riboside transporter; also transports thiamine with low affinity; major transporter for 5-aminoimidazole-4-carboxamide-1-beta-D-ribofuranoside (acadesine) uptake.
sv92382	69892	16	5.38E-06	*HFI1*	*TADA1*	69485 - 70951	1,467 bp	Adaptor protein required for structural integrity of the SAGA complex; a histone acetyltransferase-coactivator complex that is involved in global regulation of gene expression through acetylation and transcription functions
sv82926	75860	15	8.12E-06	*ALR1*	-	74400 - 76979	2,580 bp	Plasma membrane Mg(2+) transporter; expression and turnover are regulated by Mg(2+) concentration; overexpression confers increased tolerance to Al(3+) and Ga(3+) ions.
sv71799	458866	13	1.02E-05	*SNZ1*	-	458408 - 459301	894 bp	Subunit of a two-component pyridoxal-5'-phosphate synthase; involved in pyridoxine (vitamin B6) biosynthesis from glyceraldehyde-3-phosphate, ribose-5-phosphate and ammonia liberated from glutamine by glutaminase.

Table 3. List of genes found across GWAS μMax variants in Fold change

Fold Change								
Variant	**Position**	**Chromosome**	**p-value**	**Gene**	**Human orthologue**	**Gene position**	**Length**	**Function**
sv86664	461411	15	1.43E-07	*YOR072W*	-	461502 - 461816	315 bp	Putative protein of unknown function; conserved across S. cerevisiae strains; partially overlaps the dubious gene YOR072W-A; diploid deletion strains are methotrexate, paraquat and wortmannin sensitive
sv86663	461395	15	5.61E-06	*YOR072W*	-	461502 - 461816	315 bp	
sv86656	460871	15	5.50E-07	*NRT1*	-	459480 - 461276	1,797 bp	High-affinity nicotinamide riboside transporter; also transports thiamine with low affinity; major transporter for 5-aminoimidazole-4-carboxamide-1-beta-D-ribofuranoside (acadesine) uptake.
sv86657	461014	15	1.11E-06	*NRT1*	-	459480 - 461276	1,797 bp	

7.3. Quantitative growth variation in PQ-exposure

Our preliminary results revealed differential responses to PQ exposure among four parental strains (Supplementary Figure 1). The SA strain exhibited resistance in PQ exposure without impacting its µMax. Conversely, the WE strain showed susceptibility, decreasing its reproductive fitness upon PQ exposure. To study the phenotypic diversity of the segregants, we exposed the cross SA x WE to PQ (75 µg/mL) to measure the phenotypic changes as a quantitative trait. We conducted growth curve analyses on the 96 segregant strains under both control conditions (to assess natural variability) and PQ exposure. In addition, the resulting fold change values were calculated. We extracted the µMax from these data and used it as a phenotypic trait for subsequent QTL mapping analysis.

In both control and PQ exposure conditions, the SA x WE cross yielded few transgressive segregants. Under control conditions, only four strains (4.16%) exhibited positive transgressive behavior, exceeding the parental growth rates by at least two standard deviations (Figure 4A). When exposed to PQ, we identified two positive transgressive strains (2.08%) and one negative transgressor (1.04%) (Figure 4B). These findings might be attributed to epistatic interactions or the limited genetic variability associated with using one resistant and one susceptible parental strain in PQ-response. Although we analyzed the distribution based on fold change, no significant differences were observed in phenotypic changes (Figure 4C).

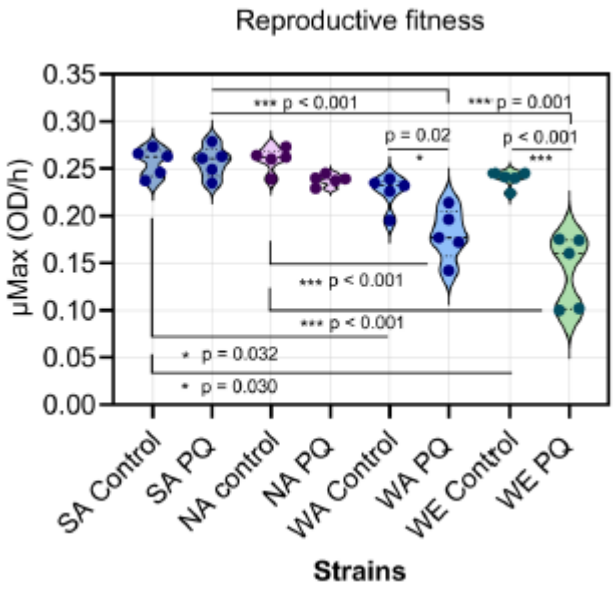

Supplementary Figure 1. Reproductive fitness in S. cerevisiae parental strains against PQ exposure. Calculation of μMax in the four strains under control conditions and PQ treated (75 μg/mL). N= 5, Shapiro Wilk normality test *P*-value > 0.05, Kruskal Wallis test *P*-value <0.05 (control and fold change). ANOVA test *P*-value < 0.05, post-hoc Tukey (AUC and PQ). *P*-value ≤ 0.05 (*), *P*-value < 0.01 (**), *P*-value < 0.001 (***), *P*-value < 0.0001 (****), ns = not significant (*P*-value > 0.05). Statistical analysis was performed in SPSS software version 20.0 and plotted in GraphPad.

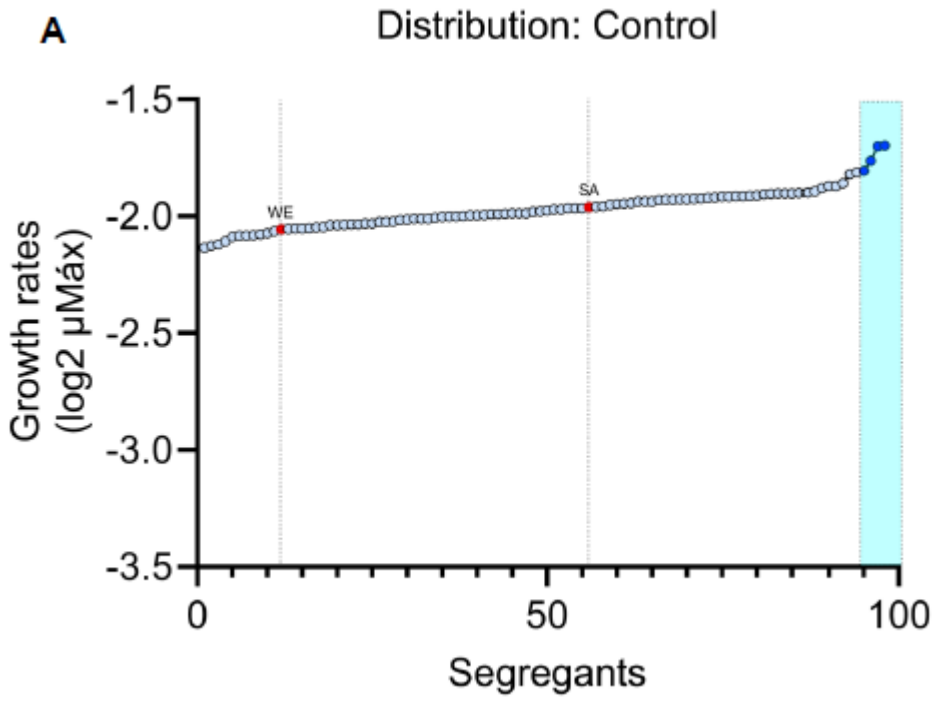
A
Distribution: Control
Growth rates (log2 µMáx)
-1.5
-2.0
-2.5
-3.0
-3.5
WE
SA
0
50
100
Segregants

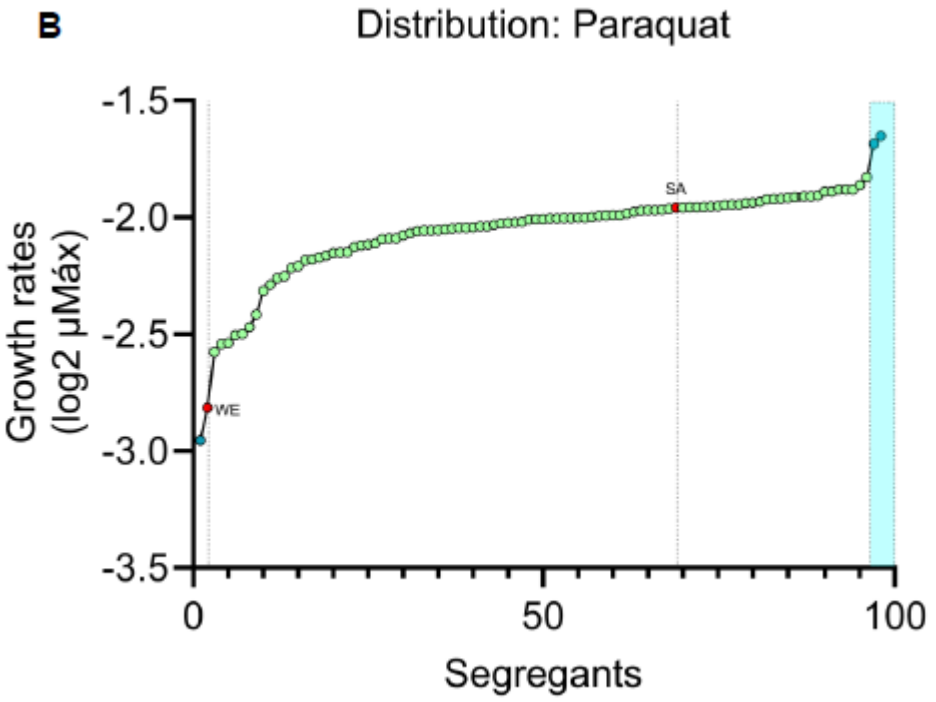
B
Distribution: Paraquat
Growth rates (log2 µMáx)
-1.5
-2.0
-2.5
-3.0
-3.5
WE
SA
0
50
100
Segregants

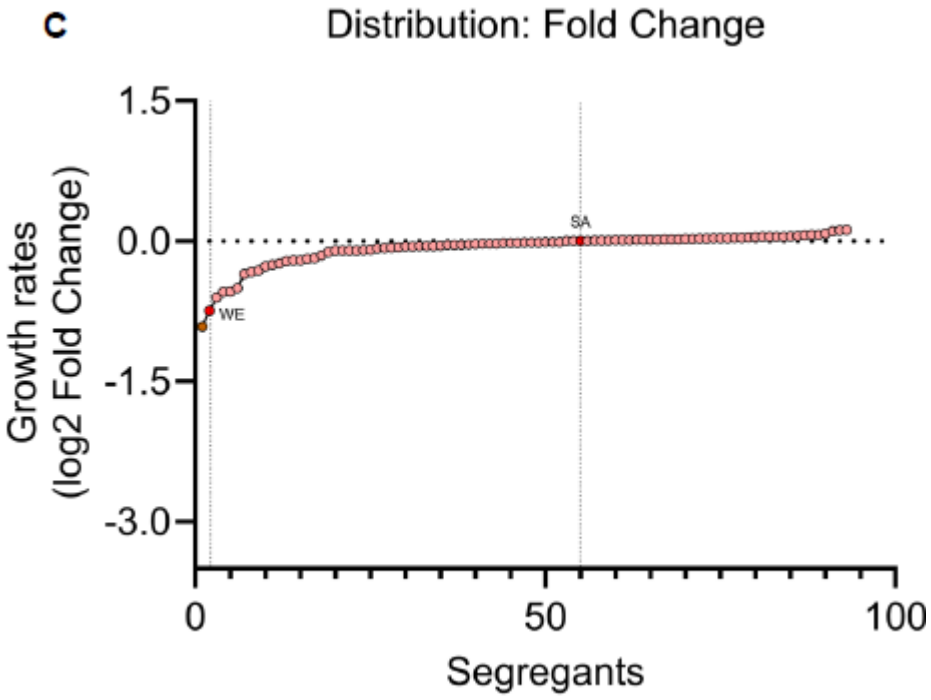

Figure 4. Distribution of Saccharomyces cerevisiae segregants in control conditions, PQ-exposure and fold change (PQ/control) according to their growth parameters. (A) Distribution of the yeast segregants according to their μMax in the control condition (B) Distribution of the yeast segregants according to their μMax in PQ treatment (C) Distribution of the yeast segregants according to their μMax in fold change. N sample = 96 segregants of S. cerevisiae (cross SA x WE). The log in base 2 of the μMax and transgressive segregants was calculated by 2 standard deviations. Red dots = founder strains, blue dots = transgressive segregants (control and PQ), orange dots = transgressive segregant (fold change). Statistical analysis was performed and plotted in GraphPad.

7.4. QTL mapping in segregants and µMax as a phenotypic trait

To identify candidate genes associated with growth rate variation under control conditions, PQ exposure, and fold change (PQ/control), we conducted linkage analysis to map QTLs using µMax as a trait. Through permutation testing, we successfully identified significant QTL peaks in two of the analyzed conditions.

In our QTL mapping, we found no significant peaks in the control condition (Figure 5A), while in the PQ-exposure, we identified a significant QTL, at marker *SAW1*, located on chromosome 1, with a LOD score of 2.87 (*P*-value = 0.028), exceeding the significance threshold of 2.63 (Figure 5B). This result suggests that the *SAW1* locus is associated with variation in growth rate under PQ stress. To identify potential candidate genes, we analyzed a 40 kb region both upstream and downstream of the *SAW* marker using Ensembl (https://www.ensembl.org). We decided not to explore this genomic region because we prioritized validating fold change results since they offer to unveil relative changes and eliminate individual variations and the normalization in this context gave us information about gene-environment interaction, where these genes may vary under different environmental conditions. In our analysis of fold change, we identified a significant QTL peak at the *CKA2* marker on chromosome 15, with a LOD score of 2.74 (*P*-value = 0.044). This LOD score exceeded the significance threshold of 2.68 (Figure 5C). We identified potential candidate genes in this region, and we employed the same strategy used for PQ exposure analysis (Figure 5D and Table

4). In this region, we also found the candidate gene *NRT1*, as in the GWAS analyses (Table 4).

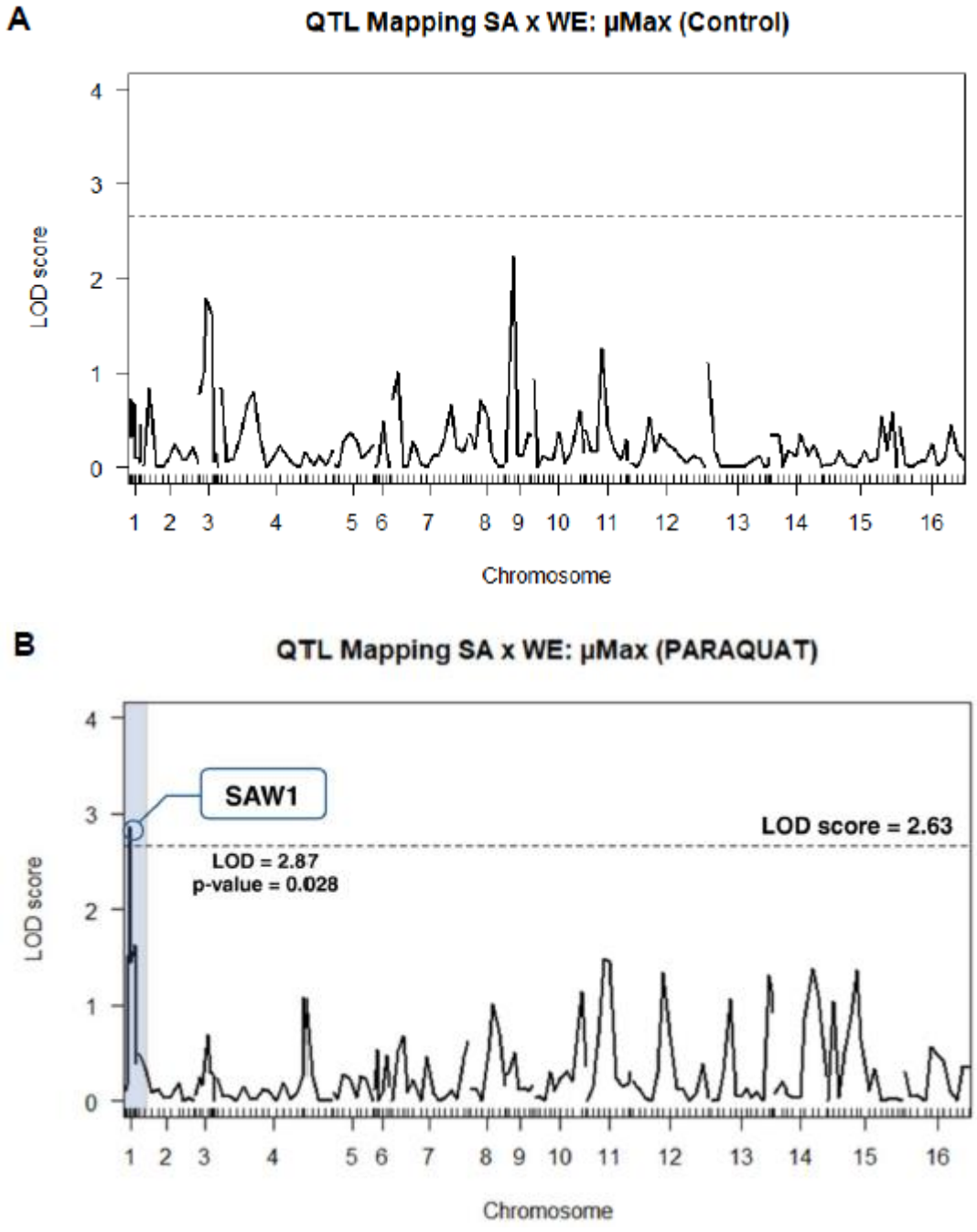

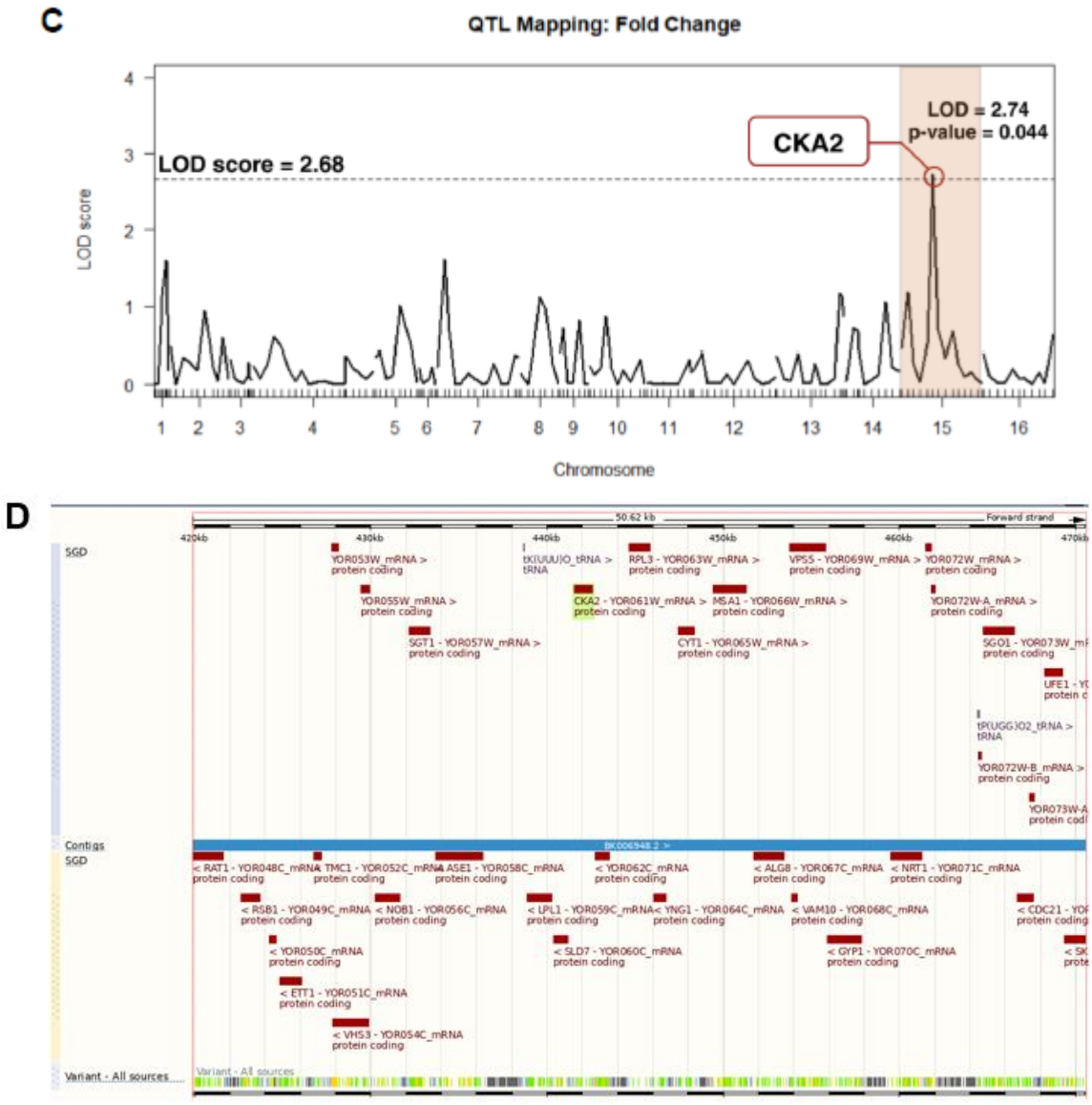

Figure 5. Markers found in QTL mapping associated with a genomic region, using the S288C reference genome. (A) Linkage analysis using μMáx as a phenotypic trait in the 96 strains of the cross SAxWE in the control condition (B) Linkage analysis using μMáx as a phenotypic trait in the 96 strains of the cross SAxWE in PQ-exposure. LOD score 2.63 (C) Linkage analysis using the fold change (PQ/control) as a phenotypic trait in the 96 strains of the cross SAxWE.

LOD score 2.68 (D) Genomic region in chromosome 15, found through *CKA2* marker associated with QTL mapping in fold change (Chromosome XV: 419,891-470,511 (ensembl.org)). N sample = 3. We calculated LOD scores using a non-parametric model determined through permutations. For each trait and cross, phenotype values were permuted within the tetrads 1000 times and the maximum score of the LOD scores were recorded each time. A significant QTL is recognized when the LOD score is greater than the 0.05 tail of the 1000 LOD scores obtained. The phenotypic variance score explained for a QTL is calculated using Formula 1, where “n” represents the sample size. Formula 1: Percentage of variance explained = $100(1–10^{(-2LOD/n)})$. Plotted in Rstudio.

Table 4. List of genes found in the genomic region of chromosome 15 through QTL mapping in Fold change

Genomic region: Chromosome 15			
Yeast gene	Human Orthologue	Position	Function
VPS5	*SNX1*	453768 - 455795	Nexin-1 homolog; required for localizing membrane proteins from a prevacuolar/late endosomal compartment back to late Golgi; structural component of retromer membrane coat complex
RPL3	*RPL3*	444686 - 445849	Ribosomal 60S subunit protein L3; homologous to mammalian ribosomal protein L3 and bacterial L3; plays an important role in function of eIF5B in stimulating 3' end processing of 18S rRNA.
NRT1	-	459480 - 461276	High-affinity nicotinamide riboside transporter; also transports thiamine with low affinity; major transporter for 5-aminoimidazole-4-carboxamide-1-beta-D-ribofuranoside (acadesine) uptake.
CKA2	*CSNK2*	441534 - 442553	Alpha catalytic subunit of casein kinase 2 (CK2); CK2 is a Ser/Thr protein kinase with roles in cell growth and proliferation.
CYT1	*CYC1*	447439 - 448368	Cytochrome c1; component of the mitochondrial respiratory chain; expression is regulated by the heme-activated.
SGT1	*SUGT1*	432186 - 433373	Cochaperone protein; regulates activity of adenylyl cyclase Cyr1p; involved in kinetochore complex assembly; associates with the SCF (Skp1p/Cdc53p/F box protein) ubiquitin ligase complex.
MSA	-	449436 - 451325	Activator of G1-specific transcription factors MBF and SBF; involved in regulation of the timing of G1-specific gene transcription and cell cycle initiation.
SGO1	-	464771 - 466543	Component of the spindle checkpoint; involved in sensing lack of tension on mitotic chromosomes; protects centromeric Rec8p at meiosis I; required for accurate chromosomal segregation at meiosis II and for mitotic chromosome stability.
VAM10	-	453869 - 454213	Protein involved in vacuole morphogenesis; acts at an early step of homotypic vacuole fusion that is required for vacuole tethering.
GYP1	*TBC1D22A* *TBC1D22B*	455907- 457820	Cis-golgi GTPase-activating protein (GAP) for yeast Rabs; the Rab family members are Ypt1p (in vivo) and for Ypt1p, Sec4p, Ypt7p, and Ypt51p (in vitro); involved in vesicle docking and fusion; interacts with autophagosome component Atg8p.
ALG8	*ALG8*	451729 - 453462	Glucosyl transferase; involved in N-linked glycosylation; adds glucose to the dolichol-linked oligosaccharide precursor prior to transfer to protein during lipid-linked oligosaccharide biosynthesis
YNG1	-	446079 - 446738	Subunit of the NuA3 histone acetyltransferase complex; this complex acetylates histone H3; contains PHD finger domain that interacts with methylated histone H3.
SLD7	-	440390 - 441163	Protein with a role in chromosomal DNA replication; interacts with Sld3p and reduces its affinity for Cdc45p.
LPL1	*FAM135B*	438906 - 440258	Phospholipase; contains lipase specific GXSXG motif; maintains lipid droplet (LD) morphology; induced by transcription factor Rpn4p.
ASE1	*PRC1*	433688 - 436345	Mitotic spindle midzone-localized microtubule bundling protein; microtubule-associated protein (MAP) family member; required for spindle elongation and stabilization.
NOB1	*NOB1*	430247 - 431626	Protein involved in proteasomal and 40S ribosomal subunit biogenesis; required for cleavage of the 20S pre-rRNA to generate the mature 18S rRNA.
VHS3	*PPCDC*	427833 - 429857	Negative regulatory subunit of protein phosphatase 1 Ppz1p; involved in coenzyme A biosynthesis.
RSB1	-	422668 - 423732	Sphingoid long-chain base (LCB) efflux transporter; integral membrane transporter that localizes to the plasma membrane and may transport long chain bases (LCBs) from the cytoplasmic side toward the extracytoplasmic side of the membrane.
TMC1	-	426772 - 427224	AN1-type zinc finger protein, effector of proteotoxic stress response; stress-inducible transcriptional target of Rpn4p; induced by nitrogen limitation, weak acid, misfolded proteins

We decided to investigate potential genetic variants in association with yeast reproductive growth through SIFT prediction. We compared the number of variants in *NRT1* and *YOR072W* genes in the four founder strains and the reference S288C and their corresponding µMax in PQ exposure. Our findings showed a differential number of non-synonymous variants in these genes (Table 5) and a significant negative correlation was observed between the number of variants of *NRT1* and µMax (*P*-value = 0.042, *r* = -0.8928, Pearson) (Figure 6A), suggesting a strong contribution of these variants to decreased µMax. In contrast, no significant correlation was found between *YOR072W* and its reproductive fitness (*P*-value = ns, *r* = -0.7205, Pearson) (Figure 6B).

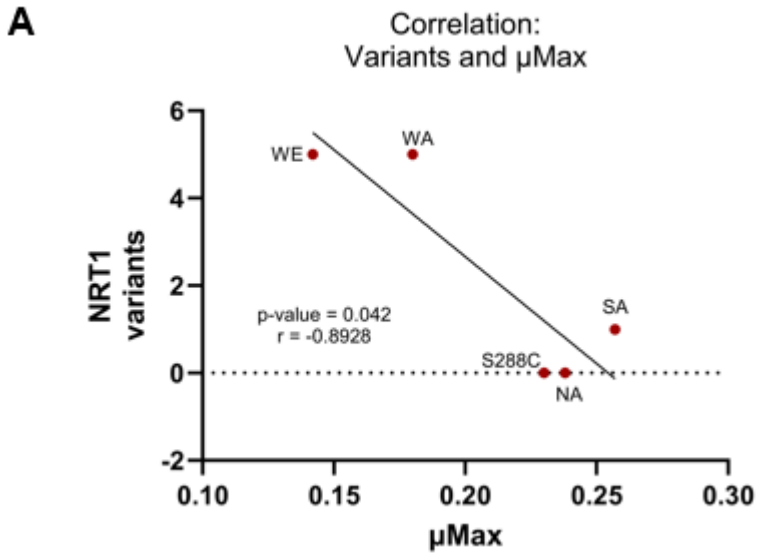

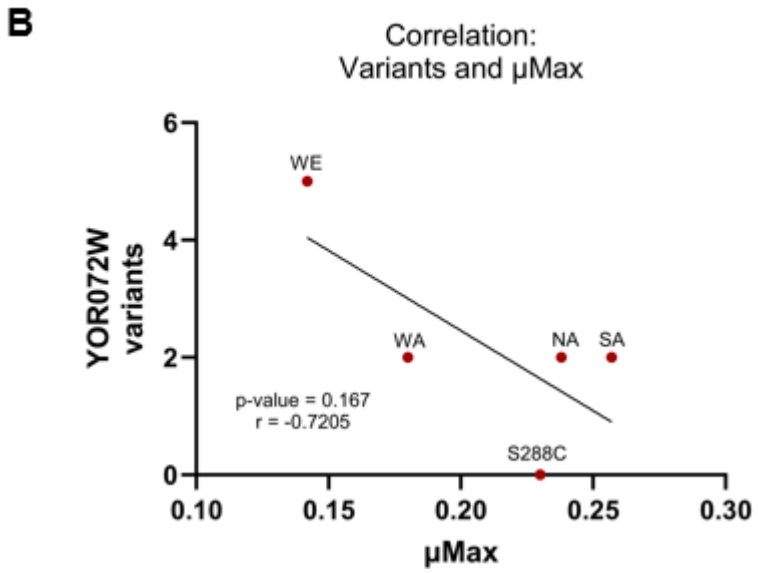

Figure 6. **Pearson correlations in NRT1 and YOR072W genes in yeast strains**. The potential effects of variants in each gene of the four yeast strains were determined using SIFT. The number of variants in NRT1 and YOR072W genes was correlated with µMax. (A) Plot of Pearson correlation between the number of variants in NRT1 and µMax. (B) Plot of Pearson correlation between the number of variants in YOR072W and µMax. Shapiro Wilk test *P*-value > 0.05. *P*-value ≤ 0.05 (*), *P*-value < 0.01 (**), *P*-value < 0.001 (***), *P*-value < 0.0001 (****), ns = not significant (*P*-value > 0.05). Statistical analysis was performed in SPSS software version 20.0 and plotted in GraphPad.

Table 5. Variants in NRT1 and YOR072W genes in four parental and reference strains. The potential effects of variants in each gene of the four yeast strains and reference were determined using SIFT.

µMax	0.257	0.238	0.180	0.142	0.230		
				NRT1			
Position	SA	NA	WA	WE	S288C	Variant Type	SIFT Prediction
459550	T	T	T	G	T	NONSYNONYMOUS	TOLERATED
459560	C	C	C	T	C	NONSYNONYMOUS	TOLERATED
459568	G	G	A	G	G	NONSYNONYMOUS	TOLERATED
459843	T	T	A	T	T	NONSYNONYMOUS	TOLERATED
460379	T	T	A	T	T	NONSYNONYMOUS	TOLERATED
460430	A	A	A	T	A	NONSYNONYMOUS	TOLERATED
460865	A	C	C	C	C	NONSYNONYMOUS	TOLERATED
460871	A	A	C	C	A	NONSYNONYMOUS	TOLERATED
461164	G	G	G	T	G	NONSYNONYMOUS	TOLERATED
461249	A	A	T	A	A	NONSYNONYMOUS	TOLERATED
				YOR072W			
Position	SA	NA	WA	WE	S288C	Variant Type	SIFT Prediction
461625	C	T	T	T	T	NONSYNONYMOUS	DELETERIOUS
461644	C	C	C	C	T	NONSYNONYMOUS	TOLERATED
461659	T	T	C	C	T	NONSYNONYMOUS	TOLERATED
461683	G	G	G	A	G	NONSYNONYMOUS	TOLERATED
461760	A	A	A	G	A	NONSYNONYMOUS	TOLERATED
461776	T	C	T	T	T	NONSYNONYMOUS	DELETERIOUS
461814	T	T	T	C	T	STOP-LOSS	NA

8. Chapter 3: To validate candidate modifier genes of the paraquat susceptibility/resistance phenotype in yeast strains with pre-existing targeted gene deletions.

9. EXPERIMENTAL PROCEDURES: Chapter 3

9.1. Growth curves conditions: phenotyping

Yeast cells were pre-cultured in 200 µL of YNB medium supplemented with uracil (0.2% uracil) for 48 h at 28 °C. For the experimental run, the four yeast strains were inoculated to an optical density (OD) of 0.03-0.1 (wavelength of 620 nm) in 200 µL of medium and incubated without shaking at 28 °C for 48 h in different conditions, i) control (YNB media, 2% glucose) and PQ (Sigma Aldrich-Merck, CAS No. 75365-73-0) at 75 µg/mL for the phenotyping in 1,011 isolates; ii) control (YNB media, 2% glucose), PQ 200 µg/mL, nicotinamide riboside chloride (NR), dissolved in distilled water (Cayman Chemicals, CAS No. 23111-00-4) at 20 µM and co-treatment PQ 200 µg/mL and NR 20 µM for the validation assays in a Tecan Sunrise absorbance microplate reader (Tecan Trading AG, Männedorf, Switzerland). OD was measured every 30 min using a 620 nm filter. Each experiment was performed in triplicate. Growth rates for each strain were calculated as previously described (García-Ríos et al., 2014; Quispe et al., 2017). Briefly, OD measurements as a function of time were fitted to the mathematical

model of the re-parameterized Gompertz sigmoid curve describing microbiological temporal growth, previously proposed (Zwietering et al., 1990) from which growth rates were obtained. The parameters of each curve were processed in the GrowthRates software to obtain OD max, μMax, and the average time of the lag phase.

9.2. Deleting yeast

To validate the phenotypes found in response to PQ exposure, we decided to use deletion strains of the genes identified in both the GWAS and QTL mapping. Some of the strains were provided by Professor Jonas Warringer, while others were purchased from Euroscarf (www.euroscarf.de). We used strains BY4743 and S288C as reference strains.

9.3. Induced pluripotent stem cells (iPSC) culture and treatments

The iPSC lines used in this study were previously generated from *GBA*-PD patients and control individuals and characterized (Schöndorf et al., 2014). For all iPSC lines, informed consent was obtained from patients prior to cell donation using a written form. The protocol was approved by the Ethics Committee of the Medical Faculty and the University Hospital Tübingen (Ethikkommission der Medizinischen Fakultät am Universitätsklinikum Tübingen). iPSCs were maintained in hESC medium containing knockout DMEM (Gibco Life

Technologies), 20% knockout serum replacement (Gibco Life Technologies), 1% non-essential amino acids (Gibco Life Technologies), 1% penicillin/streptomycin (P/S, Merck Millipore), 1% GlutaMAX Supplement (Gibco Life Technologies) and 500 µM β-mercaptoethanol (Sigma-Aldrich) supplemented with 10 ng/ml FGF2 (Peprotech). iPSCs were routinely passaged onto MMC-treated CF-1 mouse embryonic fibroblasts (MEF) (Globalstem MTI ThermoFisher) with addition of 10 µM Rock inhibitor Y-27632 2HCl (Selleckchem). iPSCs were differentiated into dopaminergic neurons according to Kriks et al. (Kriks et al., 2011). Cells were grown for 11 days on Matrigel (Corning) in hESC medium. Differentiation was based on exposure to LDN193189 (100 nM, Axon Medchem) from days 0–11, SB431542 (10 µM, Selleckchem) from days 0–5, SHH (100 ng/mL, Peprotech), purmorphamine (PMA; 2 µM, EMD) and FGF8 (100 ng/mL, Peprotech) from days 1–7 and CHIR99021 (CHIR; 3 µM, Axon Medchem) from days 3–13. hESC medium was gradually shifted to N2 medium (DMEM/Ham's F12, 1% P/S, 1% GlutaMAX and N2 supplement from Gibco Life Technologies), starting on day 5 of differentiation. On day 11, medium was changed to N2/B27 medium containing DMEM/Ham's F12, Neurobasal medium, N2 and B27 supplement, 1% P/S and 1% Glutamax (N2 and B27 supplement; Gibco Life Technologies) supplemented with CHIR (3 µM, until day 13) and brain-derived neurotrophic factor (BDNF; 20 ng/ml; Peprotech), ascorbic acid (AA; 200 µM, Sigma-Aldrich), glial cell line-derived neurotrophic factor (GDNF; 20 ng/ml; Peprotech), transforming growth factor type β3 (TGFβ3, 1 ng/ml; Peprotech), dibutyryl cAMP (0.5 mM; Applichem),

and DAPT (10 µM; Selleckchem) for 9 days. On day 20, cells were dissociated using Accutase (Sigma-Aldrich) and replated under high cell density conditions on dishes pre-coated with 15 µg/ml polyornithine and 1 µg/ml laminin in differentiation medium (N2/B27 medium +BDNF, AA, GDNF, dbcAMP, TGFβ3 and DAPT). Neurons were maintained *in vitro* for 45-55 days and then used for PQ and NR experiments.

9.4. Cell viability assay

Cells were seeded into a 96-well plate (1x104 cell per well). After 24 h, benzoates-TPP+ compounds were added at increasing concentrations into the wells and incubated for 48 and 72 h, in culture DMEM medium supplemented with 10% FBS, 100 U/mL of penicillin and 100 µg/mL of streptomycin in a humidified 5% CO_2 at 37°C. After this time, the cells were washed twice with PBS (phosphate buffer saline) 1X, and then 100 µL of 0.5 mg/mL MTT solution was added to each well. After 2 h of incubation, MTT was removed, and crystals of formazan were dissolved in 40 µL of DMSO. Absorbance was measured at 570 nm with a microplate ELISA reader (Infinite F50 Tecan Group Ltd., Swiss).

9.5. Bright field microscopy

Dopaminergic neurons maintained *in vitro* were used to analyze viability by brightfield microscopy under the conditions at 24 hours: PBS, PBS and NR at 1 mM, PQ at 500 µM and the co-treatment of PQ at 500 µM and NR at 1 mM.

Images were captured using a 40X objective (NA 0.75, Nikon) and a CoolSnap HQ2-- CCD camera via bright field microscopy.

10. RESULTS: Chapter 3

10.1. Validation of modifier genes identified in GWAS and QTL mapping

After identifying genes in both GWAS, PQ-exposure and fold change (PQ/control), we decided to validate those genes. The identified genes were *SNZ1*, *HFI1*, *WHI2*, *ALR1*, *RPB2*, *NRT1*, and *YOR072W*. Notably, *NRT1* and *YOR072W* were found in both GWAS and QTL mapping. To experimentally evaluate the phenotypic consequences associated with these genes, we utilized commercially available yeast deletion strains from Eurocarf and provided by Professor Jonas Warringer, University of Gothenburg. Using yeast strains with each gene deleted, we aimed to investigate their potential impact on the yeast response to PQ and phenotype changes. We decided to perform physiological growth kinetics experiments, using µMax as a phenotypic trait to validate in deleting strains. Due to observed drug resistance, likely attributed to subtelomeric regions, we increased the PQ concentration to 200 µg/mL to further challenge these strains. Previous studies have suggested that genes in these regions contribute to individual quantitative variation and play a crucial role in the adaptive response to environmental factors (Cubillos et al., 2011; Quispe et al., 2017). Significant differences between the control condition and PQ exposure (200 µg/mL) were

observed in the reference strains S288C (*P*-value = 0.0059, ANOVA) and BY4743 (*P*-value = 0.0015, ANOVA). However, significant differences were only found in the deleting strains Δ*yor072w* (*P*-value = 0.0015, ANOVA) and Δ*rpb2* (*P*-value < 0.0001, ANOVA) (Figure 7A).

Recent studies suggest that a decrease in nicotinamide adenine dinucleotide (NAD^+) levels may contribute to PD. Supplementation with nicotinamide riboside, a precursor of NAD^+, could potentially restore NAD^+ levels (Pérez et al., 2021; Schöndorf et al., 2018). To investigate the potential benefits of NR supplementation, we decided to include it in our experiments. We selected strain S288C to assess differential responses and determine if NR could prevent the fitness decline observed upon PQ exposure. We found significant differences in μMax between the control condition and PQ exposure at 200 μg/mL (*P*-value < 0.0001, ANOVA (Figure 7B). Interestingly, the co-treatment of PQ (200 μg/mL) and NR (20 μM) significantly prevented the observed decrease in μMax compared to PQ treatment alone (*P*-value < 0.0001, ANOVA) (Figure 7B). We also observed significant differences between NR and PQ exposure (*P*-value < 0.0001, ANOVA) as well as between NR and the co-treatment (PQ and NR) (*P*-value = 0.0316, ANOVA). As expected, we did not observe any significant differences between the control condition and NR supplementation (*ujhg*-value = ns, ANOVA), as NR was solely used as an internal control (Figure 7B).

Given that *Nrt1* is the primary transporter for NR uptake into cells, we decided to use a Δ*nrt1* strain to investigate the role of NR supplementation. We found no

significant differences between the groups (Figure 7C). These findings provide evidence that *Nrt1* is essential for NR transport and NAD^+ enrichment pathway, but it also has a role in PQ toxicity, suggesting that *Nrt1* serves multiple activities and functions. Additionally, our findings suggest that NR does not utilize alternative transporters or pathways to exert its effects. Due to the close genomic proximity of *NRT1* and *YOR072W*, and their identification in both GWAS and QTL mapping, we used a Δ*yor072w* strain to investigate its role in NAD^+ metabolism. We found significant differences between control condition and PQ treatment (*P*-value < 0.0001, ANOVA). Moreover, co-treatment with PQ and NR prevented the PQ-induced phenotype, increasing μMax (*P*-value = 0.0002, ANOVA) (Figure 7D). These results strongly suggest that YOR072W is not essential for NAD^+ metabolism, as Δ*yor072w* yeast strain can still respond to NR supplementation. However, *Yor072w* could play a role in PQ toxicity because Δ*yor072w* is more susceptible to PQ exposure.

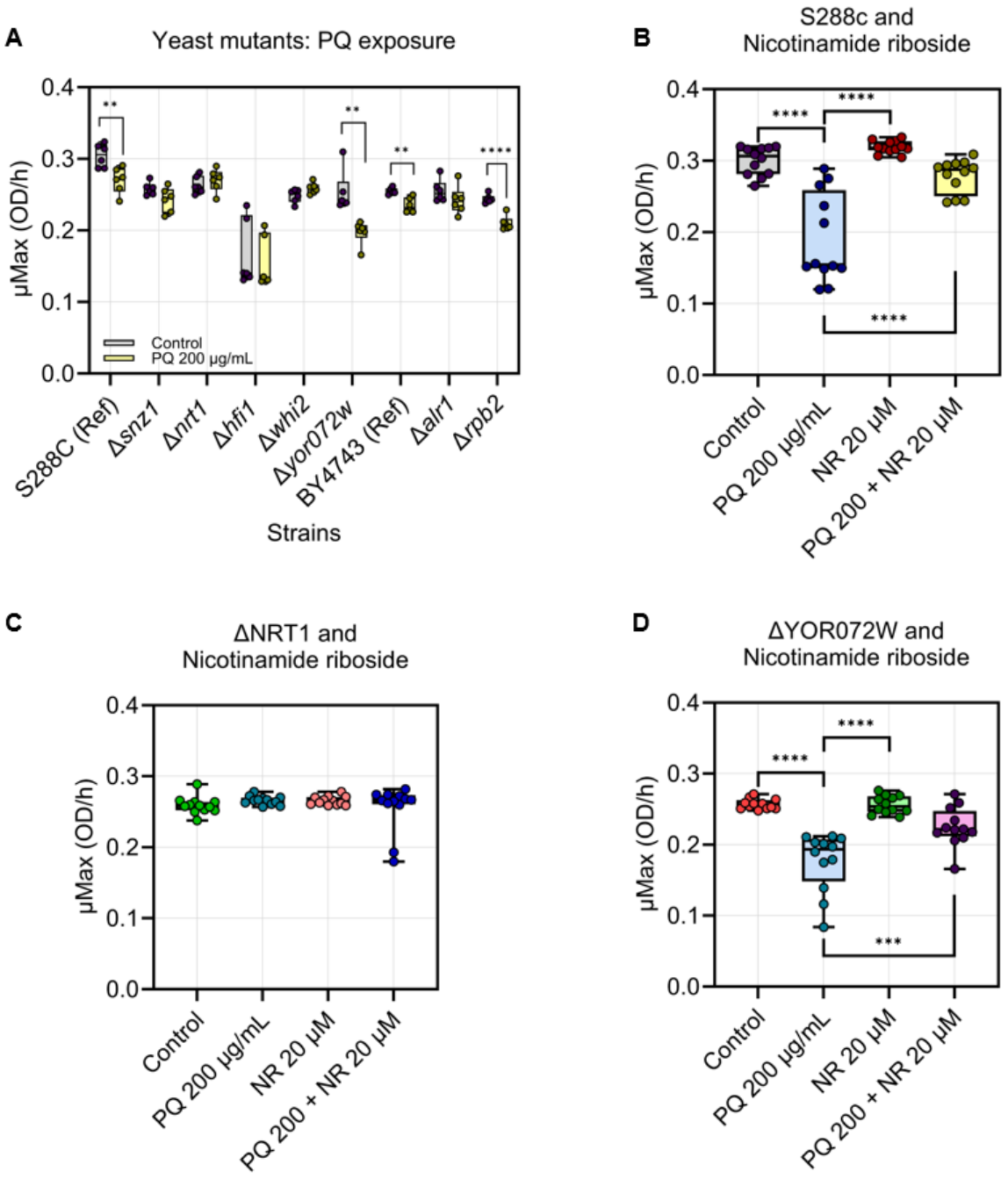

Figure 7. Validation of growth phenotypes using genes identified in GWAS (µMax). (A) Deleting strains of the genes found in the GWAS (µMax) and calculation of the growth parameter µMax in control condition and PQ-exposure

(200 µg/mL). (B) calculation of the growth parameter µMax of S288C strain in 4 conditions: Control, PQ (200 µg/mL), NR 20 µM and co-treatment PQ and NR. (C) Deleting strain in NRT1 gene found in the GWAS (µMax) and calculation of the growth parameter µMax in 4 conditions: Control, PQ (200 µg/mL), NR 20 µM and co-treatment PQ and NR. (D) Deleting strain in YOR072W gene found in the GWAS (µMax) and calculation of the growth parameter µMax in 4 conditions: Control, PQ (200 µg/mL), NR 20 µM and co-treatment PQ and NR. N sample = 12. Shapiro Wilk normality test *P*-value > 0.05. ANOVA test *P*-value < 0.05, post-hoc Dunnett. *P*-value ≤ 0.05 (*), *P*-value < 0.01 (**), *P*-value < 0.001 (***), *P*-value < 0.0001 (****), ns = not significant (*P*-value > 0.05). Statistical analysis was performed in SPSS software version 20.0 and plotted in GraphPad.

10.2. Treatment of PQ and NR in dopaminergic neurons from iPSCs

In addition to our findings in yeast, we established a collaboration with Professor Michela Deleidi, who conducted experiments on dopaminergic neurons iPSC from GBA-PD patients. These cells were treated with NR to investigate their capacity to prevent the toxic effects of PQ exposure on cell viability. Bright-field microscopy revealed no significant differences in PBS samples (Figure 8A) or cotreatment PBS and NR at 1 mM (Figure 8B). However, we found increased cell death when the cells were exposed to PQ (500 µM) (Figure 8C), while the co-treatment with PQ and NR 1mM effectively prevented cell death (Figure 8D), suggesting a preventive effect of NR in cell viability.

To confirm the previous findings, we perform an MTT analysis to determine cell viability. Our results showed no significant differences in cellular viability in PBS or PBS combined with NR at 1 mM conditions (*P*-value = ns, T-Test) (Figure 8E). In contrast, PQ exposure significantly reduced cellular viability compared to the control condition (PBS) (*P*-value < 0.0001, T-Test) (Figure 8F). However, the combination of PQ and NR partially prevented the toxic effects of PQ exposure (*P*-value = 0.0001, T-Test) (Figure 8G), resulting in increased cell viability.

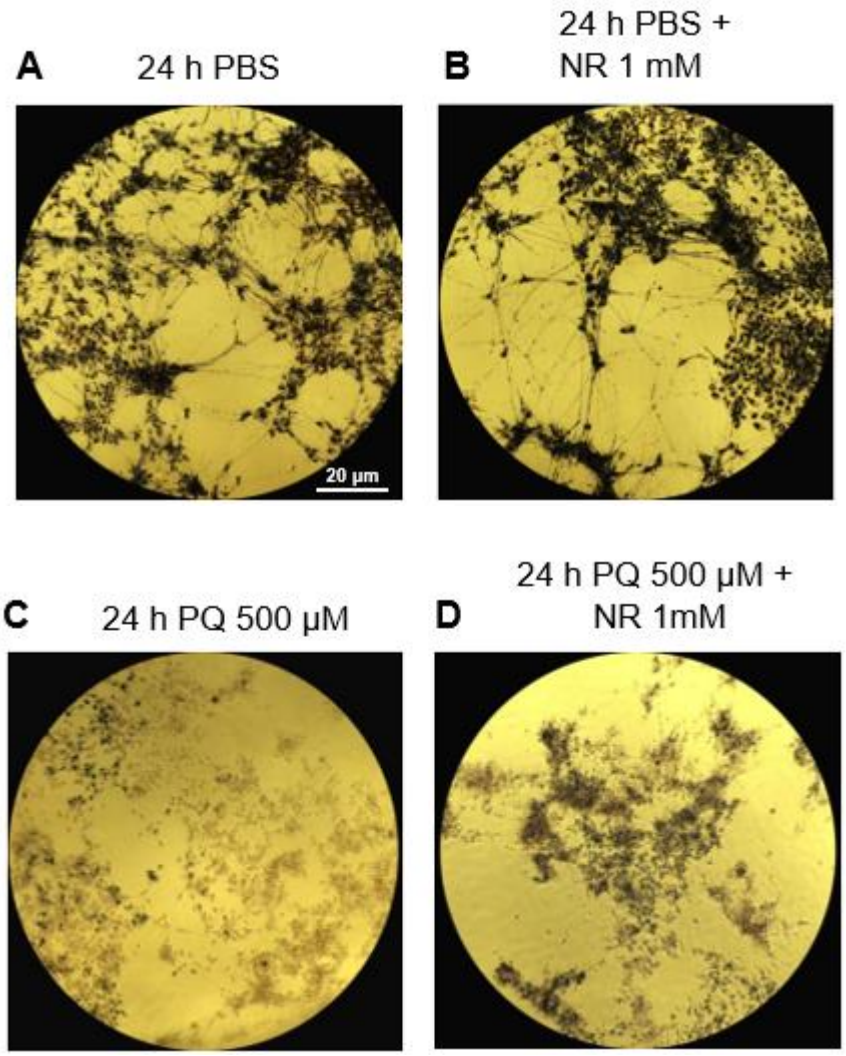

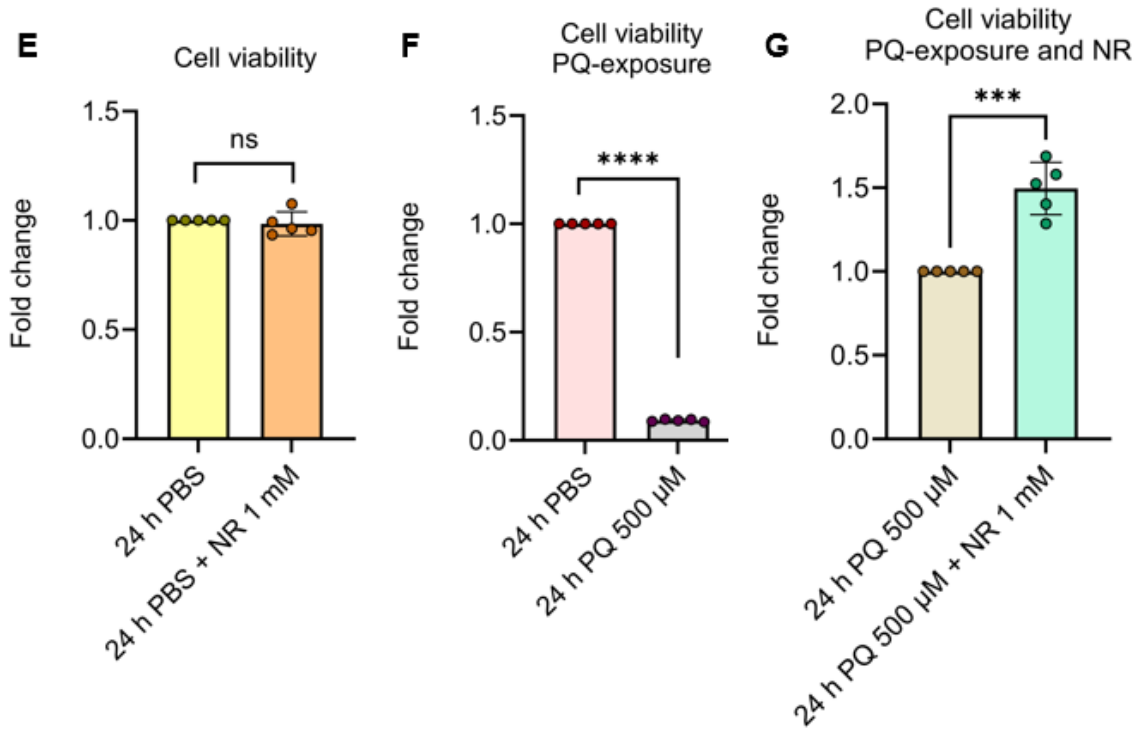

Figure 8. **Treatment of NR in dopaminergic neurons from iPSCs exposed to PQ**. Cell viability by brightfield microscopy in dopaminergic neurons from iPSCs of GBA-PD patients in (A) control condition (PBS), (B) PBS and 1 mM NR, (C) PQ 500 uM exposure and (D) PQ and NR co-treatment. Cell viability through MTT assays. (E) PBS condition and PBS with NR 1 mM, (F) PBS and PQ, (G) PQ and PQ and NR co-treatment. Shapiro Wilk normality test *P*-value > 0.05. T-test *P*-value < 0.05. *P*-value ≤ 0.05 (*), *P*-value < 0.01 (**), *P*-value < 0.001 (***), *P*-value < 0.0001 (****), ns = not significant (*P*-value > 0.05). Statistical analysis was performed in SPSS software version 20.0 and plotted in GraphPad.

11. DISCUSSION

Saccharomyces cerevisiae is a model system that has allowed understanding of relevant biological, cellular, and genomics processes over time (Bai et al., 2022b; Karathia et al., 2011b; Oftadeh et al., 2021b). Sourced from diverse ecological niches and geographic locations, with genetically and phenotypically diverse, the yeast strains employed in this study possess genetic and phenotypic characteristics shaped by environment-specific alleles (Cubillos et al., 2011; Jara et al., 2014).

The yeast isolates used in this thesis project exhibit high genetic diversity ($\pi = 3 \times 10^{-3}$) and low linkage disequilibrium ($LD_{1/2}$= 500 bp), being successful for GWAS analysis (Peter et al., 2018). These characteristics are essential to contribute to higher-resolution mapping since the genes with low linkage disequilibrium can be able to recombine independently during breeding, increasing the precise identification of the genetic variants underlying phenotypic complex traits, and even reducing the likelihood of multiple variants being inherited together (Slatkin, 2008). On the other hand, families of yeast, created through the crossing of two founder strains, have been a valuable biological system for linkage mapping. These panels of families have revealed a high number of QTLs, being able to identify genomic regions with complex traits (Cubillos et al., 2013). These genetic mapping techniques enabled us to precisely pinpoint specific regions of the genome, especially genetic variants linked to the phenotypes of interest. This has

significantly advanced our understanding of the phenotypic responses associated with PQ.

Our findings demonstrate that the effect of PQ on μMax varies among a genetically diverse panel of *S. cerevisiae* strains. PQ decreased μMax in 36 of the 603 isolates analyzed, indicating increased susceptibility in comparison to control conditions. Notably, 29 of the isolates tested were resistant to PQ exposure. These strain-specific differences suggest a transcriptional response mediated by Gcn4, a transcription factor involved in amino acid biosynthesis and metabolism. Gcn4 may also regulate the expression of genes encoding antioxidant enzymes (Fendt et al., 2010; Mascarenhas et al., 2008). This suggests that PQ-resistant strains exhibit a complex response, potentially involving enhanced metabolic efficiency to compensate for the energy required for detoxification and repair processes. In contrast, susceptible strains might downregulate Gcn4 activity in response to PQ exposure.

Beyond reducing replicative lifespan and inhibiting cell division (Jarolim et al., 2004b; Nestelbacher et al., 2000b). PQ exposure is a potent inducer of oxidative stress, which contributes to mitochondrial damage, mtDNA loss, and impaired oxidative phosphorylation, thus exacerbating the negative effects on cell viability in both mammalian cells and yeast (Y. Li et al., 2021; Stenberg et al., 2022; Tiên Nguyên-nhu & Knoops, 2003). Furthermore, PQ exposure apparently inhibits quinolinate phosphoribosyl transferase in bacteria, resulting in decreased NAD^+ levels. This reduction in NAD^+ availability can compromise cellular energy

production, exacerbating the detrimental effects of oxidative stress (Heitkamp & Brown, 1981).

Previous studies in humans have demonstrated that the increase in NAD^+ levels may play a role as a potential neuroprotective factor for healthy aging and neurodegenerative diseases (Pérez et al., 2021). NAD^+ is an essential redox cofactor in mitochondrial respiration and serves as a substrate in DNA repair, histone, and protein deacetylation, even a second messenger generation (Brakedal et al., 2022; Pérez et al., 2021). Reports indicate that NAD^+ consumption is extremely necessary for these pathways and needs continuous and prolonged replenishment. Studies have shown that NAD+ levels decrease with age and the NAD^+/NADH ratio is crucial for maintaining a balance in these processes. Enhancing this ratio prevents an imbalance that could cause ATP depletion, leading to mitochondrial dysfunction and eventually the development of neurodegenerative diseases such as PD (Brakedal et al., 2022; Wakade & Chong, 2014).

Mitophagy is a highly coordinated process that selectively degrades defective organelles, preserving mitochondrial functional stability, which allows maintaining cellular homeostasis. Reports indicate that impaired mitophagy may actively contribute to PD pathogenesis. Mitophagy is regulated by *PINK*, which encodes a protein involved in autophagic degradation (Youle & Narendra, 2011). Mutations in PINK can alter mitophagy and perturb mitochondrial bioenergetics and NAD^+ redox status (Bingol & Sheng, 2016; Lehmann et al., 2017; Scarffe et al., 2014;

Youle & Narendra, 2011). These findings suggest a link between mitochondrial dysfunction and PD, highlighting the role of mitophagy and NAD^+ metabolism in preventing PD.

NAD^+ possesses antioxidant properties that regulate different cellular processes and enhance the oxidative status in PD. However, patients with PD exhibit low NAD^+ levels, necessitating the implementation of new strategies for NAD^+ supplementation through molecule intermediates. Recent studies investigated the potential NAD^+ precursors, such as nicotinamide riboside (NR) to prevent age-related metabolic impairment. NR significantly enhances the mitochondrial function in PD dopaminergic neurons in iPSC and prevents age-related loss of dopaminergic neurons and motor impairments in fly models of GBA-PD (Schöndorf et al., 2018). Additionally, NR can be imported into cells through the equilibrium nucleoside transporter (ENT) family of transporters. Once inside the cell, NR is metabolized to nicotinamide (Nam), a precursor of NAD^+ (Kropotov et al., 2021).

Our GWAS analysis of *S. cerevisiae* isolates, using µMax as a phenotypic trait under PQ conditions and fold change GWAS to analyze genotype-phenotype interactions, identified significant variants. These variants were mapped to candidate genes in the reference genome based on their genomic location. GWAS PQ and GWAS fold change analysis revealed a gene on chromosome 15, *YOR071C*, which encodes the high-affinity NR transporter *Nrt1* (P. A. Belenky et al., 2008). Additionally, QTL mapping of the fold change in a 96-segregant SA x

WE cross, using µMax as a phenotypic trait, identified a genomic region on chromosome 15 (Marker *CKA2* in significant peak) containing the *YOR071C* gene. The convergence of these two independent analyses on the same candidate gene, *YOR071C*, underscores its potential relevance to our research on PD.

In yeast, NR supplementation has been shown to increase NAD^+ levels, activate sir2, and extend replicative lifespan (P. Belenky, Racette, et al., 2007). Yeast utilizes multiple pathways to metabolize NR into NAD^+. The primary pathway involves the kinases *Nrk1* and *Nrk2*, which phosphorylate NR for conversion to NAD^+. Alternatively, the enzymes *Urh1* and *Pnp1* can degrade NR to nicotinamide, which can then be recycled to produce NAD^+ (P. A. Belenky et al., 2008). The *NRT1* gene encodes the *Nrt1* protein, a membrane protein primarily associated with thiamine transport but exhibiting low affinity. However, mutants of *nrt1* have been shown to reduce NR utilization by 93%, indicating that *Nrt1* plays a significant role in NR transport (P. Belenky et al., 2011; P. A. Belenky et al., 2008). Our findings align with previous literature, as we observed no differences in µMax when comparing the *NRT1*-deficient strain exposed to NR alone or in combination with PQ. It had no discernible impact on the yeast growth-related phenotype, as the NR did not enter the system to exert any effect. Intriguingly, we also found no differences in PQ exposure, suggesting that *NRT1* and NR may be involved in this response.

In humans, organic cation transporters (OCT), specifically the transporters OCT2 (SLC22A2) and MATE-1 (SLC47A1), belonging to the multidrug resistance protein family have been described. Both are responsible for mediating PQ transport and subsequently accumulation within cells, producing cytotoxicity (Chen et al., 2007). While in humans PQ transport mechanisms have been described, they have not yet been elucidated in yeast. In our results the *nrt1* mutant showed no significant changes in μMax in any condition, indicating that PQ exposure remains unaffected in the absence of transporter activity. *Nrt1* is a transporter with selectivities for different molecules. For example, it can transport 5-Aminoimidazole-4-carboxamide-1-β-D-ribofuranoside (Ceschin et al., 2014), 5-fluorocytosine (Paluszynski et al., 2006), and thiamine (Mojzita & Hohmann, 2006). If our hypothesis is correct *Nrt1* might also facilitate PQ transport. To test this, it is necessary to determine if *Nrt1* overexpression in yeast increases PQ toxicity within the cells. Furthermore, it is relevant to confirm through experiments competitive inhibition whether *Nrt1* interacts with PQ and directly mediates its transport, either as a primary or alternative pathway. Understanding how PQ is transported into the cell could be a strong proxy for elucidating its mechanisms of action.

The active and functional transporters mediate the intervention of NR into the cell, increasing ATP production and mitochondrial membrane potential. Thus, it reduces oxidative stress, increasing the NAD^+ metabolism in PD models (Pérez et al., 2021). The effects of PQ disrupt the balance in the redox cycle, leading to

mitochondrial fragmentation through ROS and reactive nitrogen species and ultimately apoptosis (Alural et al., 2015; Djukic et al., 2007; Donaher & Van den Hurk, 2023b; Houzé et al., 1990; Xiong et al., 2019) The damage in dopaminergic neurons is mediated by cellular and molecular events in association with oxidation into the cell, being contributing factors in PD pathogenesis (Dinis-Oliveira et al., 2006; See et al., 2022). Here, NR is relevant because it has a potential therapeutic role in the prevention of toxic effects caused by PQ. This is consistent with our findings demonstrating that the S288C yeast strain when exposed to PQ, significantly increased the μMax as a physiological reproductive growth, while when co-treatment with NR, the toxic effect is lower, since increasing the μMax improves reproductive fitness. These results showed a protective effect of NR when it is supplemented in the yeast strains exposed to PQ. In collaboration with Professor Michela Deleidi, our findings were confirmed, because experiments using iPSC-derived dopaminergic neurons from GBA-PD patients, demonstrated reduction in cell viability in neurons with PQ exposure, while when NR is co-treated, the cell death was prevented, suggesting again the protective role of NR in this human cell models, being a strong supplement candidate for PD induced by PQ and even other pesticides.

The prevention of NR has effects when the cells or organisms are exposed to PQ. The effect is mediated by sirtuin 1 (SIRT1), which is an NAD^+-dependent protein deacetylase with roles in different processes, such as apoptosis, inflammation, and cell proliferation (Ding et al., 2016; X. Li et al., 2020). *Sirt1* promotes the

stability of nuclear factor E2-related factor 2 (NRF2), increasing the transcriptional activity and expression of their protein. These changes in transcript levels upregulate the expression of *SOD*, *CAT*, and *GSH* such antioxidant factors relevant to oxidative stress induced by stressors *(Chao et al., 2022; S. Li et al., 2016)*. The protective role of *Sirt1* prevents PQ-induced damage using its antioxidant effects in mouse type II alveolar epithelial cells, regulating the deacetylation and activation of the NRF2/ARE antioxidant pathway (Ding et al., 2016).

12. CONCLUSIONS

This thesis project investigated cellular, molecular, and genetic mechanisms in four diverse genetic backgrounds of *S. cerevisiae against* PQ toxicity, allowing the unveiling of differential responses. These PQ susceptibilities and resistances could be good proxies for a study in humans. For designing new strategies, it is necessary to have a deeper understanding of the biology of resistant strains and to prevent pesticide-induced PD, such as PQ exposition. To investigate the gene-environmental interaction approaches like GWAS and QTL mapping were used. In this study we used a collection of 1,011 isolates from diverse ecological niches and geographical for GWAS and segregants from crosses of founder yeast strains, enabling us to identify variants and markers associated with those differential responses to PQ defined as susceptibility and resistance. These findings revealed candidate genes and processes associated with mitochondrial metabolism, particularly the role of NAD^+ metabolism in response to PQ and to offer potential therapeutic targets for PD. Here, we demonstrated that NR can effectively prevent the toxic effects of PQ, like reproductive fitness and cell viability in yeast models and dopaminergic neurons from iPSC from GBA-PD patients, respectively, indicating NR as a promising therapeutic agent for PD induced by PQ toxicity.

In conclusion, our thesis study represents a valuable source of information about the underlying processes of PD through cellular and molecular responses associated with PQ toxicity in genetically diverse yeast strains. In addition, the use of GWAS and QTL mapping like powerful genetic techniques gave us a deeper understanding of the gene-environmental interaction and identify candidate genes. Our GWAS and linkage studies in yeast strains identified the *NRT1* gene, as a strong candidate, which encodes the *Nrt1* transporter regulating NR transport and preventing the toxic effects of PQ, apparently, through enhancing mitochondrial NAD^+ metabolism, suggesting potential therapeutic targets for interventions aimed at preventing or treating PQ-induced toxicity in PD.

13. FUTURE DIRECTIONS

In the future is relevant to integrate our findings in PQ with transcriptomic analysis in combination with biological network enrichment to elucidate the major pathways, critical routes, and even interaction with other molecules. Subsequent studies in yeast mutants and other organisms with central nervous systems could be a valuable approach for new therapies in pesticide-induced PD.

14. REFERENCES

1. Aitman, T. J., Boone, C., Churchill, G. A., Hengartner, M. O., Mackay, T. F. C., & Stemple, D. L. (2011). The future of model organisms in human disease research. *Nature Reviews. Genetics*, *12*(8), 575–582.
2. Akhter, F., Chen, D., Yan, S. F., & Yan, S. S. (2017). Mitochondrial Perturbation in Alzheimer's Disease and Diabetes. *Progress in Molecular Biology and Translational Science*, *146*, 341–361.
3. Alural, B., Ozerdem, A., Allmer, J., Genc, K., & Genc, S. (2015). Lithium protects against paraquat neurotoxicity by NRF2 activation and miR-34a inhibition in SH-SY5Y cells. *Frontiers in Cellular Neuroscience*, *9*, 209.
4. Bai, F.-Y., Han, D.-Y., Duan, S.-F., & Wang, Q.-M. (2022a). The Ecology and Evolution of the Baker's Yeast. *Genes*, *13*(2). https://doi.org/10.3390/genes13020230
5. Bai, F.-Y., Han, D.-Y., Duan, S.-F., & Wang, Q.-M. (2022b). The Ecology and Evolution of the Baker's Yeast. *Genes*, *13*(2). https://doi.org/10.3390/genes13020230
6. Ball, N., Teo, W.-P., Chandra, S., & Chapman, J. (2019). Parkinson's Disease and the Environment. *Frontiers in Neurology*, *10*, 218.
7. Bastías-Candia, S., Zolezzi, J. M., & Inestrosa, N. C. (2019). Revisiting the Paraquat-Induced Sporadic Parkinson's Disease-Like Model. *Molecular Neurobiology*, *56*(2), 1044–1055.
8. Belenky, P. A., Moga, T. G., & Brenner, C. (2008). Saccharomyces cerevisiae YOR071C encodes the high affinity nicotinamide riboside transporter Nrt1. *The Journal of Biological Chemistry*, *283*(13), 8075–8079.
9. Belenky, P., Bogan, K. L., & Brenner, C. (2007). NAD+ metabolism in health and disease. *Trends in Biochemical Sciences*, *32*(1), 12–19.
10. Belenky, P., Racette, F. G., Bogan, K. L., McClure, J. M., Smith, J. S., & Brenner, C. (2007). Nicotinamide riboside promotes Sir2 silencing and extends lifespan via Nrk and Urh1/Pnp1/Meu1 pathways to NAD+. *Cell*, *129*(3), 473–484.
11. Belenky, P., Stebbins, R., Bogan, K. L., Evans, C. R., & Brenner, C. (2011). Nrt1 and Tna1-independent export of NAD+ precursor vitamins promotes NAD+ homeostasis and allows engineering of vitamin production. *PloS One*, *6*(5), e19710.
12. Berry, C., La Vecchia, C., & Nicotera, P. (2010). Paraquat and Parkinson's disease. *Cell Death and Differentiation*, *17*(7), 1115–1125.
13. Bingol, B., & Sheng, M. (2016). Mechanisms of mitophagy: PINK1, Parkin, USP30 and beyond. *Free Radical Biology & Medicine*, *100*, 210–222.
14. Blauwendraat, C., Nalls, M. A., & Singleton, A. B. (2020). The genetic architecture of Parkinson's disease. *Lancet Neurology*, *19*(2), 170–178.
15. Blauwendraat, C., Reed, X., Krohn, L., Heilbron, K., Bandres-Ciga, S., Tan,

M., Gibbs, J. R., Hernandez, D. G., Kumaran, R., Langston, R., Bonet-Ponce, L., Alcalay, R. N., Hassin-Baer, S., Greenbaum, L., Iwaki, H., Leonard, H. L., Grenn, F. P., Ruskey, J. A., Sabir, M., … Singleton, A. B. (2020). Genetic modifiers of risk and age at onset in GBA associated Parkinson's disease and Lewy body dementia. *Brain: A Journal of Neurology*, *143*(1), 234–248.

16. Blesa, J., Foffani, G., Dehay, B., Bezard, E., & Obeso, J. A. (2022). Motor and non-motor circuit disturbances in early Parkinson disease: which happens first? *Nature Reviews. Neuroscience*, *23*(2), 115–128.
17. Bloom, J. S., Ehrenreich, I. M., Loo, W. T., Lite, T.-L. V., & Kruglyak, L. (2013). Finding the sources of missing heritability in a yeast cross. *Nature*, *494*(7436), 234–237.
18. Brakedal, B., Dölle, C., Riemer, F., Ma, Y., Nido, G. S., Skeie, G. O., Craven, A. R., Schwarzlmüller, T., Brekke, N., Diab, J., Sverkeli, L., Skjeie, V., Varhaug, K., Tysnes, O.-B., Peng, S., Haugarvoll, K., Ziegler, M., Grüner, R., Eidelberg, D., & Tzoulis, C. (2022). The NADPARK study: A randomized phase I trial of nicotinamide riboside supplementation in Parkinson's disease. *Cell Metabolism*, *34*(3), 396–407.e6.
19. Brice, C., Cubillos, F. A., Dequin, S., Camarasa, C., & Martínez, C. (2018). Adaptability of the Saccharomyces cerevisiae yeasts to wine fermentation conditions relies on their strong ability to consume nitrogen. *PloS One*, *13*(2), e0192383.
20. Brockmann, K., Schulte, C., Hauser, A.-K., Lichtner, P., Huber, H., Maetzler, W., Berg, D., & Gasser, T. (2013). SNCA: major genetic modifier of age at onset of Parkinson's disease. *Movement Disorders: Official Journal of the Movement Disorder Society*, *28*(9), 1217–1221.
21. Brooker, S. M., Naylor, G. E., & Krainc, D. (2024). Cell biology of Parkinson's disease: Mechanisms of synaptic, lysosomal, and mitochondrial dysfunction. *Current Opinion in Neurobiology*, *85*, 102841.
22. Burbulla, L. F., & Krüger, R. (2011). Converging environmental and genetic pathways in the pathogenesis of Parkinson's disease. *Journal of the Neurological Sciences*, *306*(1-2), 1–8.
23. Cannon, J. R., & Greenamyre, J. T. (2013). Gene-environment interactions in Parkinson's disease: specific evidence in humans and mammalian models. *Neurobiology of Disease*, *57*, 38–46.
24. Ceschin, J., Saint-Marc, C., Laporte, J., Labriet, A., Philippe, C., Moenner, M., Daignan-Fornier, B., & Pinson, B. (2014). Identification of yeast and human 5-aminoimidazole-4-carboxamide-1-β-d-ribofuranoside (AICAr) transporters. *The Journal of Biological Chemistry*, *289*(24), 16844–16854.
25. Chang, D., Nalls, M. A., Hallgrímsdóttir, I. B., Hunkapiller, J., van der Brug, M., Cai, F., International Parkinson's Disease Genomics Consortium, 23andMe Research Team, Kerchner, G. A., Ayalon, G., Bingol, B., Sheng, M., Hinds, D., Behrens, T. W., Singleton, A. B., Bhangale, T. R., & Graham, R. R. (2017). A meta-analysis of genome-wide association studies

identifies 17 new Parkinson's disease risk loci. *Nature Genetics*, *49*(10), 1511–1516.

26. Chao, C.-C., Huang, C.-L., Cheng, J.-J., Chiou, C.-T., Lee, I.-J., Yang, Y.-C., Hsu, T.-H., Yei, C.-E., Lin, P.-Y., Chen, J.-J., & Huang, N.-K. (2022). SRT1720 as an SIRT1 activator for alleviating paraquat-induced models of Parkinson's disease. *Redox Biology*, *58*, 102534.
27. Chen, Y., Zhang, S., Sorani, M., & Giacomini, K. M. (2007). Transport of paraquat by human organic cation transporters and multidrug and toxic compound extrusion family. *The Journal of Pharmacology and Experimental Therapeutics*, *322*(2), 695–700.
28. Cicchetti, F., Lapointe, N., Roberge-Tremblay, A., Saint-Pierre, M., Jimenez, L., Ficke, B. W., & Gross, R. E. (2005). Systemic exposure to paraquat and maneb models early Parkinson's disease in young adult rats. *Neurobiology of Disease*, *20*(2), 360–371.
29. Cooper, A. A., Gitler, A. D., Cashikar, A., Haynes, C. M., Hill, K. J., Bhullar, B., Liu, K., Xu, K., Strathearn, K. E., Liu, F., Cao, S., Caldwell, K. A., Caldwell, G. A., Marsischky, G., Kolodner, R. D., Labaer, J., Rochet, J.-C., Bonini, N. M., & Lindquist, S. (2006). Alpha-synuclein blocks ER-Golgi traffic and Rab1 rescues neuron loss in Parkinson's models. *Science*, *313*(5785), 324–328.
30. Coria, J., & Elgueta, S. (2022). Towards safer use of pesticides in Chile. *Environmental Science and Pollution Research International*, *29*(16), 22785–22797.
31. Cristóvão, A. C., Campos, F. L., Je, G., Esteves, M., Guhathakurta, S., Yang, L., Beal, M. F., Fonseca, B. M., Salgado, A. J., Queiroz, J., Sousa, N., Bernardino, L., Alves, G., Yoon, K.-S., & Kim, Y.-S. (2020). Characterization of a Parkinson's disease rat model using an upgraded paraquat exposure paradigm. *The European Journal of Neuroscience*, *52*(4), 3242–3255.
32. Cubillos, F. A., Billi, E., Zörgö, E., Parts, L., Fargier, P., Omholt, S., Blomberg, A., Warringer, J., Louis, E. J., & Liti, G. (2011). Assessing the complex architecture of polygenic traits in diverged yeast populations. *Molecular Ecology*, *20*(7), 1401–1413.
33. Cubillos, F. A., Louis, E. J., & Liti, G. (2009). Generation of a large set of genetically tractable haploid and diploid Saccharomyces strains. *FEMS Yeast Research*, *9*(8), 1217–1225.
34. Cubillos, F. A., Parts, L., Salinas, F., Bergström, A., Scovacricchi, E., Zia, A., Illingworth, C. J. R., Mustonen, V., Ibstedt, S., Warringer, J., Louis, E. J., Durbin, R., & Liti, G. (2013). High-resolution mapping of complex traits with a four-parent advanced intercross yeast population. *Genetics*, *195*(3), 1141–1155.
35. Dardiotis, E., Xiromerisiou, G., Hadjichristodoulou, C., Tsatsakis, A. M., Wilks, M. F., & Hadjigeorgiou, G. M. (2013). The interplay between environmental and genetic factors in Parkinson's disease susceptibility: the

evidence for pesticides. *Toxicology*, *307*, 17–23.
36. de Lau, L. M. L., & Breteler, M. M. B. (2006). Epidemiology of Parkinson's disease. *Lancet Neurology*, *5*(6), 525–535.
37. Ding, Y.-W., Zhao, G.-J., Li, X.-L., Hong, G.-L., Li, M.-F., Qiu, Q.-M., Wu, B., & Lu, Z.-Q. (2016). SIRT1 exerts protective effects against paraquat-induced injury in mouse type II alveolar epithelial cells by deacetylating NRF2 in vitro. *International Journal of Molecular Medicine*, *37*(4), 1049–1058.
38. Dinis-Oliveira, R. J., Remião, F., Carmo, H., Duarte, J. A., Navarro, A. S., Bastos, M. L., & Carvalho, F. (2006). Paraquat exposure as an etiological factor of Parkinson's disease. *Neurotoxicology*, *27*(6), 1110–1122.
39. Djukic, M., Jovanovic, M. C., Ninkovic, M., Vasiljevic, I., & Jovanovic, M. (2007). The role of nitric oxide in paraquat-induced oxidative stress in rat striatum. *Annals of Agricultural and Environmental Medicine: AAEM*, *14*(2), 247–252.
40. Domínguez-Oliva, A., Hernández-Ávalos, I., Martínez-Burnes, J., Olmos-Hernández, A., Verduzco-Mendoza, A., & Mota-Rojas, D. (2023). The Importance of Animal Models in Biomedical Research: Current Insights and Applications. *Animals : An Open Access Journal from MDPI*, *13*(7). https://doi.org/10.3390/ani13071223
41. Donaher, S. E., & Van den Hurk, P. (2023a). Ecotoxicology of the herbicide paraquat: effects on wildlife and knowledge gaps. *Ecotoxicology* , *32*(9), 1187–1199.
42. Donaher, S. E., & Van den Hurk, P. (2023b). Ecotoxicology of the herbicide paraquat: effects on wildlife and knowledge gaps. *Ecotoxicology* , *32*(9), 1187–1199.
43. Elkholy, A. R., El-Sheakh, A. R., & Suddek, G. M. (2023). Nilotinib alleviates paraquat-induced hepatic and pulmonary injury in rats via the Nrf2/Nf-kB axis. *International Immunopharmacology*, *124*(Pt A), 110886.
44. Fendt, S.-M., Oliveira, A. P., Christen, S., Picotti, P., Dechant, R. C., & Sauer, U. (2010). Unraveling condition-dependent networks of transcription factors that control metabolic pathway activity in yeast. *Molecular Systems Biology*, *6*, 432.
45. Gaare, J. J., Dölle, C., Brakedal, B., Brügger, K., Haugarvoll, K., Nido, G. S., & Tzoulis, C. (2023). Nicotinamide riboside supplementation is not associated with altered methylation homeostasis in Parkinson's disease. *iScience*, *26*(3), 106278.
46. Gao, H.-M., & Hong, J.-S. (2011). Gene-environment interactions: key to unraveling the mystery of Parkinson's disease. *Progress in Neurobiology*, *94*(1), 1–19.
47. García-Ríos, E., López-Malo, M., & Guillamón, J. M. (2014). Global phenotypic and genomic comparison of two Saccharomyces cerevisiae wine strains reveals a novel role of the sulfur assimilation pathway in adaptation at low temperature fermentations. *BMC Genomics*, *15*(1), 1059.

48. Goker-Alpan, O., Schiffmann, R., LaMarca, M. E., Nussbaum, R. L., McInerney-Leo, A., & Sidransky, E. (2004). Parkinsonism among Gaucher disease carriers. *Journal of Medical Genetics*, *41*(12), 937–940.
49. Gupta, R., Advani, D., Yadav, D., Ambasta, R. K., & Kumar, P. (2023). Dissecting the Relationship Between Neuropsychiatric and Neurodegenerative Disorders. *Molecular Neurobiology*. https://doi.org/10.1007/s12035-023-03502-9
50. Haldane, J. B. S. (1941). The relative importance of principal and modifying genes in determining some human diseases. *Journal of Genetics*, *41*(2-3), 149–157.
51. Hamza, T. H., & Payami, H. (2010). The heritability of risk and age at onset of Parkinson's disease after accounting for known genetic risk factors. *Journal of Human Genetics*, *55*(4), 241–243.
52. Han, S., Kim, S., Kim, H., Shin, H.-W., Na, K.-S., & Suh, H. S. (2019). Prevalence and incidence of Parkinson's disease and drug-induced parkinsonism in Korea. *BMC Public Health*, *19*(1), 1328.
53. Hansson, L., & Häggström, M. H. (1986). Metabolic effects of paraquat onSaccharomyces cerevisiae. *Current Microbiology*, *13*(2), 81–83.
54. Heitkamp, M., & Brown, O. (1981). Inhibition of NAD biosynthesis by paraquat in Escherichia coli. *Biochimica et Biophysica Acta, General Subjects*, *676*(3), 345–349.
55. Houzé, P., Baud, F. J., Mouy, R., Bismuth, C., Bourdon, R., & Scherrmann, J. M. (1990). Toxicokinetics of paraquat in humans. *Human & Experimental Toxicology*, *9*(1), 5–12.
56. Hsieh, Y.-W., Lin, J.-L., Lee, S.-Y., Weng, C.-H., Yang, H.-Y., Liu, S.-H., Wang, I.-K., Liang, C.-C., Chang, C.-T., & Yen, T.-H. (2013). Paraquat poisoning in pediatric patients. *Pediatric Emergency Care*, *29*(4), 487–491.
57. Hyun, C. H., Yoon, C. Y., Lee, H.-J., & Lee, S.-J. (2013). LRRK2 as a Potential Genetic Modifier of Synucleinopathies: Interlacing the Two Major Genetic Factors of Parkinson's Disease. *Experimental Neurobiology*, *22*(4), 249–257.
58. Islam, M. S., Azim, F., Saju, H., Zargaran, A., Shirzad, M., Kamal, M., Fatema, K., Rehman, S., Azad, M. A. M., & Ebrahimi-Barough, S. (2021). Pesticides and Parkinson's disease: Current and future perspective. *Journal of Chemical Neuroanatomy*, *115*, 101966.
59. Jara, M., Cubillos, F. A., García, V., Salinas, F., Aguilera, O., Liti, G., & Martínez, C. (2014). Mapping genetic variants underlying differences in the central nitrogen metabolism in fermenter yeasts. *PloS One*, *9*(1), e86533.
60. Jarolim, S., Millen, J., Heeren, G., Laun, P., Goldfarb, D. S., & Breitenbach, M. (2004a). A novel assay for replicative lifespan in Saccharomyces cerevisiae. *FEMS Yeast Research*, *5*(2), 169–177.
61. Jarolim, S., Millen, J., Heeren, G., Laun, P., Goldfarb, D. S., & Breitenbach, M. (2004b). A novel assay for replicative lifespan in Saccharomyces cerevisiae. *FEMS Yeast Research*, *5*(2), 169–177.

62. Johansson, M. E., Toni, I., Kessels, R. P. C., Bloem, B. R., & Helmich, R. C. (2024). Clinical severity in Parkinson's disease is determined by decline in cortical compensation. *Brain: A Journal of Neurology*, *147*(3), 871–886.
63. Johnson, B. S., McCaffery, J. M., Lindquist, S., & Gitler, A. D. (2008). A yeast TDP-43 proteinopathy model: Exploring the molecular determinants of TDP-43 aggregation and cellular toxicity. *Proceedings of the National Academy of Sciences of the United States of America*, *105*(17), 6439–6444.
64. Kachroo, A. H., Laurent, J. M., Yellman, C. M., Meyer, A. G., Wilke, C. O., & Marcotte, E. M. (2015). Evolution. Systematic humanization of yeast genes reveals conserved functions and genetic modularity. *Science*, *348*(6237), 921–925.
65. Kang, M. J., Gil, S. J., & Koh, H. C. (2009). Paraquat induces alternation of the dopamine catabolic pathways and glutathione levels in the substantia nigra of mice. *Toxicology Letters*, *188*(2), 148–152.
66. Karathia, H., Vilaprinyo, E., Sorribas, A., & Alves, R. (2011a). Saccharomyces cerevisiae as a model organism: a comparative study. *PloS One*, *6*(2), e16015.
67. Karathia, H., Vilaprinyo, E., Sorribas, A., & Alves, R. (2011b). Saccharomyces cerevisiae as a model organism: a comparative study. *PloS One*, *6*(2), e16015.
68. Kearney, J. A., & Jorge, B. S. (2012). Genetic modifiers of neurological disease. In *eLS*. John Wiley & Sons, Ltd. https://doi.org/10.1002/9780470015902.a0023856
69. Klein, A. D., & Mazzulli, J. R. (2018). Is Parkinson's disease a lysosomal disorder? *Brain: A Journal of Neurology*, *141*(8), 2255–2262.
70. Klein, A. D., & Outeiro, T. F. (2023). Glucocerebrosidase mutations disrupt the lysosome and now the mitochondria. *Nature Communications*, *14*(1), 6383.
71. Kriks, S., Shim, J.-W., Piao, J., Ganat, Y. M., Wakeman, D. R., Xie, Z., Carrillo-Reid, L., Auyeung, G., Antonacci, C., Buch, A., Yang, L., Beal, M. F., Surmeier, D. J., Kordower, J. H., Tabar, V., & Studer, L. (2011). Dopamine neurons derived from human ES cells efficiently engraft in animal models of Parkinson's disease. *Nature*, *480*(7378), 547–551.
72. Kropotov, A., Kulikova, V., Nerinovski, K., Yakimov, A., Svetlova, M., Solovjeva, L., Sudnitsyna, J., Migaud, M. E., Khodorkovskiy, M., Ziegler, M., & Nikiforov, A. (2021). Equilibrative Nucleoside Transporters Mediate the Import of Nicotinamide Riboside and Nicotinic Acid Riboside into Human Cells. *International Journal of Molecular Sciences*, *22*(3). https://doi.org/10.3390/ijms22031391
73. Kumar, S., Gupta, S., Bansal, Y. S., Bal, A., Rastogi, P., Muthu, V., & Arora, V. (2021). Pulmonary histopathology in fatal paraquat poisoning. *Autopsy & Case Reports*, *11*, e2021342.
74. Latourelle, J. C., Hendricks, A. E., Pankratz, N., Wilk, J. B., Halter, C.,

Nichols, W. C., Gusella, J. F., Destefano, A. L., Myers, R. H., Foroud, T., & PSG-Progeni GenePD Investigators, Coordinators, and Molecular Genetic Laboratories. (2011). Genomewide linkage study of modifiers of LRRK2-related Parkinson's disease. *Movement Disorders: Official Journal of the Movement Disorder Society*, *26*(11), 2039–2044.

75. Lehmann, S., Loh, S. H. Y., & Martins, L. M. (2017). Enhancing NAD salvage metabolism is neuroprotective in a PINK1 model of Parkinson's disease. *Biology Open*, *6*(2), 141–147.
76. LeWitt, P. A., & Chaudhuri, K. R. (2020). Unmet needs in Parkinson disease: Motor and non-motor. *Parkinsonism & Related Disorders*, *80 Suppl 1*, S7–S12.
77. Li, D., Mastaglia, F. L., Fletcher, S., & Wilton, S. D. (2020). Progress in the molecular pathogenesis and nucleic acid therapeutics for Parkinson's disease in the precision medicine era. *Medicinal Research Reviews*, *40*(6), 2650–2681.
78. Lippert, C., Listgarten, J., Liu, Y., Kadie, C. M., Davidson, R. I., & Heckerman, D. (2011). FaST linear mixed models for genome-wide association studies. *Nature Methods*, *8*(10), 833–835.
79. Li, S., Zhao, G., Chen, L., Ding, Y., Lian, J., Hong, G., & Lu, Z. (2016). Resveratrol protects mice from paraquat-induced lung injury: The important role of SIRT1 and NRF2 antioxidant pathways. *Molecular Medicine Reports*, *13*(2), 1833–1838.
80. Liu, W., Li, L., Ye, H., Chen, H., Shen, W., Zhong, Y., Tian, T., & He, H. (2017). From Saccharomyces cerevisiae to human: The important gene co-expression modules. *Biomedical Reports*, *7*(2), 153–158.
81. Liu, X., Yang, H., & Liu, Z. (2022). Signaling pathways involved in paraquat-induced pulmonary toxicity: Molecular mechanisms and potential therapeutic drugs. *International Immunopharmacology*, *113*(Pt A), 109301.
82. Li, X., Feng, Y., Wang, X.-X., Truong, D., & Wu, Y.-C. (2020). The Critical Role of SIRT1 in Parkinson's Disease: Mechanism and Therapeutic Considerations. *Aging and Disease*, *11*(6), 1608–1622.
83. Li, Y., Zhong, X., Ye, J., Guo, H., & Long, Y. (2021). Proteome of Saccharomyces cerevisiae under paraquat stress regulated by therapeutic concentration of copper ions. *Ecotoxicology and Environmental Safety*, *217*, 112245.
84. Marder, K., Levy, G., Louis, E. D., Mejia-Santana, H., Cote, L., Andrews, H., Harris, J., Waters, C., Ford, B., Frucht, S., Fahn, S., & Ottman, R. (2003). Familial aggregation of early- and late-onset Parkinson's disease. *Annals of Neurology*, *54*(4), 507–513.
85. Marian, A. J. (2002). Modifier genes for hypertrophic cardiomyopathy. *Current Opinion in Cardiology*, *17*(3), 242–252.
86. Mascarenhas, C., Edwards-Ingram, L. C., Zeef, L., Shenton, D., Ashe, M. P., & Grant, C. M. (2008). Gcn4 is required for the response to peroxide stress in the yeast Saccharomyces cerevisiae. *Molecular Biology of the*

Cell, *19*(7), 2995–3007.

87. McCormack, A. L., Thiruchelvam, M., Manning-Bog, A. B., Thiffault, C., Langston, J. W., Cory-Slechta, D. A., & Di Monte, D. A. (2002). Environmental risk factors and Parkinson's disease: selective degeneration of nigral dopaminergic neurons caused by the herbicide paraquat. *Neurobiology of Disease*, *10*(2), 119–127.
88. Menezes, R., Tenreiro, S., Macedo, D., Santos, C. N., & Outeiro, T. F. (2015). From the baker to the bedside: yeast models of Parkinson's disease. *Microbial Cell Factories*, *2*(8), 262–279.
89. Mischley, L. K., Shankland, E., Liu, S. Z., Bhayana, S., Fox, D. J., & Marcinek, D. J. (2023). ATP and NAD Deficiency in Parkinson's Disease. *Nutrients*, *15*(4). https://doi.org/10.3390/nu15040943
90. Mojzita, D., & Hohmann, S. (2006). Pdc2 coordinates expression of the THI regulon in the yeast Saccharomyces cerevisiae. *Molecular Genetics and Genomics: MGG*, *276*(2), 147–161.
91. Mülleder, M., Capuano, F., Pir, P., Christen, S., Sauer, U., Oliver, S. G., & Ralser, M. (2012). A prototrophic deletion mutant collection for yeast metabolomics and systems biology. *Nature Biotechnology*, *30*(12), 1176–1178.
92. Nadeau, J. H. (2001). Modifier genes in mice and humans. *Nature Reviews. Genetics*, *2*(3), 165–174.
93. Nalls, M. A., Blauwendraat, C., Vallerga, C. L., Heilbron, K., Bandres-Ciga, S., Chang, D., Tan, M., Kia, D. A., Noyce, A. J., Xue, A., Bras, J., Young, E., von Coelln, R., Simón-Sánchez, J., Schulte, C., Sharma, M., Krohn, L., Pihlstrøm, L., Siitonen, A., … International Parkinson's Disease Genomics Consortium. (2019). Identification of novel risk loci, causal insights, and heritable risk for Parkinson's disease: a meta-analysis of genome-wide association studies. *Lancet Neurology*, *18*(12), 1091–1102.
94. Nestelbacher, R., Laun, P., Vondráková, D., Pichová, A., Schüller, C., & Breitenbach, M. (2000a). The influence of oxygen toxicity on yeast mother cell-specific aging. *Experimental Gerontology*, *35*(1), 63–70.
95. Nestelbacher, R., Laun, P., Vondráková, D., Pichová, A., Schüller, C., & Breitenbach, M. (2000b). The influence of oxygen toxicity on yeast mother cell-specific aging. *Experimental Gerontology*, *35*(1), 63–70.
96. Ngo, K. J., Paul, K. C., Wong, D., Kusters, C. D. J., Bronstein, J. M., Ritz, B., & Fogel, B. L. (2024). Lysosomal genes contribute to Parkinson's disease near agriculture with high intensity pesticide use. *NPJ Parkinson's Disease*, *10*(1), 87.
97. O'Brien, K. P., Remm, M., & Sonnhammer, E. L. L. (2005). Inparanoid: a comprehensive database of eukaryotic orthologs. *Nucleic Acids Research*, *33*(Database issue), D476–D480.
98. Oftadeh, O., Salvy, P., Masid, M., Curvat, M., Miskovic, L., & Hatzimanikatis, V. (2021a). A genome-scale metabolic model of Saccharomyces cerevisiae that integrates expression constraints and

reaction thermodynamics. *Nature Communications*, *12*(1), 4790.

99. Oftadeh, O., Salvy, P., Masid, M., Curvat, M., Miskovic, L., & Hatzimanikatis, V. (2021b). A genome-scale metabolic model of Saccharomyces cerevisiae that integrates expression constraints and reaction thermodynamics. *Nature Communications*, *12*(1), 4790.
100. Olivares, G. H., Olguín, P., & Klein, A. D. (2019). Modeling Parkinson's Disease Heterogeneity to Accelerate Precision Medicine. *Trends in Molecular Medicine*, *25*(12), 1052–1055.
101. Ossowska, K., Smiałowska, M., Kuter, K., Wierońska, J., Zieba, B., Wardas, J., Nowak, P., Dabrowska, J., Bortel, A., Biedka, I., Schulze, G., & Rommelspacher, H. (2006). Degeneration of dopaminergic mesocortical neurons and activation of compensatory processes induced by a long-term paraquat administration in rats: implications for Parkinson's disease. *Neuroscience*, *141*(4), 2155–2165.
102. Outeiro, T. F., & Lindquist, S. (2003). Yeast cells provide insight into alpha-synuclein biology and pathobiology. *Science*, *302*(5651), 1772–1775.
103. Ou, Z., Pan, J., Tang, S., Duan, D., Yu, D., Nong, H., & Wang, Z. (2021). Global Trends in the Incidence, Prevalence, and Years Lived With Disability of Parkinson's Disease in 204 Countries/Territories From 1990 to 2019. *Frontiers in Public Health*, *9*, 776847.
104. Paluszynski, J. P., Klassen, R., Rohe, M., & Meinhardt, F. (2006). Various cytosine/adenine permease homologues are involved in the toxicity of 5-fluorocytosine in Saccharomyces cerevisiae. *Yeast* , *23*(9), 707–715.
105. Pan-Montojo, F., Anichtchik, O., Dening, Y., Knels, L., Pursche, S., Jung, R., Jackson, S., Gille, G., Spillantini, M. G., Reichmann, H., & Funk, R. H. W. (2010). Progression of Parkinson's disease pathology is reproduced by intragastric administration of rotenone in mice. *PloS One*, *5*(1), e8762.
106. Paul, K. C., Cockburn, M., Gong, Y., Bronstein, J., & Ritz, B. (2024). Agricultural paraquat dichloride use and Parkinson's disease in California's Central Valley. *International Journal of Epidemiology*, *53*(1). https://doi.org/10.1093/ije/dyae004
107. Pereira, C., Costa, V., Martins, L. M., & Saraiva, L. (2015). A yeast model of the Parkinson's disease-associated protein Parkin. *Experimental Cell Research*, *333*(1), 73–79.
108. Pérez, M. J., Baden, P., & Deleidi, M. (2021). Progresses in both basic research and clinical trials of NAD+ in Parkinson's disease. *Mechanisms of Ageing and Development*, *197*, 111499.
109. Peter, J., De Chiara, M., Friedrich, A., Yue, J.-X., Pflieger, D., Bergström, A., Sigwalt, A., Barre, B., Freel, K., Llored, A., Cruaud, C., Labadie, K., Aury, J.-M., Istace, B., Lebrigand, K., Barbry, P., Engelen, S., Lemainque, A., Wincker, P., … Schacherer, J. (2018). Genome evolution across 1,011 Saccharomyces cerevisiae isolates. *Nature*, *556*(7701), 339–344.
110. Polymeropoulos, M. H., Lavedan, C., Leroy, E., Ide, S. E., Dehejia, A., Dutra, A., Pike, B., Root, H., Rubenstein, J., Boyer, R., Stenroos, E. S.,

Chandrasekharappa, S., Athanassiadou, A., Papapetropoulos, T., Johnson, W. G., Lazzarini, A. M., Duvoisin, R. C., Di Iorio, G., Golbe, L. I., & Nussbaum, R. L. (1997). Mutation in the alpha-synuclein gene identified in families with Parkinson's disease. *Science*, *276*(5321), 2045–2047.

111. Pouchieu, C., Piel, C., Carles, C., Gruber, A., Helmer, C., Tual, S., Marcotullio, E., Lebailly, P., & Baldi, I. (2018). Pesticide use in agriculture and Parkinson's disease in the AGRICAN cohort study. *International Journal of Epidemiology*, *47*(1), 299–310.
112. Prasad, K., Winnik, B., Thiruchelvam, M. J., Buckley, B., Mirochnitchenko, O., & Richfield, E. K. (2007). Prolonged toxicokinetics and toxicodynamics of paraquat in mouse brain. *Environmental Health Perspectives*, *115*(10), 1448–1453.
113. Pretty, J., & Bharucha, Z. P. (2015). Integrated Pest Management for Sustainable Intensification of Agriculture in Asia and Africa. *Insects*, *6*(1), 152–182.
114. Quispe, X., Tapia, S. M., Villarroel, C., Oporto, C., Abarca, V., García, V., Martínez, C., & Cubillos, F. A. (2017). Genetic basis of mycotoxin susceptibility differences between budding yeast isolates. *Scientific Reports*, *7*(1), 9173.
115. Rahit, K. M. T. H., & Tarailo-Graovac, M. (2020). Genetic Modifiers and Rare Mendelian Disease. *Genes*, *11*(3). https://doi.org/10.3390/genes11030239
116. Romero-Aguilar, L., Vázquez-Meza, H., Guerra-Sánchez, G., Luqueño-Bocardo, O. I., & Pardo, J. P. (2022). The Mitochondrial Alternative Oxidase in Is Not Involved in Response to Oxidative Stress Induced by Paraquat. *Journal of Fungi (Basel, Switzerland)*, *8*(11). https://doi.org/10.3390/jof8111221
117. Ross, O. A., & Rademakers, R. (2016). Modifiers of LRRK2 parkinsonism: new therapeutic targets. *Lancet Neurology*, *15*(12), 1200–1201.
118. Rubilar, J. C., Outeiro, T. F., & Klein, A. D. (2024). The lysosomal β-glucocerebrosidase strikes mitochondria: implications for Parkinson's therapeutics. *Brain: A Journal of Neurology*. https://doi.org/10.1093/brain/awae070
119. Salinas, F., de Boer, C. G., Abarca, V., García, V., Cuevas, M., Araos, S., Larrondo, L. F., Martínez, C., & Cubillos, F. A. (2016). Natural variation in non-coding regions underlying phenotypic diversity in budding yeast. *Scientific Reports*, *6*, 21849.
120. Satake, W., Nakabayashi, Y., Mizuta, I., Hirota, Y., Ito, C., Kubo, M., Kawaguchi, T., Tsunoda, T., Watanabe, M., Takeda, A., Tomiyama, H., Nakashima, K., Hasegawa, K., Obata, F., Yoshikawa, T., Kawakami, H., Sakoda, S., Yamamoto, M., Hattori, N., … Toda, T. (2009). Genome-wide association study identifies common variants at four loci as genetic risk factors for Parkinson's disease. *Nature Genetics*, *41*(12), 1303–1307.
121. Scarffe, L. A., Stevens, D. A., Dawson, V. L., & Dawson, T. M. (2014).

Parkin and PINK1: much more than mitophagy. *Trends in Neurosciences*, *37*(6), 315–324.

122. Schöndorf, D. C., Aureli, M., McAllister, F. E., Hindley, C. J., Mayer, F., Schmid, B., Sardi, S. P., Valsecchi, M., Hoffmann, S., Schwarz, L. K., Hedrich, U., Berg, D., Shihabuddin, L. S., Hu, J., Pruszak, J., Gygi, S. P., Sonnino, S., Gasser, T., & Deleidi, M. (2014). iPSC-derived neurons from GBA1-associated Parkinson's disease patients show autophagic defects and impaired calcium homeostasis. *Nature Communications*, *5*, 4028.
123. Schöndorf, D. C., Ivanyuk, D., Baden, P., Sanchez-Martinez, A., De Cicco, S., Yu, C., Giunta, I., Schwarz, L. K., Di Napoli, G., Panagiotakopoulou, V., Nestel, S., Keatinge, M., Pruszak, J., Bandmann, O., Heimrich, B., Gasser, T., Whitworth, A. J., & Deleidi, M. (2018). The NAD+ Precursor Nicotinamide Riboside Rescues Mitochondrial Defects and Neuronal Loss in iPSC and Fly Models of Parkinson's Disease. *Cell Reports*, *23*(10), 2976–2988.
124. See, W. Z. C., Naidu, R., & Tang, K. S. (2022). Cellular and Molecular Events Leading to Paraquat-Induced Apoptosis: Mechanistic Insights into Parkinson's Disease Pathophysiology. *Molecular Neurobiology*, *59*(6), 3353–3369.
125. See, W. Z. C., Naidu, R., & Tang, K. S. (2024). Paraquat and Parkinson's Disease: The Molecular Crosstalk of Upstream Signal Transduction Pathways Leading to Apoptosis. *Current Neuropharmacology*, *22*(1), 140–151.
126. Sharma, D. R., Thapa, R. B., & Manandhar, H. K. (2012). Use of pesticides in Nepal and impacts on human health and environment. *Journal of Agriculture of Western Australia*. https://www.cabdirect.org/cabdirect/abstract/20133093039
127. Sharma, P., & Mittal, P. (2024). Paraquat (herbicide) as a cause of Parkinson's Disease. *Parkinsonism & Related Disorders*, *119*, 105932.
128. Shi, L., Yu, G., Li, Y., Zhao, L., Wen, Z., Tao, Y., Wang, W., & Jian, X. (2022). The toxicokinetics of acute paraquat poisoning in specific patients: a case series. *The Journal of International Medical Research*, *50*(9), 3000605221122745.
129. Shi, M., Zeng, M., Jian, T., Yu, G., Genjiafu, A., Zhang, X., Guo, L., Shang, R., Zhou, Z., Zhang, T., Jian, X., & Kan, B. (2023). A mass event of paraquat poisoning via inhalation. *Frontiers in Public Health*, *11*, 1309708.
130. Sidransky, E., Nalls, M. A., Aasly, J. O., Aharon-Peretz, J., Annesi, G., Barbosa, E. R., Bar-Shira, A., Berg, D., Bras, J., Brice, A., Chen, C.-M., Clark, L. N., Condroyer, C., De Marco, E. V., Dürr, A., Eblan, M. J., Fahn, S., Farrer, M. J., Fung, H.-C., … Ziegler, S. G. (2009). Multicenter analysis of glucocerebrosidase mutations in Parkinson's disease. *The New England Journal of Medicine*, *361*(17), 1651–1661.
131. Singleton, A. B., Farrer, M. J., & Bonifati, V. (2013). The genetics of Parkinson's disease: progress and therapeutic implications. *Movement*

Disorders: Official Journal of the Movement Disorder Society, *28*(1), 14–23.

132. Slatkin, M. (2008). Linkage disequilibrium--understanding the evolutionary past and mapping the medical future. *Nature Reviews. Genetics*, *9*(6), 477–485.
133. Stenberg, S., Li, J., Gjuvsland, A. B., Persson, K., Demitz-Helin, E., González Peña, C., Yue, J.-X., Gilchrist, C., Ärengård, T., Ghiaci, P., Larsson-Berglund, L., Zackrisson, M., Smits, S., Hallin, J., Höög, J. L., Molin, M., Liti, G., Omholt, S. W., & Warringer, J. (2022). Genetically controlled mtDNA deletions prevent ROS damage by arresting oxidative phosphorylation. *eLife*, *11*. https://doi.org/10.7554/eLife.76095
134. Sukumar, C. A., Shanbhag, V., & Shastry, A. B. (2019). Paraquat: The Poison Potion. *Indian Journal of Critical Care Medicine: Peer-Reviewed, Official Publication of Indian Society of Critical Care Medicine*, *23*(Suppl 4), S263–S266.
135. Tanner, C. M., Kamel, F., Ross, G. W., Hoppin, J. A., Goldman, S. M., Korell, M., Marras, C., Bhudhikanok, G. S., Kasten, M., Chade, A. R., Comyns, K., Richards, M. B., Meng, C., Priestley, B., Fernandez, H. H., Cambi, F., Umbach, D. M., Blair, A., Sandler, D. P., & Langston, J. W. (2011). Rotenone, paraquat, and Parkinson's disease. *Environmental Health Perspectives*, *119*(6), 866–872.
136. Tanner, C. M., Ottman, R., Goldman, S. M., Ellenberg, J., Chan, P., Mayeux, R., & Langston, J. W. (1999). Parkinson disease in twins: an etiologic study. *JAMA: The Journal of the American Medical Association*, *281*(4), 341–346.
137. Tenreiro, S., Franssens, V., Winderickx, J., & Outeiro, T. F. (2017). Yeast models of Parkinson's disease-associated molecular pathologies. *Current Opinion in Genetics & Development*, *44*, 74–83.
138. Tiên Nguyên-nhu, N., & Knoops, B. (2003). Mitochondrial and cytosolic expression of human peroxiredoxin 5 in Saccharomyces cerevisiae protect yeast cells from oxidative stress induced by paraquat. *FEBS Letters*, *544*(1-3), 148–152.
139. Torres-Rojas, C., Zhuang, D., Jimenez-Carrion, P., Silva, I., O'Callaghan, J. P., Lu, L., Zhao, W., Mulligan, M. K., Williams, R. W., & Jones, B. C. (2020). Systems Genetics and Systems Biology Analysis of Paraquat Neurotoxicity in BXD Recombinant Inbred Mice. *Toxicological Sciences: An Official Journal of the Society of Toxicology*, *176*(1), 137–146.
140. Tudi, M., Daniel Ruan, H., Wang, L., Lyu, J., Sadler, R., Connell, D., Chu, C., & Phung, D. T. (2021). Agriculture Development, Pesticide Application and Its Impact on the Environment. *International Journal of Environmental Research and Public Health*, *18*(3). https://doi.org/10.3390/ijerph18031112
141. Uversky, V. N. (2004). Neurotoxicant-induced animal models of Parkinson's disease: understanding the role of rotenone, maneb and paraquat in neurodegeneration. *Cell and Tissue Research*, *318*(1), 225–

241.
142. Wakade, C., & Chong, R. (2014). A novel treatment target for Parkinson's disease. *Journal of the Neurological Sciences*, *347*(1-2), 34–38.
143. Warringer, J., Zörgö, E., Cubillos, F. A., Zia, A., Gjuvsland, A., Simpson, J. T., Forsmark, A., Durbin, R., Omholt, S. W., Louis, E. J., Liti, G., Moses, A., & Blomberg, A. (2011). Trait variation in yeast is defined by population history. *PLoS Genetics*, *7*(6), e1002111.
144. Willingham, S., Outeiro, T. F., DeVit, M. J., Lindquist, S. L., & Muchowski, P. J. (2003). Yeast genes that enhance the toxicity of a mutant huntingtin fragment or alpha-synuclein. *Science*, *302*(5651), 1769–1772.
145. Winzeler, E. A., Shoemaker, D. D., Astromoff, A., Liang, H., Anderson, K., Andre, B., Bangham, R., Benito, R., Boeke, J. D., Bussey, H., Chu, A. M., Connelly, C., Davis, K., Dietrich, F., Dow, S. W., El Bakkoury, M., Foury, F., Friend, S. H., Gentalen, E., … Davis, R. W. (1999). Functional characterization of the S. cerevisiae genome by gene deletion and parallel analysis. *Science*, *285*(5429), 901–906.
146. Xiong, G., Zhao, L., Yan, M., Wang, X., Zhou, Z., & Chang, X. (2019). N-acetylcysteine alleviated paraquat-induced mitochondrial fragmentation and autophagy in primary murine neural progenitor cells. *Journal of Applied Toxicology: JAT*, *39*(11), 1557–1567.
147. Youle, R. J., & Narendra, D. P. (2011). Mechanisms of mitophagy. *Nature Reviews. Molecular Cell Biology*, *12*(1), 9–14.
148. Zhang, X.-F., Thompson, M., & Xu, Y.-H. (2016). Multifactorial theory applied to the neurotoxicity of paraquat and paraquat-induced mechanisms of developing Parkinson's disease. *Laboratory Investigation; a Journal of Technical Methods and Pathology*, *96*(5), 496–507.
149. Zhu, J.-H., Guo, F., Shelburne, J., Watkins, S., & Chu, C. T. (2003). Localization of phosphorylated ERK/MAP kinases to mitochondria and autophagosomes in Lewy body diseases. *Brain Pathology* , *13*(4), 473–481.
150. Zwietering, M. H., Jongenburger, I., Rombouts, F. M., & van 't Riet, K. (1990). Modeling of the bacterial growth curve. *Applied and Environmental Microbiology*, *56*(6), 1875–1881.

15. APPENDIX: Publications

BRAIN
REVIEW ARTICLE

The lysosomal β-glucocerebrosidase strikes mitochondria: implications for Parkinson's therapeutics

Juan Carlos Rubilar,[1] Tiago Fleming Outeiro[2,3,4,5] and Andrés D. Klein[1]

Parkinson's disease is a neurodegenerative disorder primarily known for typical motor features that arise due to the loss of dopaminergic neurons in the substantia nigra. However, the precise molecular aetiology of the disease is still unclear. Several cellular pathways have been linked to Parkinson's disease, including the autophagy-lysosome pathway, α-synuclein aggregation and mitochondrial function. Interestingly, the mechanistic link between *GBA1*, the gene that encodes for lysosomal β-glucocerebrosidase (GCase), and Parkinson's disease lies in the interplay between GCase functions in the lysosome and mitochondria. GCase mutations alter mitochondria-lysosome contact sites. In the lysosome, reduced GCase activity leads to glycosphingolipid build-up, disrupting lysosomal function and autophagy, thereby triggering α-synuclein accumulation. Additionally, α-synuclein aggregates reduce GCase activity, creating a self-perpetuating cycle of lysosomal dysfunction and α-synuclein accumulation. GCase can also be imported into the mitochondria, where it promotes the integrity and function of mitochondrial complex I. Thus, GCase mutations that impair its normal function increase oxidative stress in mitochondria, the compartment where dopamine is oxidized. In turn, the accumulation of oxidized dopamine adducts further impairs GCase activity, creating a second cycle of GCase dysfunction. The oxidative state triggered by GCase dysfunction can also induce mitochondrial DNA damage which, in turn, can cause dopaminergic cell death. In this review, we highlight the pivotal role of GCase in Parkinson's disease pathogenesis and discuss promising examples of GCase-based therapeutics, such as gene and enzyme replacement therapies, small molecule chaperones and substrate reduction therapies, among others, as potential therapeutic interventions.

1 Centro de Genética y Genómica, Facultad de Medicina, Clínica Alemana Universidad del Desarrollo, Santiago 7780272, Chile
2 Department of Experimental Neurodegeneration, Center for Biostructural Imaging of Neurodegeneration, University Medical Center Göttingen, 37073, Göttingen, Germany
3 Max Planck Institute for Natural Sciences, 37073, Göttingen, Germany
4 Translational and Clinical Research Institute, Faculty of Medical Sciences, Newcastle University, Framlington Place, Newcastle Upon Tyne, NE2 4HH, UK
5 Scientific Employee with an Honorary Contract at Deutsches Zentrum für Neurodegenerative Erkrankungen (DZNE), 37075, Göttingen, Germany

Correspondence to: Andrés D. Klein
Centro de Genética y Genómica, Facultad de Medicina, Clínica Alemana Universidad del Desarrollo, Av. La Plaza 680, Santiago, 7780272, Chile
E-mail: andresklein@udd.cl

Received November 30, 2023. Revised January 31, 2024. Accepted February 14, 2024. Advance access publication March 4, 2024

Correspondence may also be addressed to: Tiago Fleming Outeiro
Department of Experimental Neurodegeneration, Center for Biostructural Imaging of Neurodegeneration, University Medical Center Göttingen, Von-Siebold-Straße 3a, 37075, Göttingen, Germany
E-mail: tiago.outeiro@med.uni-goettingen.de

Keywords: Parkinson's disease; Gaucher's disease; lysosome; mitochondria; neurodegeneration; therapeutics

Introduction

Parkinson's disease (PD) is a prevalent age-associated neurodegenerative condition characterized by symptoms such as bradykinesia, resting tremor, rigidity and postural instability. Additionally, PD manifests various non-motor features, including cognitive impairment, sleep abnormalities, hyposmia, cognitive dysfunction, constipation, pain or sensory disturbances.[1]

The global burden of disability and mortality related to PD is increasing at a faster rate compared to other neurological disorders. Over the past 25 years, the prevalence of PD has approximately doubled with an estimated 8.5 million individuals living with PD worldwide in 2019.[2-4]

Neuropathologically, PD is characterized by the loss of dopaminergic neurons (DA) from the substantia nigra and the accumulation of proteinaceous inclusions rich in the protein α-synuclein (α-syn) within cells, primarily in the brain. In the brain, the accumulation of α-syn typically begins either in the lower brainstem or in olfactory bulb and, as disease progresses, is thought to spread to the substantia nigra and to other brain regions.[5] However, emerging studies suggest that PD may exist in multiple clinical subtypes, differing in their neuropathological classification, genetic subtyping, biomarker signatures and mechanisms of disease, including variation in misfolded α-syn accumulation.[6] Recent studies also suggest that, at least in some cases, α-syn aggregation may originate in dopaminergic neurons in the gut, subsequently propagating to the brain through the vagus nerve.[7] Therefore, it will be important to continue integrating various modalities of biological information in order to improve our understanding of different forms of PD.[6,8]

While the majority of PD cases have no known genetic alteration, deciphering the contribution of genetic factors in PD is extremely important for our understanding of the molecular mechanisms underlying the disease. These factors range from highly penetrant rare DNA variants found in familial cases, to more common variants with smaller individual effects in sporadic cases. Historically, linkage studies in large PD families led to the discovery of genes such as *SNCA* (α-syn), *LRKK2*, DJ-1 (*PARK7*) and *PINK1*, among others.[9-11] These, and other PD-associated genes, have been connected to intracellular trafficking and mitochondrial biology. Next generation sequencing studies, including exome and genome sequencing, have further advanced our understanding of PD genetics. Genome-wide association studies (GWASs) have already identified ~90 independent common risk signals associated with PD, highlighting the involvement of the lysosome and related organelles in the pathogenesis of the disease.[12]

GCase and other lysosomal hydrolases strike the lysosome in Parkinson's disease

The *GBA1* gene encodes for the lysosomal β-glucocerebrosidase (GCase), an essential enzyme involved in sphingolipid metabolism. GCase breaks down glucosylceramide (GlcCer) into ceramide and glucose. Biallelic mutations in the *GBA1* gene lead to Gaucher's disease (GD), a lysosomal storage disorder characterized by the accumulation of GlcCer, glucosylsphingosine (GlcSph) and other glycosphingolipids (GSLs) within cells.[13] GD exhibits a highly diverse range of phenotypes, including neuropathic and non-neuropathic forms. The underlying molecular mechanism responsible for this variability remains unknown. However, it has been suggested that genomic modifiers may play a significant role.[14,15] GD is a rare condition in the general population, with an incidence of ~1 in 40 000 to 1 in 60 000 births. Importantly, certain populations, such as Ashkenazi Jews, have a higher incidence of ~1 in 800 individuals.[16,17]

The connection between *GBA1* mutations and PD initially emerged from anecdotal cases observed in relatives of GD patients, particularly within the Jewish population. At first, it was perceived as a mere coincidence due to the high prevalence of both diseases in this population.[18,19] However, a genomic study of 99 PD Ashkenazi patients showed that 31% of them presented variants in at least one *GBA1* allele.[20] This observation was further confirmed when a large-scale GWAS, including 5691 patients with PD (780 Ashkenazi Jews) and 4898 controls (387 Ashkenazi Jews) revealed that mutations in one allele of the *GBA1* gene substantially increase the risk of developing PD.[21] Subsequent investigations further confirmed the association between *GBA1* and PD and expanded it to include other variants in lysosomal genes, such as *GALC*, *CTSB*, *ATP6V0A1*, *SMPD1*, and others, across various human populations.[22-24]

In the general population, ~5% of PD patients carry a *GBA1* mutation, but this prevalence can rise to as high as 30% among individuals of Ashkenazi Jewish descent.[19,25,26] For reasons still unknown, the mean age at onset of PD among patients harbouring *GBA1* mutations is 4–5 years earlier than non-carriers; these individuals experience more rapid progression of motor impairment and cognitive decline and have reduced survival rates.[27] Intriguingly, GCase is abundantly expressed in the brain, particularly within dopaminergic neurons.[28] As a result, dysfunctional GCase may interfere with their normal function.

The genetic landscape of *GBA1* is extensive, with over 350 described mutations in a protein of 497 amino acids.[29] These variants encompass amino acid substitutions, insertions, deletions and complex alleles. Among them, the most common ones are c.1226A>G (p.N370S), c.1342G>C (p.D409H), and c.1448T>C (p.L444P). Homozygosity for these mutations results in GD and a significant reduction in GCase activity.[30] Interestingly, other *GBA1* variants like c.1093G>A (p.E326 K) are associated with PD but do not cause GD when present in homozygosity.[31] Instead, they only lead to a subtle reduction in GCase activity.[30,32] Systematic studies have been conducted to evaluate the risk of PD associated with each specific *GBA1* mutation. A web browser tool has been designed for this purpose,[33] emphasizing the predictive role of *GBA1* mutations as biomarkers for PD symptoms and progression.

It is important to note that a mutation in *GBA1* or other in lysosomal genes is not sufficient to trigger PD. This suggests an interaction with other genetic and/or environmental factors is necessary for PD to manifest, and is a research field that requires continued attention.

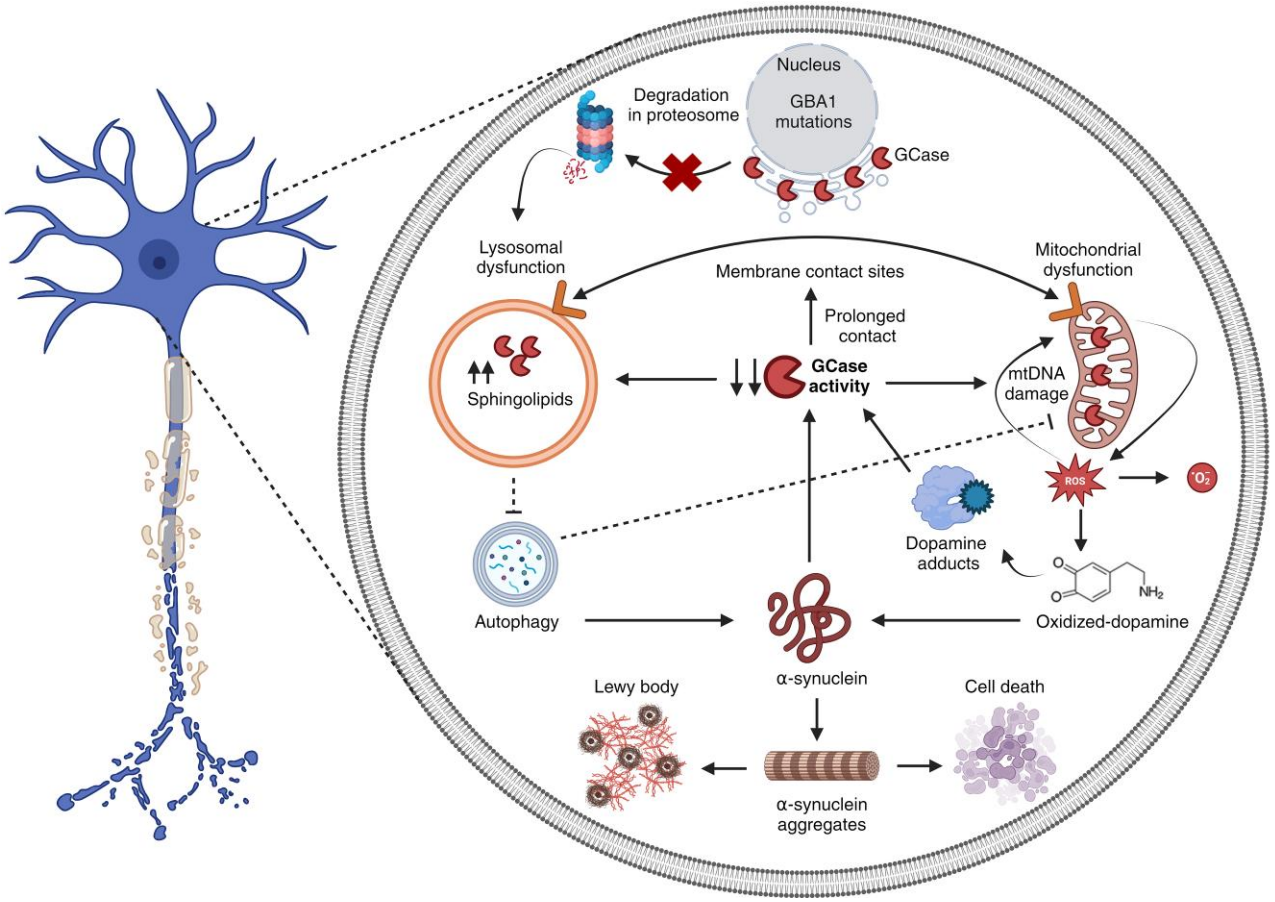

Figure 1 GCase exists in lysosomes and in mitochondria and plays a significant role in PD. Reduced GCase activity within the lysosomes leads to elevated sphingolipid levels and hinders autophagic flux, resulting in the aggregation of α-syn into putatively toxic clusters. In turn, the accumulation of α-syn impairs GCase activity, initiating a detrimental cycle of cellular self-destruction. GCase also supports the proper functioning of mitochondrial complex I and maintains mitochondrial integrity. Alterations in GCase activity cause an increase in reactive oxygen species (ROS), leading to dopamine oxidation, intensifying α-syn aggregation, and further impairment of GCase activity, creating a second destructive cycle. Additionally, autophagy deficiencies impair the elimination of damaged mitochondria, leading to an additional rise in ROS levels. ROS damages mtDNA, which triggers α-syn accumulation and cell death. Furthermore, the lysosome and mitochondria are connected through membrane contact sites (MCS), facilitating the exchange of molecules, including toxic lipids and probably dysfunctional GCase. Black arrows indicate promotion of a mechanism and 'T' indicates inhibition. GCase = β-glucocerebrosidase; PD = Parkinson's disease. Figure created with BioRender.com.

Molecular mechanisms linking GCase to Parkinson's disease

The mechanistic link between GCase mutations and PD is being continuously refined as new studies emerge (Fig. 1). Loss-of-function variants in *GBA1* have been found to trigger lysosomal dysfunction. For instance, CRISPR/Cas9 gene-edited isogenic human dopaminergic-like neuroblastoma cells lacking CGase or bearing the p.N370S or p.L444P variants show lysosomal alkalinization, accompanied by less protein breakdown within lysosomes but not total protein degradation. This was analysed by measuring the degradation rate of long-lived proteins labelled with radioactive valine in the presence of ammonium chloride and leupeptin.[34] Furthermore, a reduction in the activity of cathepsin D, β-hexosaminidase and acid phosphatase was observed only when the activity was analysed in isolated lysosomes, but not in the total homogenates. These changes are accompanied by increased levels of GCase substrates determined by LC/MS-MS and α-syn aggregation.[34] The build-up of GlcCer and the aggregation of α-syn has been replicated many cell types, including in human induced pluripotent stem (iPS) neurons[34] and others,[35] where lysosomal dysfunction was measured as reduced dextran degradation and accumulation of enlarged lysotracker positive vacuolar structures.[36] A non-genetic mechanism that decreases GCase and other lysosomal activities resulting in increased GlcCer and other sphingolipids is ageing,[37-41] a major risk factor for both genetic and sporadic PD.[42]

Biochemical studies directly implicate GlcCer on α-syn oligomerization and fibril formation in a reversible process, upon GluCer depletion.[43] Emerging evidence suggests that accumulation of long-chain GSLs (≥22 chains), but not short-chain species, induce α-syn neuropathology *in vivo*. Notably, reducing long-chain GSLs by 30%–40% can prevent or reverse α-syn neuropathology, but only in the presence of fully functional cathepsins,[44] whose activity depends on the acidic pH of the lysosome that is disturbed by GCase mutations.[34] Furthermore, α-syn has been shown to inhibit the normal activity of wild-type GCase enzyme in neurons and in brain tissue from idiopathic PD cases, establishing a bidirectional cycle between α-syn and GCase that may contribute to a self-propagating disease process.[36] Interestingly, a recent study showed that GlcCer can self-assemble and form amyloid-like aggregates *in vitro*, and that these can, in turn, induce α-syn aggregation.[45]

Genetic studies using knockdowns of lysosomal storage disorder (LSD) genes in a *Drosophila* model of PD validated 15 lysosomal genes as modifiers (enhancers) of α-syn-induced locomotor dysfunction. Among them are the orthologues of *GBA1*, *GLB1*, *IDS*, *NPC1*, *SCARB2*, *SMPD1*, *CTSD*, *GNPTAB*, *SLC17A5* and others, which have been reported as PD susceptibility factors in humans.[46] Collectively, these results, including others, establish the lysosome and related organelles as contributors to the aetiology of PD.[47]

In addition, human induced pluripotent stem cell (iPSC) dopaminergic neurons carrying *GBA1* mutations exhibit elevated cytoplasmic calcium levels and impaired autophagy flux, as evidenced by a decreased degree of co-localization between LC3+ vacuoles and LAMP1+ compared to controls. These alterations were reversible after gene corrections.[48] It is important to note that our understanding of the mechanistic links between mutated GCase and PD is still evolving, and further research is necessary to fully elucidate the complex interplay between these factors.

GCase strikes the mitochondria

The initial description of alterations in mitochondrial complex I in PD were reported by Schapira and colleagues[49] in 1989. Subsequent genomic studies revealed mutations in mitochondrial genes like *PINK1*, *DJ-1*, *PARK2*[11,50,51] among many others, further validated this discovery. These findings have been extensively investigated, unveiling the role of mitochondrial dysfunction in the pathophysiology of PD.[52-54] The fact that pharmacological inhibition of GCase activity with conduritol B epoxide (CBE) or mitochondrial complex I inhibition with rotenone lead to similar effects on dopamine and serotonin turnover in SH-SY5Y cells,[55] suggested that GCase could participate in mitochondrial-related pathways and/or that rotenone could have an effect in the lysosome.

Compelling evidence from GD animal models and GD human-derived cells suggest a link between GCase and mitochondria.[56,57] For instance, chemical GCase inhibition with CBE leads to decreased adenosine diphosphate (ADP) phosphorylation, which occurs in mitochondria, reduced mitochondrial membrane potential and increased free radical formation and damage, together with accumulation of α-syn in a human dopaminergic cell line.[58] Consistently, studies using a murine model of neuropathic GD showed dysfunctional and fragmented mitochondria with impaired respiration, reduced respiratory chain complex activities, and a decreased potential maintained by reversal of the ATP synthase.[59] *Gba1* deficient cells also show reduction in mitochondrial calcium uptake due to decreased levels of the mitochondrial calcium uniporter.[60] Similar findings have been described in human GCase p.N370S iPSC-dopaminergic neurons, which also show mitochondrial calcium dysregulation, reduced mitochondrial membrane potential and oxygen consumption rate, indicating mitochondrial failure.[61]

If GCase indeed plays a role in mitochondrial function, then cells with reduced GCase activity should be more vulnerable to toxins that block mitochondrial function. One of those compounds is MPP+ (1-methyl-4-phenylpyridinium), which is injected into mice as its precursor, MPTP, to induce parkinsonism.[62] This vulnerability is evident in p.L444P GCase heterozygous mice, where MPTP-induced neurotoxicity manifests as greater loss of nigrostriatal DA neurons and motor deficits compared to wild-type animals. Importantly, both *Gba1* overexpression and α-syn depletion mitigated these MPTP-induced effects, highlighting the critical interplay between lysosomal GCase activity and mitochondrial health.[62] Supporting this connection, iPSC-derived neurons from *GBA1*-PD patients exhibit depleted NAD+, a key mitochondrial metabolite involved in bioenergetics and mitophagy.[63] NAD+ levels can be restored by nicotinamide riboside (NR) administration, rescuing both mitochondrial function and motor deficits in a *GBA1*-PD fly model.[64] These findings underscore the pivotal role of GCase in safeguarding mitochondrial function and suggest its potential as a therapeutic target for mitigating *GBA1*-PD-related pathology.

The generalized block in the autophagic flux triggered by lysosomal dysfunctional GCase[48] can, potentially, aggravate mitochondrial abnormalities. GD animal models, 3D human neurospheres and post-mortem brain tissue from PD patients carrying *GBA1* mutations present mitophagy dysfunction and oxidative damage.[59,65,66] Impaired autophagic and mitochondrial functions are partially restored by enzyme replacement therapies in peripheral blood mononuclear cells (PBMCs) derived from GD patients,[67] suggesting that mitochondrial dysfunction participates in the pathophysiology of GCase depletion.

Another mechanism that regulates GCase levels, in addition to the effect of genetic mutations, is proteasomal-mediated protein degradation. At least two E3 ubiquitin ligases have been reported to interact with both wild-type and mutant GCases to control their degradation. ITCH ubiquitinates GCase in Lys48 and TRIP12 at Lys293.[68,69] TRIP12 overexpression leads to decreased GCase levels, increased α-syn accumulation, and to mitochondrial dysfunction.[69] Elevated levels of TRIP12 are also observed in human PD brain and α-syn-based mouse models.[69] These results indicate that reduced levels of GCase, independent of the molecular mechanism that leads to its reduction, cause mitochondrial defects.

Although research models tend to oversimplify the pathological disease context, organelles are not isolated in cells. They are often connected, communicating and exchanging signalling molecules such as proteins, lipids, metabolites, etc. Under normal conditions the mitochondria and the lysosome interact through contact sites. Remarkably, dopaminergic neurons derived from *GBA1*-PD patients exhibit prolonged interactions between mitochondria and lysosomes. This extended time of contact is a result of a malfunction in the untethering protein TBC1D15, which is responsible for mediating Rab7 GTP hydrolysis to release the contact.[70] The administration of a small molecule chaperone, which enhances GCase activity, effectively restored lysosome-mitochondria dynamics measured as the average time that these organelles are physically in contact, mitochondrial density, oxidative phosphorylation and ATP concentration in GCase mutant neurons.[71] This supports a potential involvement of lysosome-mitochondria contact sites in PD pathology. Notably, the same chaperone increased GCase activity, reduced GluCer and GlcSph accumulation, and decreased insoluble α-syn species in brains of *Gba1*$^{D409V/+}$ mice.[72] This indicates that this small chaperone also has the potential to modulate GCase activity *in vivo*.

Up to this point, most of the presented evidence is correlative. However, two pieces of data directly link GCase function to PD and mitochondria. One recent study explored the GCase-interacting proteome of wild-type (WT), p.L444P and p.E326 K GCase mutants using FLAG-tags. This unbiased approach revealed that both wild-type and mutant enzymes interact with several mitochondrial proteins, including mitochondrial quality control proteins HSP60 (a chaperonin protein essential for the folding and assembly of newly imported proteins in the mitochondria) and LONP1 (a mitochondrial matrix protein) in HEK cells and human iPSC-derived dopaminergic neurons. To confirm the mitochondrial localization, subcellular fractionation was performed followed by western blotting and super resolution imaging on a conventional fluorescence microscope.[73] In the future, complementary imaging techniques, such as electron microscopy, could be used to further validate these findings. The role of

GCase in mitochondria was also explored in this groundbreaking research. The authors showed that mitochondrial GCase promotes the maintenance of mitochondrial complex I measured as the ratio of NADH oxidase/co-enzyme Q reductase activities.[73,74] This study aligns with our own research findings, which suggest that another chaperonin protein, HSP10, may become sequestered by α-syn in the cytosol, consequently impacting mitochondrial function.[75]

Studies using midbrain organoids show an increased interaction between mutant GCase and LONP1 when compared to the wild-type enzyme, leading to α-syn aggregation and the dysfunction of mitochondrial complex I. In addition, dysfunctional GCase increases the production of mitochondrial reactive oxygen species (ROS) species.[73] ROS lead to dopamine oxidation in a non-enzymatic reaction within mitochondria that results in the formation of dopamine adducts that, in turn, inhibit GCase function, thereby exacerbating the pathology and creating another amplification cycle.[76] Consistently, in PD and GD there is generalized oxidative damage, probably partially mediated by GCase dysfunction, which is reflected by reduced plasma glutathione levels.[77,78] Compelling evidence shows that oxidative stress can trigger mitochondrial DNA (mtDNA) damage, which has been proposed as a blood biomarker for PD.[79,80] A recent study demonstrated that injecting damaged mtDNA into the brains of mice led to the death of dopaminergic cells. This was accompanied by an increase in phosphorylated α-syn, the accumulation of lipofuscin granules (presumably in lysosomes), and motor impairments. In contrast, injecting healthy mtDNA did not induce these effects.[81] Taken together, these results support that GCase plays a major role in oxidative stress homeostasis in the mitochondria, which in turn leads to α-syn aggregation. Furthermore, the GCase-mitochondrial connection may explain why some mutations that in homozygosity do not cause GD, such as c.1093G>A (p.E326K), could be associated with PD by disrupting mitochondrial function.

The interplay between GCase, α-syn and the endoplasmic reticulum (ER) has also garnered significant research attention. Mutations in GCase have been shown to induce ER stress, a known trigger of apoptosis,[82] and can be targeted for degradation by ER-associated protein degradation (ERAD) via the proteasome,[83] contributing to GD severity[84] and potentially explaining the association between p.E326K and PD. Mechanistic studies in iPSC-derived dopaminergic neurons carrying the heterozygous p.N370S GCase mutation revealed ER misprocessing accompanied by ER stress pathway activation, lipid accumulation, intracellular α-syn aggregation and its subsequent secretion (not in exosomes).[85] Notably, iPSC-derived neurons harbouring *SNCA* (α-syn) triplications exhibited ER fragmentation and aggregation of insoluble, likely membrane-bound GCase, suggesting an interaction between α-syn and specific GCase chaperones within the ER.[86] While a strategy targeting ER proteostasis by blocking ryanodine receptors (RyRs) successfully increased soluble GCase levels, it unfortunately had minimal impact on GCase trafficking in patient neurons, hinting at potential downstream ER factors hindering hydrolase trafficking.[86] Collectively, these studies highlight a potential toxic gain-of-function in GCase, induced either by GCase mutations or α-syn overexpression.[82]

GCase and sphingolipid metabolism in Parkinson's disease

If variants in *GBA1* and/or other lysosomal genes increase PD risk, then changes in their activities should be observed in patients. Reduced GCase activity and several other sphingolipid hydrolases are observed in PD midbrain post-mortem studies and in patient-derived fibroblasts.[40,87] Lower GCase activity has been also found in CSF of PD patients,[88-90] in dried blood spots[91,92] and in PBMCs.[93,94] However, exceptions to these findings have been reported. A recent study did not found changes in GCase activity in blood dried spots in PD patients in an Ashkenazi Jewish cohort.[95] These differences can be partially due to the methodology applied. Striking differences are observed when lysosomal enzymes are measured in total homogenates versus in isolated lysosomes.[34]

The consequence of lower GCase activity in the lysosome should be substrate build-up. In this regard, there are also contradictory data. A lipidomic analysis of in the putamen and cerebellum of controls, PD-*GBA1* and sporadic PD showed no evidence for substrate accumulation in affected brains independent of *GBA1* mutations.[96] However, a recent lipidomic analysis in the striatum, the occipital cortex, middle temporal gyrus and cingulate gyrus from idiopathic PD, PD-GBA1 and age- and sex-matched controls ($n = 21$ for each group) showed a small but significant elevation in gangliosides in most of the PD and PD-GBA1 brain regions, suggesting that gangliosides, but not glucosylceramides, may participate in the pathological cascade. However, the lipid levels in the substantia nigra were not assessed in this study.[97] Another study, including 109 PD-*GBA1* patients and 118 controls, reported elevated plasma hexosylceramides and hexosylsphingosine levels in PD patients, while ceramides were found to be reduced in patients.[98] Moreover, the study found sex differences, with a preferential shunting from hexosylceramide to hexosylsphingosine in males, and to ceramides in females. This study supports sex-related pathophysiologic differences in GCase function, which have not been addressed before and should be included in future GCase-related clinical studies.

As PD is a complex and heterogeneous disease, and not every patient shows decreased GCase activity of glycosphingolipid accumulation, customized therapies should be designed based on the biology of each patient. In this regard, large consortia, such as the PD progression markers initiative (PPMI), the International Parkinson's Disease Genomics Consortium (IPDGC), the Molecular Integration in Neurological Diagnosis (MIND) Initiative, the Parkinson's Disease Biomarker's Program (PDBP) and the Personalized Parkinson Project (PPP), were developed to usher in a precision medicine era.[99-103] Analogously, it has been proposed that PD animal models of different genetic backgrounds, that show different severities and progressions, are necessary for investigating customized therapies,[104-106] including GCase-focused approaches.

Therapeutic targeting of GCase

While targeting GCase may not lead to improvements in every PD patient, it holds potential for assisting a significant number of individuals. Numerous therapeutic approaches initially developed for GD,[107] along with novel approaches currently under development, could be repurposed for PD. These strategies encompass small molecules that enhance GCase activity, enzyme replacement therapies, gene therapies, substrate reduction therapies, chaperones and genetic modifiers of GCase activity.[108] However, a major challenge resides in ensuring treatment crosses the blood–brain barrier to reach the brain at the necessary levels (Fig. 2).

A groundbreaking study demonstrated that a small molecule activator of GCase,[109] effectively reduces the accumulation of glucosylceramide and hexosylsphingosine, while promoting α-syn clearance in dopaminergic lines derived from human iPS cells obtained from PD patients with mutations in *SNCA* (triplication or A53T), *GBA1*, *PARK9* genes, as well as idiopathic PD neurons. This indicates the potential of GCase activation in diverse genetic backgrounds.[110]

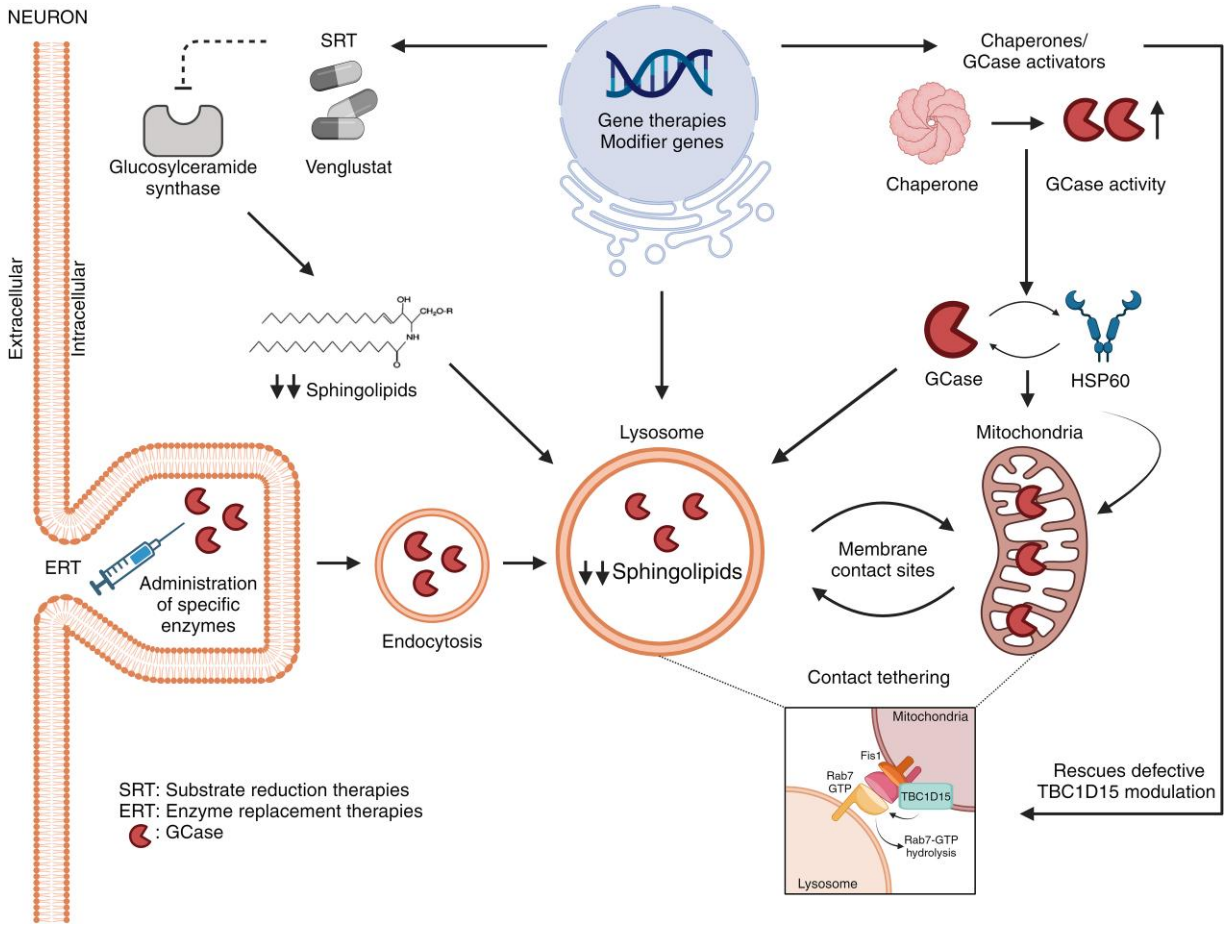

Figure 2 GCase and glycosphingolipid-targeted therapeutic approaches for PD. GCase and GSL-targeted therapies can be categorized as follows: (i) delivery of non-mutated enzyme, such as gene therapy delivered to the nucleus or enzyme replacement therapies (ERT), which are taken up by the endocytic pathway and directed to the lysosome; (ii) targeting the defective enzyme using small molecules, including chaperones that aid in proper protein folding and other types of activators; (iii) modifier genes that regulate GCase enzyme activity or pathological cascades; and (iv) reducing substrate biosynthesis (substrate reduction therapies, SRT) by inhibiting glucosylceramide synthase at the endoplasmic reticulum (ER) or acid ceramidase in the lysosome. Although some of these therapies are targeted to one specific organelle, the lysosome and the mitochondria can exchange therapeutic contents through their membrane contact sites (MCS). Mechanistically, untethering lysosome-mitochondria contact sites involves the recruitment of cytosolic TBC1D15 to mitochondria via Fis1 protein. Subsequently, TBC1D15 interacts with Rab7 GTP in the lysosome, allowing Rab7 GTP hydrolysis. In the GDP state, Rab7 loses localization to the lysosomal membrane, leading to lysosome-mitochondria untethering contact sites. GCase = β-glucocerebrosidase; PD = Parkinson's disease. Figure created with BioRender.com.

Similar findings were observed in the brains of *Gba1*$^{D409V/+}$ heterozygous mouse models using another GCase activator.[72]

Additional small molecules that exhibit promising potential in enhancing GCase activity have been reported, and others are under development. These include iminosugars, ambroxol, other competitive, yet reversible, GCase inhibitors that facilitate the transport of GCase to the lysosome, and non-inhibitory chaperones or activators that do not compete for the active site. Their therapeutic application in GD and PD and effectiveness towards specific mutations must be investigated.[111] Ambroxol, an over-the-counter expectorant widely used in Europe and in other world regions,[112] gained significant attention as a potential treatment for certain forms of GD and PD following its identification as a GCase chaperone.[113] Ambroxol binds to GCase, facilitating its trafficking to the lysosome, and in a low pH it is released, increasing GCase activity in cultured macrophages derived from GD and *GBA1*-PD patients by ∼3.5-fold, while reducing substrate levels by ∼2-fold when compared to untreated cells.[114] Similar results were observed in patient-derived fibroblasts.[115] Ambroxol decreases both tau and α-syn levels in an *in vitro* murine cholinergic model heterozygous for the p.N370S/WT GCase mutation[116] and in transgenic mice overexpressing human α-syn.[117] Furthermore, oral administration of ambroxol increases brain GCase activity in non-human primates.[118] Notably, ambroxol crosses the blood–brain barrier in humans and is well tolerated in PD patients.[119] Currently, multiple clinical trials investigating the efficacy of ambroxol in treating PD are underway across different locations worldwide (NCT02941822, NCT05778617, NCT05830396, NCT05287503, NCT02914366, NCT04388969, NCT0458825).

Recently, a phase 1B clinical trial (NCT05819359) investigated an allosteric GCase activator, which showed good tolerability.[120] *In vitro*, this molecule was able to double GCase activity in wild-type and mutated enzymes. Notably, the CSF concentrations of the GCase activator mirrored the unbound plasma fraction, suggesting efficacious brain penetration.[120] The clinical benefit will be further assessed in a larger phase 2 study. Exploring therapeutic strategies that aim to increase GCase activity through targeting modifier genes is an intriguing, yet under-explored avenue. Modifier genes refer to loci where DNA sequence variations can alter a phenotype

that is typically independent of the target gene.[121] In this regard, we have mapped potential modifiers of GCase activity, as well as 11 other lysosomal enzymes, and of the levels of various glycosphingolipids implicated in PD.[122,123] Among the identified candidate GCase modifiers, we identified *Dmrtc2*, *Arhgef1* and *Grik5*. The latter gene encodes subunit 5 of the glutamate ionotropic kainate receptor, which has been extensively studied and for which several agonists and antagonists are known.[124] The involvement of kainite receptors (KAR) has been implicated in both genetic and environmental PD models.[125,126] Furthermore, PARKIN (*PRKN*), an E3 ligase PD susceptibility gene, interacts with some subunits of ionotropic kainite receptors, regulating its levels by proteasomal regulation.[127] Thus, PD-PARKIN neurons show high levels of KA2 receptors and enhanced glutamate excitotoxicity.[127] Whether KAR antagonists could exert beneficial effects in PD models by regulating GCase activity remains unknown.

Substrate reduction therapies (SRT) that inhibit the production of the molecules that accumulate in lysosomal storage disorders have been successfully used in patients where first line enzyme replacement therapies failed.[128] Although there is still no solid preclinical or clinical evidence of glycosphingolipid accumulation in PD,[129] a double-blind placebo-controlled clinical trial testing a glucosylceramide synthase inhibitor SRT (NCT02906020), exhibited a satisfactory safety profile but did not demonstrate any advantageous effects when compared to a placebo.[130] These results suggest that this SRT does not seem to be a viable approach for treating *GBA1*-associated PD, thereby raising doubts about the role of GlcCer in the pathology.

In contrast, a promising preclinical study with the inhibition of acid ceramidase, the lysosomal enzyme that deacylates GluCer to GluSph, prevented mTOR hyperactivity, restored autophagic flux and lowered α-syn levels in an iPSC dopaminergic neuron model of *GBA1*-PD. Administration of GluSph in wild-type cells mimicked the mTOR/α-syn abnormalities observed in *GBA1*-PD neurons, and these phenotypic alterations were prevented when GluSph treatment was in the presence of mTOR inhibitors.[131] These results suggest that GluSph, rather than GlcCer, is responsible for PD cellular alterations including autophagic block and, thus, SRT aimed at inhibiting acid ceramidase may be explored in clinical trials.

Enzyme replacement therapies, wherein the lysosomal enzyme is intravenously infused into patients, have effectively alleviated the visceral symptoms of GD and other lysosomal disorders.[132] However, a significant limitation of this approach is the inability of the infused enzyme to cross the blood–brain barrier.[132] To address this challenge, a recent study employed a fusion protein by combining a fragment of a transferrin-receptor (TfR) antibody with recombinant human or murine GCase. The TfR is responsible for transporting transferrin, an iron-binding protein, into the brain. The study demonstrated that the quinmerac GCase protein efficiently reached the mouse brain, effectively reducing the sphingolipid build-up in various GD models. These models included cortical neurons derived from embryonic null allele $Gba1^{-/-}$ mice, human pluripotent stem cell-derived neurons, and human neuroblastoma cells (H4 cells) with deleted *GBA1* or primary murine neurons harbouring a homozygous human *Gba1* mutation ($Gba^{D409V/D409V}$).[133] This approach holds immense potential for treating neuropathic diseases associated with GCase dysfunction.

Concluding remarks and outlook

In conclusion, recent evidence indicates that *GBA1* mutations can impact PD by affecting (i) the lysosome and the metabolites degraded in this compartment; (ii) mitochondrial complex I; and (iii) other organelles, such as the ER. The first and second points suggest that a loss-of-function mechanism in GCase contributes to PD pathophysiology, while the third point indicates a toxic gain-of-function effect. These two mechanisms likely occur concurrently and may explain the more severe phenotypes observed in individuals carrying mutant GCase when compared to those with sporadic PD. Irrespective of the pathological mechanisms, these findings have supported the development of GCase-centred therapeutics for PD. While GCase-based therapeutics have traditionally focused on the lysosome, the recent discovery of GCase in mitochondria expands this perspective. Considering this, GD and PD could be considered both lysosomal and mitochondrial diseases, making both organelles valid targets for therapeutic interventions. Promising strategies include small molecules that can act as chaperones, targeting modifier genes of GCase activity, and novel engineered GCase enzymes that can cross into the brain, among others. We speculate that, in combination with other strategies currently under development, such as α-syn-targeting antibodies or anti-sense oligonucleotides, or cell-based therapies, may lead to important and urgent improvements in the quality of life of PD patients.

Funding

A.D.K. is funded by Agencia Nacional de Investigación y Desarrollo (ANID)-CHILE: Fondecyt grant No 1230317. T.F.O. is supported by the Deutsche Forschungsgemeinschaft (DFG, German ResearchFoundation) under Germany's Excellence Strategy—EXC 2067/1- 390729940'.

Competing interests

The authors report no competing interests.

References

1. Sung VW, Nicholas AP. Nonmotor symptoms in Parkinson's disease: Expanding the view of Parkinson's disease beyond a pure motor, pure dopaminergic problem. *Neurol Clin*. 2013;31:S1-S16.
2. Ding C, Wu Y, Chen X, et al. Global, regional, and national burden and attributable risk factors of neurological disorders: The Global Burden of Disease study 1990–2019. *Front Public Health*. 2022;10:952161.
3. Simon DK, Tanner CM, Brundin P. Parkinson disease epidemiology, pathology, genetics, and pathophysiology. *Clin Geriatr Med*. 2020;36:1-12.
4. Marras C, Beck JC, Bower JH, et al. Prevalence of Parkinson's disease across North America. *NPJ Parkinsons Dis*. 2018;4:21.
5. Braak H, Del Tredici K, Rüb U, De Vos RAI, Jansen Steur ENH, Braak E. Staging of brain pathology related to sporadic Parkinson's disease. *Neurobiol Aging*. 2003;24:197-211.
6. Outeiro TF, Alcalay RN, Antonini A, et al. Defining the riddle in order to solve it: There is more than one "Parkinson's disease.". *Mov Disord*. 2023;38:1127-1142.
7. Kim S, Kwon SH, Kam TI, et al. Transneuronal propagation of pathologic α-synuclein from the gut to the brain models Parkinson's disease. *Neuron*. 2019;103:627-641.e7.
8. Höglinger GU, Adler CH, Berg D, et al. A biological classification of Parkinson's disease: The SynNeurGe research diagnostic criteria. *Lancet Neurol*. 2024;23:191-204.
9. Polymeropoulos MH, Lavedan C, Leroy E, et al. Mutation in the alpha-synuclein gene identified in families with Parkinson's disease. *Science*. 1997;276:2045-2047.

10. Funayama M, Hasegawa K, Kowa H, Saito M, Tsuji S, Obata F. A new locus for Parkinson's disease (PARK8) maps to chromosome 12p11.2-q13.1. *Ann Neurol*. 2002;51:296-301.
11. Bonifati V, Rizzu P, Van Baren MJ, et al. Mutations in the DJ-1 gene associated with autosomal recessive early-onset parkinsonism. *Science*. 2003;299:256-259.
12. Blauwendraat C, Nalls MA, Singleton AB. The genetic architecture of Parkinson's disease. *Lancet Neurol*. 2020;19:170-178.
13. Cox TM. Gaucher disease: Understanding the molecular pathogenesis of sphingolipidoses. *J Inherit Metab Dis*. 2001;24(Suppl 2):107-123.
14. Klein AD, Ferreira NS, Ben-Dor S, et al. Identification of modifier genes in a mouse model of Gaucher disease. *Cell Rep*. 2016;16:2546-2553.
15. Ryan E, Seehra GK, Sidransky E. Mutations, modifiers and epigenetics in Gaucher disease: Blurred boundaries between simple and complex disorders. *Mol Genet Metab*. 2019;128(1–2):10-13.
16. Rivas MA, Avila BE, Koskela J, et al. Insights into the genetic epidemiology of Crohn's and rare diseases in the Ashkenazi Jewish population. *PLoS Genet*. 2018;14:e1007329.
17. Stirnemann JÔ, Belmatoug N, Camou F, et al. A review of Gaucher disease pathophysiology, clinical presentation and treatments. *Int J Mol Sci*. 2017;18:441.
18. Nalysnyk L, Rotella P, Simeone JC, Hamed A, Weinreb N. Gaucher disease epidemiology and natural history: A comprehensive review of the literature. *Hematology*. 2017;22:65-73.
19. Inzelberg R, Hassin-Baer S, Jankovic J. Genetic movement disorders in patients of Jewish ancestry. *JAMA Neurol*. 2014;71:1567-1572.
20. Aharon-Peretz J, Rosenbaum H, Gershoni-Baruch R. Mutations in the glucocerebrosidase gene and Parkinson's disease in Ashkenazi Jews. *N Engl J Med*. 2004;351:1972-1977.
21. Sidransky E, Nalls MA, Aasly JO, et al. Multicenter analysis of glucocerebrosidase mutations in Parkinson's disease. *N Engl J Med*. 2009;361:1651-1661.
22. Chang D, Nalls MA, Hallgrímsdóttir IB, et al. A meta-analysis of genome-wide association studies identifies 17 new Parkinson's disease risk loci. *Nat Genet*. 2017;49:1511-1516.
23. Robak LA, Jansen IE, Van Rooij J, et al. Excessive burden of lysosomal storage disorder gene variants in Parkinson's disease. *Brain*. 2017;140:3191-3203.
24. Zhao YW, Pan HX, Liu Z, et al. The association between lysosomal storage disorder genes and Parkinson's disease: A large cohort study in Chinese mainland population. *Front Aging Neurosci*. 2021;13:749109.
25. Dagan E, Schlesinger I, Kurolap A, et al. LRRK2, GBA and SMPD1 founder mutations and Parkinson's disease in ashkenazi Jews. *Dement Geriatr Cogn Disord*. 2016;42(1–2):1-6.
26. Saffie Awad P, Teixeira-dos-Santos D, Santos-Lobato BL, et al. Frequency of hereditary and GBA1-related parkinsonism in Latin America: A systematic review and meta-analysis. *Mov Disord*. 2023;39(1):6-16.
27. Stoker TB, Stoker TB, Camacho M, et al. Impact of GBA1 variants on long-term clinical progression and mortality in incident Parkinson's disease. *J Neurol Neurosurg Psychiatry*. 2020;91:695-702.
28. Dopeso-Reyes IG, Sucunza D, Rico AJ, et al. Glucocerebrosidase expression patterns in the non-human primate brain. *Brain Struct Funct*. 2018;223:343-355.
29. Vieira SRL, Schapira AHV. Glucocerebrosidase mutations and Parkinson disease. *J Neural Transm (Vienna)*. 2022;129:1105-1117.
30. Montfort M, Chabás A, Vilageliu L, Grinberg D. Functional analysis of 13 GBA mutant alleles identified in Gaucher disease patients: Pathogenic changes and "modifier" polymorphisms. *Hum Mutat*. 2004;23:567-575.
31. Duran R, Mencacci NE, Angeli AV, et al. The glucocerobrosidase E326 K variant predisposes to Parkinson's disease, but does not cause Gaucher's disease. *Mov Disord*. 2013;28:232-236.
32. Liou B, Grabowski GA. Is E326 K glucocerebrosidase a polymorphic or pathological variant? *Mol Genet Metab* 2012;105:528-529.
33. Parlar SC, Grenn FP, Kim JJ, Baluwendraat C, Gan-Or Z. Classification of GBA1 variants in Parkinson's disease: The GBA1-PD browser. *Mov Disord*. 2023;38:489-495.
34. Navarro-Romero A, Fernandez-Gonzalez I, Riera J, et al. Lysosomal lipid alterations caused by glucocerebrosidase deficiency promote lysosomal dysfunction, chaperone-mediated-autophagy deficiency, and alpha-synuclein pathology. *NPJ Parkinsons Dis*. 2022;8:126.
35. Bae EJ, Yang NY, Lee C, et al. Loss of glucocerebrosidase 1 activity causes lysosomal dysfunction and α-synuclein aggregation. *Exp Mol Med*. 2015;47:e153.
36. Mazzulli JR, Xu YH, Sun Y, et al. Gaucher disease glucocerebrosidase and α-synuclein form a bidirectional pathogenic loop in synucleinopathies. *Cell*. 2011;146:37-52.
37. Rocha EM, Smith GA, Park E, et al. Progressive decline of glucocerebrosidase in aging and Parkinson's disease. *Ann Clin Transl Neurol*. 2015;2:433-438.
38. Kracun I, Rosner H, Drnovsek V, Heffer-Lauc M, Cosovic C, Lauc G. Human brain gangliosides in development, aging and disease. *Int J Dev Biol*. 1991;35:289-295.
39. Svennerholm L, Boström K, Jungbjer B, Olsson L. Membrane lipids of adult human brain: Lipid composition of frontal and temporal lobe in subjects of age 20 to 100 years. *J Neurochem*. 1994;63:1802-1811.
40. Huebecker M, Moloney EB, Van Der Spoel AC, et al. Reduced sphingolipid hydrolase activities, substrate accumulation and ganglioside decline in Parkinson's disease. *Mol Neurodegener*. 2019;14:40.
41. Hornburg D, Wu S, Moqri M, et al. Dynamic lipidome alterations associated with human health, disease and ageing. *Nat Metab*. 2023;5:1578-1594.
42. Collier TJ, Kanaan NM, Kordower JH. Ageing as a primary risk factor for Parkinson's disease: Evidence from studies of non-human primates. *Nat Rev Neurosci*. 2011;12:359-366.
43. Zunke F, Moise AC, Belur NR, et al. Reversible conformational conversion of α-synuclein into toxic assemblies by glucosylceramide. *Neuron*. 2018;97:92-107.e10.
44. Fredriksen K, Aivazidis S, Sharma K, et al. Pathological α-syn aggregation is mediated by glycosphingolipid chain length and the physiological state of α-syn in vivo. *Proc Natl Acad Sci U S A*. 2021;118:e2108489118.
45. Paul A, Jacoby G, Laor Bar-Yosef D, Beck R, Gazit E, Segal D. Glucosylceramide associated with Gaucher disease forms amyloid-like twisted ribbon fibrils that induce α-synuclein aggregation. *ACS Nano*. 2021;15:11854-11868.
46. Yu M, Ye H, De-Paula RB, et al. Functional screening of lysosomal storage disorder genes identifies modifiers of alpha-synuclein neurotoxicity. *PLoS Genet*. 2023;19:e1010760.
47. Klein AD, Mazzulli JR. Is Parkinson's disease a lysosomal disorder? *Brain*. 2018;141:2255-2262.
48. Schöndorf DC, Aureli M, McAllister FE, et al. iPSC-derived neurons from GBA1-associated Parkinson's disease patients show autophagic defects and impaired calcium homeostasis. *Nat Commun*. 2014;5:4028.
49. Schapira AHV, Cooper JM, Dexter D, Jenner P, Clark JB, Marsden CD. Mitochondrial complex I deficiency in Parkinson's disease. *Lancet*. 1989;1:1269.

50. Valente EM, Abou-Sleiman PM, Caputo V, et al. Hereditary early-onset Parkinson's disease caused by mutations in PINK1. *Science*. 2004;304:1158-1160.
51. Lücking CB, Dürr A, Bonifati V, et al. Association between early-onset Parkinson's disease and mutations in the parkin gene. *N Engl J Med*. 2000;342:1560-1567.
52. Dar GM, Ahmad E, Ali A, Mahajan B, Ashraf GM, Saluja SS. Genetic aberration analysis of mitochondrial respiratory complex I implications in the development of neurological disorders and their clinical significance. *Ageing Res Rev*. 2023;87:101906.
53. Ye H, Robak LA, Yu M, Cykowski M, Shulman JM. Genetics and pathogenesis of Parkinson's syndrome. *Annu Rev Pathol*. 2023;18:95-121.
54. Henchcliffe C, Beal FM. Mitochondrial biology and oxidative stress in Parkinson disease pathogenesis. *Nat Clin Pract Neurol*. 2008;4:600-609.
55. de la Fuente C, Burke DG, Eaton S, Heales SJR. Inhibition of neuronal mitochondrial complex I or lysosomal glucocerebrosidase is associated with increased dopamine and serotonin turnover. *Neurochem Int*. 2017;109:94-100.
56. Arévalo NB, Lamaizon CM, Cavieres VA, et al. Neuronopathic Gaucher disease: Beyond lysosomal dysfunction. *Front Mol Neurosci*. 2022;15:934820.
57. Cabrera-Reyes F, Parra-Ruiz C, Yuseff MI, Zanlungo S. Alterations in lysosome homeostasis in lipid-related disorders: Impact on metabolic tissues and immune cells. *Front Cell Dev Biol*. 2021;9:790568.
58. Cleeter MWJ, Chau KY, Gluck C, et al. Glucocerebrosidase inhibition causes mitochondrial dysfunction and free radical damage. *Neurochem Int*. 2013;62:1-7.
59. Osellame LD, Rahim AA, Hargreaves IP, et al. Mitochondria and quality control defects in a mouse model of Gaucher disease–links to Parkinson's disease. *Cell Metab*. 2013;17:941-953.
60. Plotegher N, Perocheau D, Ferrazza R, et al. Correction: Impaired cellular bioenergetics caused by GBA1 depletion sensitizes neurons to calcium overload. *Cell Death Differ*. 2020;27:2534.
61. Beccano-Kelly DA, Cherubini M, Mousba Y, et al. Calcium dysregulation combined with mitochondrial failure and electrophysiological maturity converge in Parkinson's iPSC-dopamine neurons. *iScience*. 2023;26:107044.
62. Yun SP, Kim D, Kim S, et al. α-Synuclein accumulation and GBA deficiency due to L444P GBA mutation contributes to MPTP-induced parkinsonism. *Mol Neurodegener*. 2018;13:1.
63. Lautrup S, Sinclair DA, Mattson MP, Fang EF. NAD+ in brain aging and neurodegenerative disorders. *Cell Metab*. 2019;30:630-655.
64. Schöndorf DC, Ivanyuk D, Baden P, et al. The NAD+ precursor nicotinamide riboside rescues mitochondrial defects and neuronal loss in iPSC and fly models of Parkinson's disease. *Cell Rep*. 2018;23:2976-2988.
65. Morén C, Juárez-Flores DL, Chau KY, et al. GBA mutation promotes early mitochondrial dysfunction in 3D neurosphere models. *Aging*. 2019;11:10338-10355.
66. Li H, Ham A, Ma TC, et al. Mitochondrial dysfunction and mitophagy defect triggered by heterozygous GBA mutations. *Autophagy*. 2019;15:113-130.
67. Ivanova MM, Changsila E, Iaonou C, Goker-Alpan O. Impaired autophagic and mitochondrial functions are partially restored by ERT in Gaucher and Fabry diseases. *PLoS One*. 2019;14:e0210617.
68. Maor G, Filocamo M, Horowitz M. ITCH regulates degradation of mutant glucocerebrosidase: Implications to Gaucher disease. *Hum Mol Genet*. 2013;22:1316-1327.
69. Seo BA, Kim D, Hwang H, et al. TRIP12 ubiquitination of glucocerebrosidase contributes to neurodegeneration in Parkinson's disease. *Neuron*. 2021;109:3758-3774.e11.
70. Wong YC, Ysselstein D, Krainc D. Mitochondria-lysosome contacts regulate mitochondrial fission via RAB7 GTP hydrolysis. *Nature*. 2018;554:382-386.
71. Kim S, Wong YC, Gao F, Krainc D. Dysregulation of mitochondria-lysosome contacts by GBA1 dysfunction in dopaminergic neuronal models of Parkinson's disease. *Nat Commun*. 2021;12:1807.
72. Burbulla LF, Jeon S, Zheng J, Song P, Silverman RB, KraincD. A modulator of wild-type glucocerebrosidase improves pathogenic phenotypes in dopaminergic neuronal models of Parkinson's disease. *Sci Transl Med*. 2019;11:eaau6870.
73. Baden P, Perez MJ, Raji H, et al. Glucocerebrosidase is imported into mitochondria and preserves complex I integrity and energy metabolism. *Nat Commun*. 2023;14:1930.
74. Klein AD, Outeiro TF. Glucocerebrosidase mutations disrupt the lysosome and now the mitochondria. *Nat Commun*. 2023;14(1):6383.
75. Szegő ÉM, Dominguez-Meijide A, Gerhardt E, et al. Cytosolic trapping of a mitochondrial heat shock protein is an early pathological event in synucleinopathies. *Cell Rep*. 2019;28:65-77.e6.
76. Burbulla LF, Song P, Mazzulli JR, et al. Dopamine oxidation mediates mitochondrial and lysosomal dysfunction in Parkinson's disease. *Science*. 2017;357:1255-1261.
77. Charisis S, Ntanasi E, Stamelou M, et al. Plasma glutathione and prodromal Parkinson's disease probability. *Mov Disord*. 2022;37:200-205.
78. Kartha RV, Terluk MR, Brown R, et al. Patients with Gaucher disease display systemic oxidative stress dependent on therapy status. *Mol Genet Metab Rep*. 2020;25:100667.
79. Sanders LH, McCoy J, Hu X, et al. Mitochondrial DNA damage: Molecular marker of vulnerable nigral neurons in Parkinson's disease. *Neurobiol Dis*. 2014;70:214-223.
80. Qi R, Sammler E, Gonzalez-Hunt CP, et al. A blood-based marker of mitochondrial DNA damage in Parkinson's disease. *Sci Transl Med*. 2023;15:7-eabo155.
81. Tresse E, Marturia-Navarro J, Sew WQG, et al. Mitochondrial DNA damage triggers spread of Parkinson's disease-like pathology. *Mol Psychiatry*. 2023;28(11):4902-4914.
82. Tabas I, Ron D. Integrating the mechanisms of apoptosis induced by endoplasmic reticulum stress. *Nat Cell Biol*. 2011;13:184-190.
83. Bendikov-Bar I, Ron I, Filocamo M, Horowitz M. Characterization of the ERAD process of the L444P mutant glucocerebrosidase variant. *Blood Cells Mol Dis*. 2011;46:4-10.
84. Bendikov-Bar I, Horowitz M. Gaucher disease paradigm: From ERAD to comorbidity. *Hum Mutat*. 2012;33:1398-1407.
85. Fernandes HJR, Hartfield EM, Christian HC, et al. ER stress and autophagic perturbations lead to elevated extracellular α-synuclein in GBA-N370S Parkinson's iPSC-derived dopamine neurons. *Stem Cell Reports*. 2016;6:342-356.
86. Stojkovska I, Wani WY, Zunke F, et al. Rescue of α-synuclein aggregation in Parkinson's patient neurons by synergistic enhancement of ER proteostasis and protein trafficking. *Neuron*. 2022;110:436-451.e11.
87. Thomas R, Moloney EB, Macbain ZK, Hallett PJ, Isacson O. Fibroblasts from idiopathic Parkinson's disease exhibit deficiency of lysosomal glucocerebrosidase activity associated with reduced levels of the trafficking receptor LIMP2. *Mol Brain*. 2021;14:16.
88. Lerche S, Schulte C, Wurster I, et al. The mutation matters: CSF profiles of GCase, sphingolipids, α-synuclein in PDGBA. *Mov Disord*. 2021;36:1216-1228.

89. Parnetti L, Paciotti S, Eusebi P, et al. Cerebrospinal fluid β-glucocerebrosidase activity is reduced in Parkinson's disease patients. *Mov Disord*. 2017;32:1423-1431.
90. Oftedal L, Maple-Grødem J, Dalen I, et al. Association of CSF glucocerebrosidase activity with the risk of incident dementia in patients with Parkinson disease. *Neurology*. 2023;100:E388-E395.
91. Alcalay RN, Levy OA, Waters CC, et al. Glucocerebrosidase activity in Parkinson's disease with and without GBA mutations. *Brain*. 2015;138(Pt 9):2648-2658.
92. Huh YE, Chiang MSR, Locascio JJ, et al. β-Glucocerebrosidase activity in GBA-linked Parkinson disease: The type of mutation matters. *Neurology*. 2020;95:E685-E696.
93. Avenali M, Cerri S, Ongari G, et al. Profiling the biochemical signature of GBA-related Parkinson's disease in peripheral blood mononuclear cells. *Mov Disord*. 2021;36:1267-1272.
94. Petrucci S, Ginevrino M, Trezzi I, et al. GBA-Related Parkinson's disease: Dissection of genotype-phenotype correlates in a large Italian cohort. *Mov Disord*. 2020;35:2106-2111.
95. Omer N, Giladi N, Gurevich T, et al. Glucocerebrosidase activity is not associated with Parkinson's disease risk or severity. *Mov Disord*. 2022;37:190-195.
96. Gegg ME, Sweet L, Wang BH, Shihabuddin LS, Sardi SP, Schapira AHV. No evidence for substrate accumulation in Parkinson brains with GBA mutations. *Mov Disord*. 2015;30:1085-1089.
97. Blumenreich S, Nehushtan T, Barav OB, et al. Elevation of gangliosides in four brain regions from Parkinson's disease patients with a GBA mutation. *NPJ Parkinsons Dis*. 2022;8:99.
98. Ortega R, Burbulla L, Mileva I, et al. Peripheral sphingolipids as potential biomarkers of Parkinson disease including sex-related differences (P3–11.007). *Neurology*. 2023;100(17 Supplement 2):4099.
99. Marek K, Chowdhury S, Siderowf A, et al. The Parkinson's progression markers initiative (PPMI)—Establishing a PD biomarker cohort. *Ann Clin Transl Neurol*. 2018;5:1460-1477.
100. Singleton A. Ten years of the international Parkinson disease genomics consortium: Progress and next steps. *J Parkinsons Dis*. 2020;10:19-30.
101. Tropea TF, Amari N, Han N, et al. Whole clinic research enrollment in Parkinson's disease: The Molecular Integration in Neurological Diagnosis (MIND) study. *J Parkinsons Dis*. 2021;11:757-765.
102. Rosenthal LS, Drake D, Alcalay RN, et al. The NINDS Parkinson's disease biomarkers program. *Mov Disord*. 2016;31:915-923.
103. Bloem BR, Marks WJ, Silva De Lima AL, et al. The Personalized Parkinson Project: Examining disease progression through broad biomarkers in early Parkinson's disease. *BMC Neurol*. 2019;19:160.
104. Lavoy S, Chittoor-Vinod VG, Chow CY, Martin I. Genetic modifiers of neurodegeneration in a Drosophila model of Parkinson's disease. *Genetics*. 2018;209:1345-1356.
105. Olivares GH, Olguín P, Klein AD. Modeling Parkinson's disease heterogeneity to accelerate precision medicine. *Trends Mol Med*. 2019;25:1052-1055.
106. Olguín V, Durán A, Las Heras M, et al. Genetic background matters: Population-based studies in model organisms for translational research. *Int J Mol Sci*. 2022;23:7570.
107. Klein AD, Futerman AH. Lysosomal storage disorders: Old diseases, present and future challenges. *Pediatr Endocrinol Rev*. 2013;11(Suppl 1):59-63.
108. Menozzi E, Toffoli M, Schapira AHV. Targeting the GBA1 pathway to slow Parkinson disease: Insights into clinical aspects, pathogenic mechanisms and new therapeutic avenues. *Pharmacol Ther*. 2023;246:108419.
109. Patnaik S, Zheng W, Choi JH, et al. Discovery, structure-activity relationship, and biological evaluation of noninhibitory small molecule chaperones of glucocerebrosidase. *J Med Chem*. 2012;55:5734-5748.
110. Mazzulli JR, Zunke F, Tsunemi T, et al. Activation of β-glucocerebrosidase reduces pathological α-synuclein and restores lysosomal function in Parkinson's patient midbrain neurons. *J Neurosci*. 2016;36:7693-7706.
111. Han TU, Sam R, Sidransky E. Small molecule chaperones for the treatment of Gaucher disease and GBA1-associated Parkinson disease. *Front Cell Dev Biol*. 2020;8:271.
112. Malerba M, Ragnoli B. Ambroxol in the 21st century: Pharmacological and clinical update. *Expert Opin Drug Metab Toxicol*. 2008;4:1119-1129.
113. Maegawa GHB, Tropak MB, Buttner JD, et al. Identification and characterization of ambroxol as an enzyme enhancement agent for Gaucher disease. *J Biol Chem*. 2009;284:23502-23516.
114. Kopytova AE, Rychkov GN, Nikolaev MA, et al. Ambroxol increases glucocerebrosidase (GCase) activity and restores GCase translocation in primary patient-derived macrophages in Gaucher disease and Parkinsonism. *Parkinsonism Relat Disord*. 2021;84:112-121.
115. McNeill A, Magalhaes J, Shen C, et al. Ambroxol improves lysosomal biochemistry in glucocerebrosidase mutation-linked Parkinson disease cells. *Brain*. 2014;137(Pt 5):1481-1495.
116. Yang SY, Taanman JW, Gegg M, Schapira AHV. Ambroxol reverses tau and α-synuclein accumulation in a cholinergic N370S GBA1 mutation model. *Hum Mol Genet*. 2022;31:2396-2405.
117. Migdalska-Richards A, Daly L, Bezard E, Schapira AHV. Ambroxol effects in glucocerebrosidase and α-synuclein transgenic mice. *Ann Neurol*. 2016;80:766-775.
118. Migdalska-Richards A, Ko WKD, Li Q, Bezard E, Schapira AHV. Oral ambroxol increases brain glucocerebrosidase activity in a nonhuman primate. *Synapse*. 2017;71:e21967.
119. Mullin S, Smith L, Lee K, et al. Ambroxol for the treatment of patients with Parkinson disease with and without glucocerebrosidase gene mutations: A nonrandomized, noncontrolled trial. *JAMA Neurol*. 2020;77:427-434.
120. den Heijer JM, Kruithof AC, Moerland M, et al. A phase 1B trial in GBA1-associated Parkinson's disease of BIA-28-6156, a glucocerebrosidase activator. *Mov Disord*. 2023;38:1197-1208.
121. Riordan JD, Nadeau JH. From peas to disease: Modifier genes, network resilience, and the genetics of health. *Am J Hum Genet*. 2017;101:177-191.
122. Durán A, Rebolledo-Jaramillo B, Olguin V, et al. Identification of genetic modifiers of murine hepatic β-glucocerebrosidase activity. *Biochem Biophys Rep*. 2021;28:101105.
123. Durán A, Priestman DA, Las Heras M, et al. A mouse systems genetics approach reveals common and uncommon genetic modifiers of hepatic lysosomal enzyme activities and glycosphingolipids. *Int J Mol Sci*. 2023;24:4915.
124. Conti P, Amici M, Micheli C. Selective agonists and antagonists for kainate receptors. *Mini Rev Med Chem*. 2002;2:177-184.
125. Stayte S, Laloli KJ, Rentsch P, et al. The kainate receptor antagonist UBP310 but not single deletion of GluK1, GluK2, or GluK3 subunits, inhibits MPTP-induced degeneration in the mouse midbrain. *Exp Neurol*. 2020;323:113062.
126. Regoni M, Cattaneo S, Mercatelli D, et al. Pharmacological antagonism of kainate receptor rescues dysfunction and loss of dopamine neurons in a mouse model of human parkin-induced toxicity. *Cell Death Dis*. 2020;11:963.
127. Maraschi AM, Ciammola A, Folci A, et al. Parkin regulates kainate receptors by interacting with the GluK2 subunit. *Nat Commun*. 2014;5:5182.
128. Platt FM, d'Azzo A, Davidson BL, Neufeld EF, Tifft CJ. Lysosomal storage diseases. *Nat Rev Dis Primers*. 2018;4:27.

129. Sidransky E, Arkadir D, Bauer P, et al. Substrate reduction therapy for GBA1-associated parkinsonism: Are we betting on the wrong mouse? *Mov Disord*. 2020;35:228-230.
130. Giladi N, Alcalay RN, Cutter G, et al. Safety and efficacy of venglustat in GBA1-associated Parkinson's disease: An international, multicentre, double-blind, randomised, placebo-controlled, phase 2 trial. *Lancet Neurol*. 2023;22:661-671.
131. Kumar M, Srikanth MP, Deleidi M, Hallett PJ, Isacson O, Feldman RA. Acid ceramidase involved in pathogenic cascade leading to accumulation of α-synuclein in iPSC model of GBA1-associated Parkinson's disease. *Hum Mol Genet*. 2023;32:1888-1900.
132. Concolino D, Deodato F, Parini R. Enzyme replacement therapy: Efficacy and limitations. *Ital J Pediatr*. 2018;44(Suppl 2):120.
133. Gehrlein A, Udayar V, Anastasi N, et al. Targeting neuronal lysosomal dysfunction caused by β-glucocerebrosidase deficiency with an enzyme-based brain shuttle construct. *Nat Commun*. 2023;14:2057.

International Journal of
Molecular Sciences

MDPI

Review

Genetic Background Matters: Population-Based Studies in Model Organisms for Translational Research

Valeria Olguín [1,†], Anyelo Durán [1,†], Macarena Las Heras [1], Juan Carlos Rubilar [1], Francisco A. Cubillos [2,3], Patricio Olguín [4] and Andrés D. Klein [1,*]

[1] Centro de Genética y Genómica, Facultad de Medicina, Clínica Alemana Universidad del Desarrollo, Santiago 7610658, Chile; valeria.olguin.araneda@gmail.com (V.O.); anduranm@udd.cl (A.D.); mlasherasp@udd.cl (M.L.H.); jrubilare@udd.cl (J.C.R.)
[2] Departamento de Biología, Santiago, Facultad de Química y Biología, Universidad de Santiago de Chile, Santiago 9170022, Chile; francisco.cubillos.r@usach.cl
[3] Millennium Institute for Integrative Biology (iBio), Santiago 7500565, Chile
[4] Program in Human Genetics, Institute of Biomedical Sciences, Biomedical Neurosciences Institute, Department of Neuroscience, Facultad de Medicina, Universidad de Chile, Santiago 8380453, Chile; patricioolguin@uchile.cl
* Correspondence: andresklein@udd.cl
† These authors contributed equally to this work.

Abstract: We are all similar but a bit different. These differences are partially due to variations in our genomes and are related to the heterogeneity of symptoms and responses to treatments that patients exhibit. Most animal studies are performed in one single strain with one manipulation. However, due to the lack of variability, therapies are not always reproducible when treatments are translated to humans. Panels of already sequenced organisms are valuable tools for mimicking human phenotypic heterogeneities and gene mapping. This review summarizes the current knowledge of mouse, fly, and yeast panels with insightful applications for translational research.

Keywords: systems genetics; mouse; *Drosophila*; *Saccharomyces cerevisiae*; translational research; genetic background; precision medicine; gene mapping

Citation: Olguín, V.; Durán, A.; Las Heras, M.; Rubilar, J.C.; Cubillos, F.A.; Olguín, P.; Klein, A.D. Genetic Background Matters: Population-Based Studies in Model Organisms for Translational Research. *Int. J. Mol. Sci.* **2022**, *23*, 7570. https://doi.org/10.3390/ijms23147570

Academic Editors: Mauricio A. Retamal, Rodrigo Del Rio and Darío Acuña-Castroviejo

Received: 23 May 2022
Accepted: 4 July 2022
Published: 8 July 2022

1. Precision Medicine in Humans

Precision medicine characterizes diseases at a higher resolution by genomic and other technologies, providing more accurate targeting of patient subsets with tailored therapies [1]. To make this possible, large genotyped cohorts with deep clinical annotations are required to map loci responsible for the phenotypic variability. Common approaches to gene mapping include genome-wide association studies (GWAS) and linkage analysis in families of patients with variable disease severity [1]. These studies are time-consuming and expensive due to recruiting and genotyping costs. Furthermore, it is virtually impossible with rare diseases to find large cohorts in order to assure statistical significance for the genomic mapping.

Furthermore, families presenting enough informative individuals with variable symptoms are challenging to identify [2]. Strategies using model organisms with various genetic backgrounds are valuable resources for overcoming these obstacles. In this review, we describe many panels of organisms and examples of how modeling diseases on them can accelerate the pace of discoveries toward translational research in humans.

2. Rodents as Model Organisms in Genetic Research: Advantages and Limitations

The advantages of using mouse models in biomedicine have been discussed extensively [3]. Some benefits are the following: (i) the availability of genetic tools for creating disease models by transgenic, knockout, and knock-in technologies [4–6] (https://www.

jax.org/research-and-faculty/resources/mouse-mutant-resource/available-models (accessed on 22 May 2022)); (ii) inbred mouse strains are nearly isogenic, enabling to study how the same genetic mutation modifies a phenotype of interest in different genetic backgrounds [7–11]; (iii) mouse tissues are available for omics studies which can be challenging to obtain from humans [12]. Some limitations include different evolutive pressures for mice and humans; therefore, some systems, such as the immune system, do not function similarly in both species [13].

2.1. Hybrid Mouse Diversity Panel

Currently available resources in rodents to find modifiers genes by association studies can be defined in two categories: (i) reference panels, consisting of inbred strains such as the Hybrid Mouse Diversity Panel (HMDP) and the Collaborative Cross (CC); (ii) populations derived from pseudo-random breeding of inbred strains, such as the Diversity Outbred (DO) and Heterogeneous Stock (HS) (Figure 1).

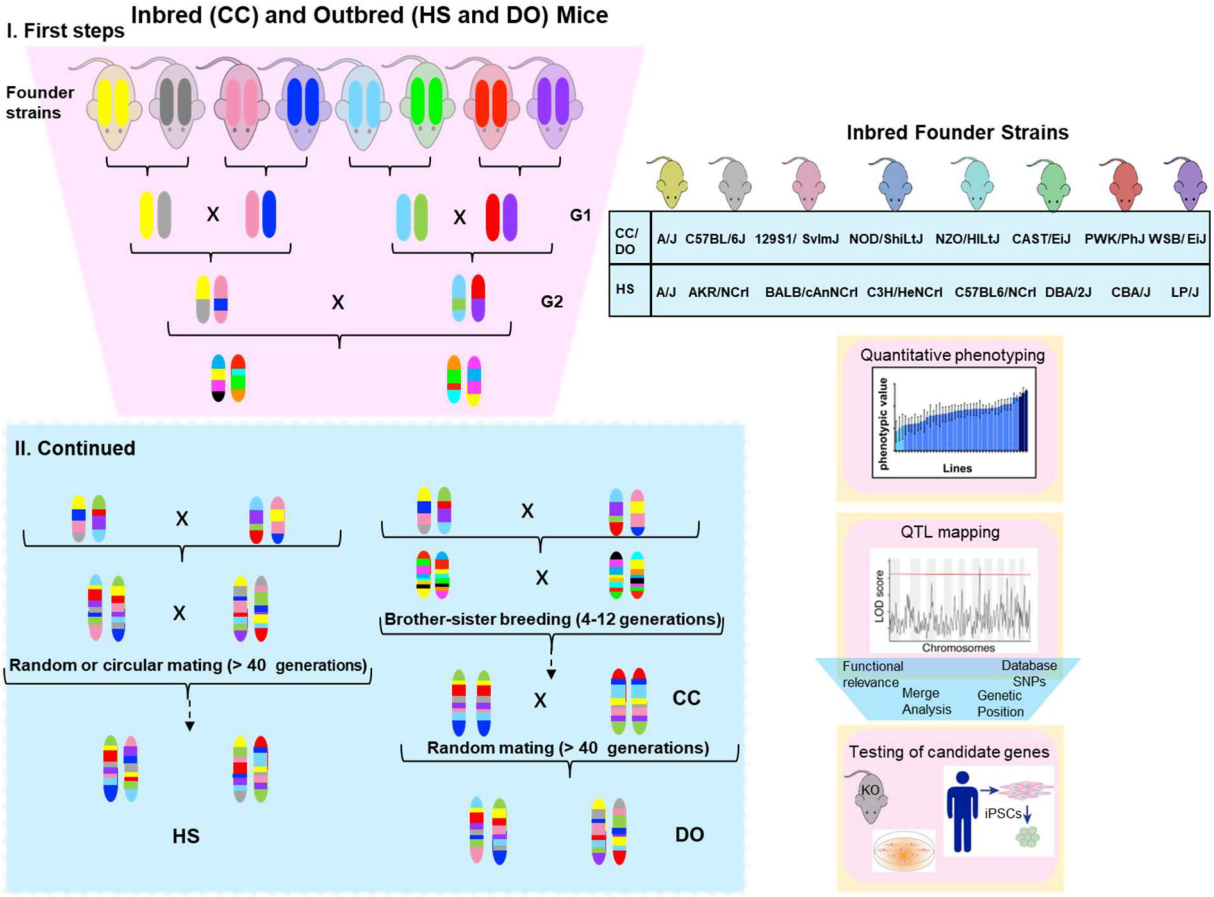

Figure 1. Breeding schemes for inbred (CC) and outbred (HS and DO) mice populations: Inbred founder strains for each panel are indicated in the right box. CC and DO populations share the same eight founder strains, five of which are standard laboratory inbred strains, while three are wild-derived strains. Colors represent the genotypes of strain chromosomes. The first steps include the combination of all eight founder genomes (outcrosses). CC is then generated as a recombinant inbred (RI) after multiple brother–sister breeding. HS and DO panels were developed as high-diversity outbred panels by over 40 generations of random outcrosses. DO was created from partially inbred Collaborative Cross (CC) mice. Quantitative phenotyping can be performed in the strains and used for gene mapping. Some signals in chromosomal locations will probably pass the threshold of significance (red line) in the LOD plot. The functional relevance of these variants can be assessed in animal models such as knockout mice and induced pluripotent stem cells (iPSC) derived from patients.

HMDP is a large panel of approximately 100 commercially available (https://www.jax.org (accessed on 22 May 2022)) and fully sequenced (www.sanger.ac.uk/science/data/mouse-genomes-project (accessed on 22 May 2022)) inbred strains: ~30 classical inbred strains and ~70 recombinant inbred (RI) strains derived mainly from crosses between C57BL/6J and DBA mice and A/J and C57BL/6J mice [14].

Advantages of using the HMDP panel are the following: (i) their genomes are known (http://mouse.cs.ucla.edu/mouseHapMap/ (accessed on 22 May 2022)); thus, it is unnecessary to spend funds performing this step; (ii) HMDP possesses ~4 million common single-nucleotide variants (SNVs), which is similar to the number present in humans [15]; (iii) high-resolution association mapping [14], which is at least an order of magnitude higher than in linkage analysis; (iv) it is possible to integrate gene mapping with other omics (transcriptomics, proteomics, and metabolomics data) [12]; (v) commercially available (from The Jackson Laboratory, Harlan, and others); (vi) sufficient bioinformatics tools for data mining of complex mouse and human disease traits, such as the Systems Genetics Resource (SGR) (http://systems.genetics.ucla.edu (accessed on 22 May 2022)); (vii) servers to perform association mapping and statistical power simulation, which are also available in R to run them in house [16].

The HMDP also has limitations. For example, extensive linkage disequilibrium (LD) blocks are observed, both within and between chromosomes, probably as a result of the selection of allelic combinations conceding higher fitness during the inbreeding [17]. Consequently, regions in LD can lead to false-positive associations in GWAS analyses. Although the HMDP has a high mapping resolution, the statistical power to detect the effect of loci is small (estimated at 50% to variants explaining 10% of the trait variance) [14]. Since most loci contributing to a complex trait have an effect size below 5% [18], variants with subtle effects cannot always be detected by the HMDP. Power can be enhanced by including additional inbred and RI strains and performing meta-analyses from other panels such as the CC or traditional crosses [19].

An exciting application of the use of mouse panels in translational research comes from crossing the classical Alzheimer's disease (AD) mouse model (5XFAD) bearing mutations in APP and PSEN1 with 28 different strains of the BXD panel (AD-BXD). The F1 represents isogenic lines that were studied in a controlled environment. The AD-BXD panel mimicked several signs of the AD patients, including phenotypic variation in disease onset and severity. As in humans, the Apoe allele significantly affected spatial memory and other behavioral tests in the AD-BXD panel. Furthermore, hippocampal gene expression in the severe and mild lines agrees with transcriptomic changes observed in patients [20].

2.2. The Collaborative Cross (CC) Panel

The CC is a large panel of RI mouse strains obtained through systematically outcrossing eight founder strains, followed by randomized breeding [21]. The founder strains of the CC include five of the widely used classical inbred laboratory strains (A/J, C57BL/6J, NOD/ShiLtJ, 129S1/SvImJ, and NZO/HILtJ), as well as three wild-derived strains descendent of three *M musculus* subspecies (WSB, Castaneous, and PWK) (Figure 1). These eight strains have been fully sequenced and carry ~45 million SNVs, four times more than those of classical laboratory mouse strains [22].

The genomes of the CC panel are known (http://csbio.unc.edu/CCstatus/CCGenomes (accessed on 22 May 2022)), which is helpful for genetic association studies. Haplotypes can be easily visualized or reconstructed as a mosaic of the genomes of the founders [23]. Parental strains capture approximately 90% of the genetic diversity seen in the *Mus musculus* species [24]. This high genetic diversity significantly reduces false candidate loci. Additionally, randomized breeding substantially increases mapping resolution by reducing population structure effects [25]. CC strains have been used to map quantitative trait loci (QTLs) to less than 5 Mb intervals [26]. Online tools are available to perform GWAS and linkage analyses [27]. Several aspects of human genetics and behavioral factors can be modeled in this system, including the heterogeneities observed in neurodevelopmental

disorders such as autistic spectrum disorders (ASDs) [28]. The CC panel allowed the discovery of novel candidate severity modifiers of ASD, e.g., *Bai3*, considered a potential target for pharmacological intervention [28].

Some considerations associated with using the CC panel are the following: (i) unique outlier phenotypes can arise in large studies, probably due to the complex genetic regulatory networks involving multiple loci with epistatic interactions [29]; in such cases, the preferred approach for identifying causal genes is traditional F2 analysis or backcrosses [30]; (ii) because identifying loci could be time-consuming, it is suggested to perform a pilot study and expand as necessary [29]; (iii) creating a panel like the CC can generate breeding complications and infertility, mainly caused by genomic incompatibility introduced by the wild-derived strains. For that reason, the initial CC project aimed to produce 1000 strains but finished with only ~100 and inspired the creation of the Diversity Outbred (DO) population.

CC lines have been used for genetic association studies of many complex traits. QTL mapping for 15 metabolism- and exercise-related traits revealed five significant loci for body weight, some of which overlapped with previous human studies [31]. Gene mapping of rotarod (exercise) performance and body weight identified 45 loci, many of them related to neurological disorders and obesity in humans, suggesting a link between physical activity and neurodegeneration [32]. A study of glucose tolerance response in the CC panel identified, only in female mice, a genomic region comprising 51 genes. This study highlighted sex differences in glucose response which should be considered in human studies [33]. The CC panel is also a valuable and reliable resource for studying host–pathogen interactions [29]. For example, to map genetic modifiers affecting the severity of *Pseudomonas aeruginosa* lung infections, 39 CC lines were inoculated with this pathogen. The phenotypic variability was enormous, ranging from complete resistance to lethality. It is particularly relevant to study the resistant lines since they have the biological secrets to design novel therapies for the susceptible. Genomic mapping and functional validation identified dihydropyrimidine dehydrogenase (*Dpyd*) and sphingosine-1-phosphate receptor 1 (*S1pr1*) as modifier genes. In a cohort of patients with cystic fibrosis, two SNVs in the *S1PR1* gene are associated with *Pseudomonas aeruginosa* infection [34], again indicating the translational relevance of multigenetic background studies in animal organisms.

2.3. Heterogeneous Stock and Diversity Outbred Populations

Both HS and DO are high-diversity outbred mice populations. The HS was established by breeding eight inbred strains and then outbreeding them in either a circular strategy or using random crosses (Figure 1) to minimize inbreeding [35]. After 50 or more generations, the HS-generated mice were a genetic mosaic of the founders' haplotypes [36,37]. On the other hand, the DO was established from partially inbred CC lines and is maintained indefinitely through pseudorandomized fashion non-sibling mating [38] (Figure 1). Since the DO is derived from the same eight founders as the CC, it presents the same allelic diversity as the CC strains. It can be used as a complementary tool in genetic association studies [39].

There are several advantages of using HS or DO mice compared to classical inbred mice. The outbred randomized mating increases the number of additional recombination sites compared to those of classically inbred mice; thus, each HS or DO mouse has a unique genome, which is a mosaic of the original eight founder lines, resembling human heterozygosity and allows high-resolution genetic mapping [39]. HS and DO mice have been used to finely map to intervals of 2.7 Mb [40] and less than 2 Mb [39], respectively. In addition, outbred animals are more vigorous and less prone to both early and late recessive allelic effects [41]. This genetic variability within both HS and DO populations results in a high degree of phenotypic variability; thus, outbred models enable the fine mapping of many phenotypic traits. Since the founders of CC and DO lines include wild-derived strains, unique behaviors can be observed compared to classical laboratory strains and represent a valuable tool for genetic behavior association studies [22]. A repository of

DO QTL studies can be shared between laboratories (https://dodb.jax.org (accessed on 22 May 2022)). Lastly, the founders of the HS and DO populations have been sequenced [42], reducing time and expense in locating the sequences.

Alternatively, some considerations must be made in the case of HS and DO mice. Since each outbred animal is genetically and phenotypically distinct, each HS and DO mouse requires genotyping and haplotype reconstruction to perform each QTL analysis [38]. High-resolution mapping can be achieved with these panels, but analyzing many animals is necessary for sufficient statistical power, which is not always possible [43]. Candidate modifiers of wild behaviors can be identified with outbred mice. However, it is challenging to validate in these panels because each animal has a unique genotype, in contrast to inbred lines [44].

An interesting translational study using the DO panel identified a diagnostic biomarker for human tuberculosis (TB). By applying machine learning algorithms to multidimensional data, the authors discovered CXCL1 as a putative biomarker of TB in the serum of mice. The biomarker was further validated in samples derived from human patients, discriminating active TB from latent infection and non-TB lung disease [45]. This study highlights the relevance of using population-based strategies to accelerate human biomarker discovery, validation, and testing.

3. *Drosophila melanogaster* as a Model Organism in Genetic Research: Advantages and Limitations

In addition to mouse models, *Drosophila melanogaster* has attracted many scientists. Flies are small, easy to manipulate in the laboratory, and cheap to maintain. They have a short life span (2 week generation interval) and produce many offspring. Flies show complex behaviors, including sleep, aggression, addiction, and social behavior [46]. Notably, about 70% of human disease-associated genes have a *Drosophila* ortholog [47]; its genome is fully sequenced and well annotated. It can be genetically modified using chemical and insertional mutagenesis, gene-specific mutations, or editions using CRISPR [47,48]. These characteristics support its use as a model system to study human diseases. As expected, the use of *Drosophila* for human research has limitations; for instance, the fly does not possess hemoglobin [49] and, thus, cannot be used for studying human pathologies related to this system.

3.1. *Drosophila melanogaster* Genetic Reference Panel (DGRP)

The DGRP is a collection of 205 inbred *Drosophila melanogaster* strains derived from a single natural population. Inseminated females were collected from the farmer's market in Raleigh, NC (USA), and their offspring were subjected to 20 generations of complete sibling mating [50] (Figure 2). The DGRP is a public resource available at the Bloomington Drosophila Stock Center (http://fly.bio.indiana.edu (accessed on 22 May 2022)) built for genomic association analyses. Currently, their genomes are available, and each line has minimal genetic variation [50]. Repeated measurements within each line are possible, enabling accuracy to increase the statistical power in GWA analyses. Since the DGRP is a publicly available resource, it allows different laboratories to correlate phenotypes on the same genotype and understand the pleiotropic effects of DNA variants and genes on multiple quantitative traits. Unlike the human genome, the fly genome has a structure with low LD between closely linked polymorphisms [51], which is favorable for accurate association mapping; thus, significant associated SNVs are likely causal or very near to a causal variant [52]. Lastly, experimentation in *Drosophila* has fewer ethical concerns compared to rodent models.

As with all study models, there are some limitations in DGRP that should be considered. Firstly, genetic variation between the lines is a snapshot of the population from which they were derived; therefore, DGRP does not represent all the possible variations of the species. Secondly, the 205 lines usually provide enough statistical power to detect common

variants with moderate to large effects [53,54], but the statistical power is still limited for rare variants (minor allele frequency (MAF) < 0.05) [51].

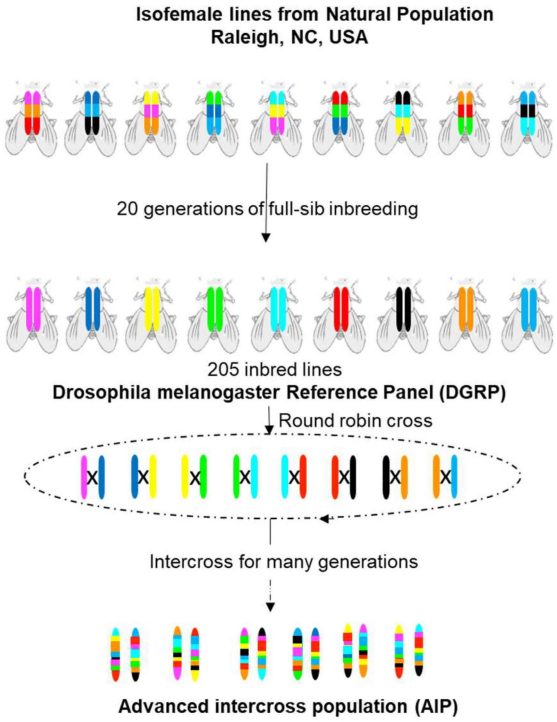

Figure 2. Generation of *Drosophila melanogaster* Genetic Reference Panel (DGRP) and Advanced Intercross Population (DGRP-AIPs). The DGRP corresponds to a sequenced panel derived from a natural fly population of Raleigh, NC (USA), and it was generated through 20 generations of full-sibling mating. The AIPs lines were derived from the DGRP by round-robin crossing and were then remapped.

3.2. DGRP for Mapping Physiological and Pathophysiological Traits

The DGRP has been used for GWA mapping of many different quantitative physiological traits, including food intake and sleep behavior [55,56]. Food intake is essential to animal fitness, and 25 modifiers with human orthologs were found [55]. Interestingly, diversity in mitochondrial haplotypes can directly mediate phenotypic variation in food intake [57]. Sleep has been increasingly explored in recent years with this model [56]. Flies resemble mammalian sleep and have become an important model species for identifying sleep regulation mechanisms. Analogous to human sleep studies, a DGRP GWAS highlighted signals in the EGFR, Wnt, Hippo, and MAPK signaling pathways, suggesting that genes affecting variation in this trait are conserved [58]. DGRP studies revealed the genetic architecture of nutrient stores (glucose, glycogen, glycerol, protein, triglycerides, and wet weight) [59], developmental plasticity [60], and circadian cycle [61].

The DGRP has been used to identify candidate modifiers of retinal degeneration [62] and neurodegeneration in a Parkinson's disease (PD) model [63]. PD is a highly variable neurodegenerative disorder where variable manifestations range from cognitive disturbances, motor alterations, and sleep and speech abnormalities to cellular pathological changes such as the formation of Lewy body inclusions and neuronal death [64]. The leucine-rich repeat kinase 2 gene G2019S mutation (LRRK2 G2019S) penetrance is incomplete and varies among ethnic populations. In the Ashkenazy Jewish population, the low penetrance (26%) of the G2019S mutant phenotype suggests that other factors, such as the genetic background, the environment, and their interaction, act as modifiers of the variable phenotype [65,66]. In this regard, it has been reported that introducing the LRRK2 G2019S mutation in the DGRP results in considerable variability in the locomotor phenotype among backgrounds [63]. Gene mapping revealed 177 candidate modifier genes enriched in path-

ways involved in the neuronal outgrowth. The study suggests a link among LRRK2, neurite regulation, and neuronal degeneration in PD [63].

3.3. Lines Derived from DGRP and DSRP

A limitation of the DGRP is its low statistical power [51], which motivated the development of DGRP-derived advanced intercross populations (AIPs). These correspond to lines generated by crossing parentals DGRP for many generations, which were then remapped [67]. By successive crossings of a subset of parentals lines, it is possible to increase the recombination rate and, consequently, the statistical power compared to the DGRP [52]. Furthermore, the extreme QTL mapping strategy in AIPs can be used to resolve the statistical limitations of the DGRP for rare variants (MAF < 0.05). Extreme QTL mapping refers to selecting individuals from the extremes of the phenotypic distribution for a trait (resembling a case–control study). Flies are pooled and sequenced, which is cheaper than sequencing all individuals of the initial population. This allows identifying alleles that segregate differentially among the distribution extremes (causal variant or in LD with it) [68,69]. The discovery of rare variants in DGRP will occur at higher frequencies in the AIPs after an extreme QTL mapping strategy.

A less applied strategy to increase the mapping power is to use DGRP and another panel for cross-validation, such as the Drosophila Synthetic Population Resource (DSPR). This collection of 1700 inbred lines is derived from 15 isogenic founder lines created from geographically distinct *Drosophila* populations [70]. However, some studies in both AIPs and DSPR lack overlap with candidate genes found in DGRP, probably due to the different genetic architecture or genetic variants between the panels.

4. *Saccharomyces cerevisiae* as a Model Organism in Genetic Research: Advantages and Limitations

Saccharomyces cerevisiae, the budding yeast, has gained prominence as a model organism in quantitative genetics because it has several experimental and biologically advantageous features. For example, it has a small and compact genome of approximately 12 million bp in haploids (about one two-hundredth of the human genome). It contains fewer introns and a lower proportion of intergenic sequences than higher eukaryotes [71]. Furthermore, it is easy to cultivate and maintain in large population size in the laboratory. In addition, two-thirds of all yeast genes share at least one domain of significant homology with human genes, and about 30% of known genes involved in human diseases have yeast orthologs [72].

One of the main advantages of yeast for quantitative genetics studies is its large genetic map. *S. cerevisiae* exhibits high meiotic recombination rates, with an average of about 90 crossovers per meiosis, allowing precise quantitative phenotyping [71,73,74]. The homologous recombination in yeast is highly efficient, facilitating the deletion of sequences or genes in vivo [72,75]. This efficient recombination permitted the generation of the first complete deletion mutant strain collection using gene replacement with the G418 resistance gene (KanMX) cassette in the reference *S. cerevisiae* strain [76]. Since then, similar panels have been available in different genetic backgrounds, demonstrating the high degree of genetic background dependencies for different phenotypes [77,78]. Yeasts have less genetic complexity than flies and rodents. Thus, it is easier to study the effect of a single gene because of the reduced genetic redundancy [79].

4.1. Analysis of Segregating Populations from Pairwise Crosses

QTL mapping in yeast has been the primary approach to uncovering genetic variants responsible for phenotypic differences between genetic backgrounds. Identifying QTLs has been achieved by analyzing segregating populations from pairwise crosses, mainly through linkage or bulk segregant analysis (BSA) [80,81]. Linkage mapping in yeast involves mating two or more haploid parental strains that show phenotypic variation and then phenotyping and genotyping a panel of recombinant offspring obtained from

these crosses. Recombination breaks allow causal loci to segregate with the phenotype of interest, and QTLs are identified using statistical tests [80,82]. The BSA also involves crossing two or more parental strains and subsequent phenotyping of their recombinant offspring [83]. However, the BSA method uses selective genotyping of subsets of segregants, commonly the extremes of the phenotypic distribution [84]. Typically, segregants undergo selective environmental pressure, where large pools are constructed. One expresses the trait of interest (selected pool), and others are not selected (control pool) or exhibit the opposite phenotype. After genotyping each marker, genetic regions of allelic enrichment are predicted as QTLs that contribute to the attribute of interest [85]. These approaches from pairwise crosses have been successfully applied to map yeast genetic variation responsible for nitrogen utilization [86], metabolic fluxes, ethanol tolerance [87], and high-temperature fermentation [88].

Most crosses constructed in yeast have involved the reference laboratory strain S288c or its derivatives crossed against a wild or fermentative isolate [89]. However, these strains only harbor a small fraction of the phenotypic variation of natural populations and have mosaic genomes of the founder strains [84,90]. Therefore, studies using biparental crosses provide a poor understanding of the relationship between the genetic background and the QTLs. These studies lack resolution since few generations are used; consequently, they are unable to reveal the complete architecture of polygenic traits. Moreover, laboratory strains often contain artificial auxotrophic markers that confound mapping experiments [91]. Investigators have recently established advanced-generation multi-parent populations (MPPs) in yeast to overcome these problems (Figure 3).

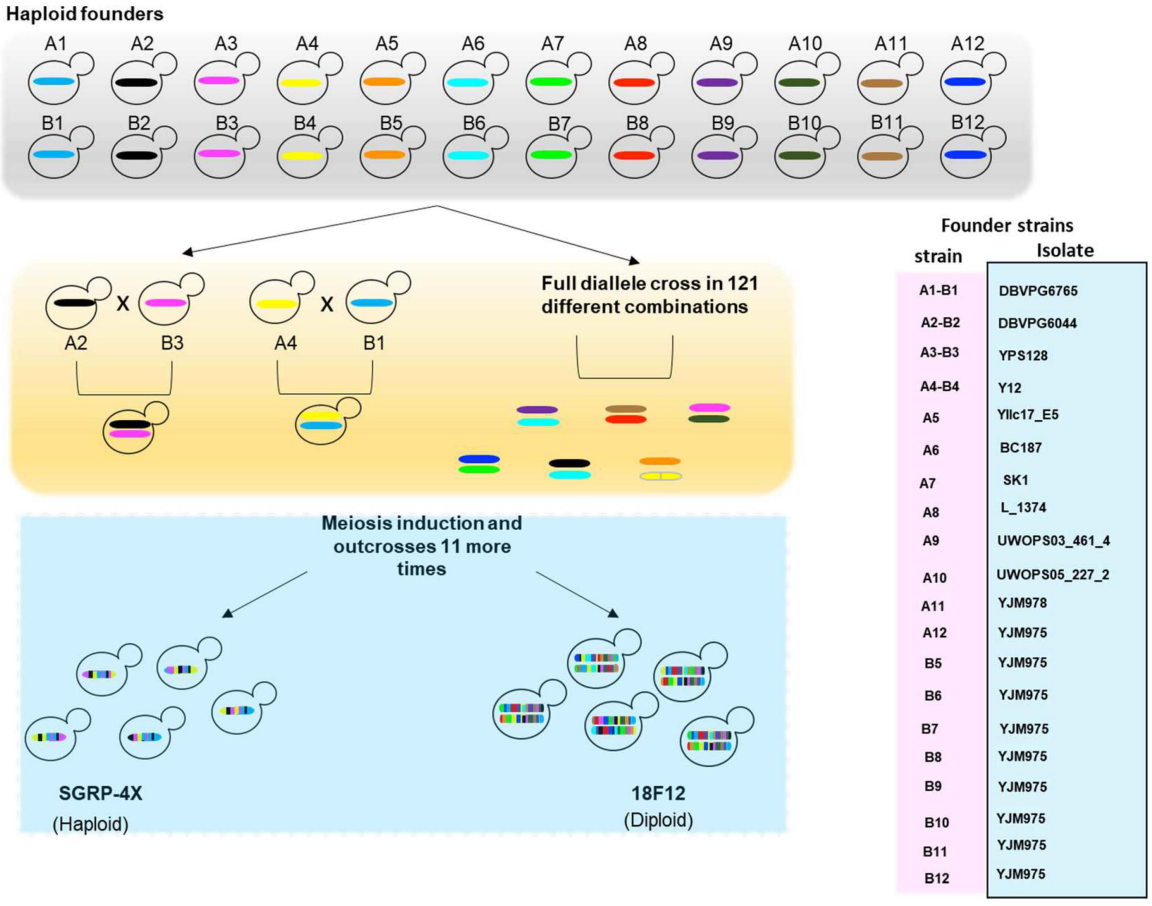

Figure 3. Cross design of SGRP-4X and 18F12 mapping populations. Haploid founder strains used for generations of these populations are indicated in the right box. Ax and Bx indicate the Mat a and Mat α haploid founder strains, respectively.

4.2. Multi-Parent Populations (MPPs)

Yeast MPPs comprise large populations with thousands to millions of individuals obtained from two main steps. Firstly, several (inbred or isogenic) founder strains from various geographical origins are crossed, and then the intercross of the resulting population is subsequentially crossed for several generations [81]. Large segregating populations are then used for mapping QTLs. The first MPP in yeast was established by Cubillos et al. [92] by crossing four strains representative of the main *S. cerevisiae* lineages (Y12 strain as representative of the SA lineage, YPS128 of the NA lineage, DBVPG6044 of the WA, and DBVPG6765 of the WE lineage) for 12 generations. The SGRP-4X contains 165 sequenced segregants, representing recombined genetic mosaics of the founder strains. Later, Linder et al. [93] extended this approach and created 18F12v1 and 18F12v2, two outbred MPPs derived from a cross of 18 genetically diverse founder strains, with each strain derived from the SGRP collection [84,92,93].

MPPs in yeast are robust mapping resources due to multiple founders and rounds of recombination in many individuals that increase both the genetic and the phenotypic diversity, s well as the linkage block resolution of the QTL mapping compared to biparental F1 or F2 populations. In fact, in yeast, it has been shown that only a few rounds of meiosis are sufficient to obtain spaced near-genic resolution [94]. Association mapping in MPPs provides more equilibrated allelic frequencies than biparental populations, increasing knowledge about the population structure [95]. Integration of this information in the QTL analysis can reduce the probability of obtaining false-positive results, thus demonstrating yeast as an accurate model system to identify dozens to hundreds of genes underlying phenotypes of interest.

4.3. Genome-Wide Association Studies (GWAS) in S. cerevisiae

GWAS utilizes the variation in large populations of unrelated individuals to provide insights into the causes of common complex traits. However, in 2012, only 36 *S. cerevisiae* genomes were available from the Saccharomyces Genome Resequencing Project, hampering GWAS studies in yeast. This situation motivated the development of a project to describe whole-genome sequence variation in numerous yeast populations (http://1002genomes.u-strasbg.fr/ (accessed on 22 May 2022)). Today, more than 2000 genomes isolated from a wide range of locations (including Australia, Europe, Russia, Vietnam, and South Africa) are available [96]. Thus, investigators can conduct GWAS in this model organism [97].

The success of GWAS in *S. cerevisiae* is a result of high diversity among natural isolates relative to humans [96], low linkage disequilibrium (extended in an average half-life of <3 kb) [98], and relatively simple quantification of phenotypes in hundreds to thousands of individuals. However, GWAS in yeast is affected by a large population structure [84,98], leading to limited statistical power and spurious associations. The increment in the number of genotyped individuals is comparable to other model organisms enabling GWAS to describe copy number variants (CNV) as having a more significant phenotypic effect than SNV in yeast and laying the foundation for GWAS in the species [99].

Many of the phenotypes addressed in yeast are directly related to the cell-autonomous features of human diseases, including neurological conditions such as Parkinson's disease [100]. Thus far, most of the disease genome-wide screenings in *S. cerevisiae* have deleted one gene at a time. To our knowledge, the genomic variability of yeast isolates is starting to be used for modeling human phenotypic variabilities. In the field of longevity and environment, a study in which 58 natural yeast strains were used led to identifying *RIM15* and *SER1* as longevity genes under caloric restrictions [101].

In the future, we expect to observe increased research using panels of organisms, where a combination of variants can be identified. This technique could be feasible in the short term for diseases that can be mimicked pharmacologically and in the medium term for disorders that can be reproduced genetically.

5. Practical Considerations and Concluding Remarks

Each of the discussed organisms and panels has advantages and disadvantages for human translational research. In addition to the already mentioned ones, researchers should consider practical factors for deciding the best model for each project. Some relevant factors are presented in Table 1.

Table 1. Practical considerations for choosing model organisms and their panels. The references are shown in brackets. When deciding the best model for a project, variables such as the percentage of homolog genes to human disease-causing genes, costs, and the possibility of automatization should be considered.

	Mus musculus	*Drosophila melanogaster*	*Saccharomyces cerevisiae*
Genome size (kb)	2,725,521 [102]	180,000 [103]	12,070 [104]
Percentage of homolog genes to human disease-causing genes	99 [105]	70 [47,106]	60 [107]
Costs to keep the panels	High	Medium	Very low
Complex behaviors	Yes	Yes	No
Discovery of cell-autonomous processes	Yes	Yes	Yes
Speed for throughput screenings and automatization of measurements	Slow	Fast	Very fast

In conclusion, the consequences of a genetic mutation can be strongly modified by the biological background in which it operates. For example, a loss-of-function mutation may be well tolerated in one genetic context and lethal in another. The most resistant individuals have the biological secrets useful for developing therapies for the most susceptible ones. Human studies are challenging; they can take a long time due to the recruitment of large cohorts, and genomic sequencing is expensive. Instead, modeling diseases in already sequenced panels of diverse model organisms followed by gene mapping and validation in smaller human cohorts can speed up translational research and precision medicine for both common and rare diseases.

Author Contributions: Conceptualization: V.O., A.D., P.O., F.A.C. and A.D.K. Writing original draft: V.O., A.D., M.L.H., J.C.R. and A.D.K. writing—review and editing: F.A.C., P.O. and A.D.K. Supervision: A.D.K. All authors have read and agreed to the published version of the manuscript.

Funding: A.D.K. is funded by the Fondo Nacional de Desarrollo Científico y Tecnológico (Fondecyt) grant No. 1180337. P.O. is funded by the Biomedical Neuroscience Institute (BNI), Iniciativa Científica Milenio, ICN09_015, Agencia Nacional de Investigación y Desarrollo ACE210007. P.O. and A.D.K. are supported by the Pew Innovation Fund, grant No. 32422.

Informed Consent Statement: Not applicable.

Conflicts of Interest: The authors declare no conflict of interest.

References

1. Ashley, E.A. Towards precision medicine. *Nat. Rev. Genet.* **2016**, *17*, 507–522. [CrossRef] [PubMed]
2. Rahit, K.M.T.H.; Tarailo-Graovac, M. Genetic Modifiers and Rare Mendelian Disease. *Genes* **2020**, *11*, 239. [CrossRef] [PubMed]
3. Canales, C.P.; Walz, K. The Mouse, a Model Organism for Biomedical Research. In *Cellular and Animal Models in Human Genomics Research*; Academic Press: Cambridge, MA, USA, 2019; pp. 119–140. [CrossRef]
4. Jinek, M.; Chylinski, K.; Fonfara, I.; Hauer, M.; Doudna, J.A.; Charpentier, E. A Programmable dual-RNA-guided DNA endonuclease in adaptive bacterial immunity. *Science* **2012**, *337*, 816–821. [CrossRef] [PubMed]
5. Platt, R.J.; Chen, S.; Zhou, Y.; Yim, M.J.; Swiech, L.; Kempton, H.R.; Dahlman, J.E.; Parnas, O.; Eisenhaure, T.M.; Jovanovic, M.; et al. CRISPR-Cas9 Knockin Mice for Genome Editing and Cancer Modeling. *Cell* **2014**, *159*, 440–455. [CrossRef] [PubMed]
6. Swiech, L.; Heidenreich, M.; Banerjee, A.; Habib, N.; Li, Y.; Trombetta, J.J.; Sur, M.; Zhang, F. In vivo interrogation of gene function in the mammalian brain using CRISPR-Cas9. *Nat. Biotechnol.* **2014**, *33*, 102–106. [CrossRef] [PubMed]
7. Calderón, J.F.; Klein, A.D. Controversies on the potential therapeutic use of rapamycin for treating a lysosomal cholesterol storage disease. *Mol. Genet. Metab. Rep.* **2018**, *15*, 135–136. [CrossRef]

8. Durán, A.; Rebolledo-Jaramillo, B.; Olguin, V.; Rojas-Herrera, M.; Heras, M.L.; Calderón, J.F.; Zanlungo, S.; Priestman, D.A.; Platt, F.M.; Klein, A.D. Identification of genetic modifiers of murine hepatic β-glucocerebrosidase activity. *Biochem. Biophys. Rep.* **2021**, *28*, 101105. [CrossRef]
9. Parra, J.; Klein, A.D.; Castro, J.; Morales, M.G.; Mosqueira, M.; Valencia, I.; Cortés, V.; Rigotti, A.; Zanlungo, S. Npc1 deficiency in the C57BL/6J genetic background enhances Niemann–Pick disease type C spleen pathology. *Biochem. Biophys. Res. Commun.* **2011**, *413*, 400–406. [CrossRef]
10. Klein, A.D.; Ferreira, N.-S.; Ben-Dor, S.; Duan, J.; Hardy, J.; Cox, T.M.; Merril, A.H., Jr.; Futerman, A.H. Identification of Modifier Genes in a Mouse Model of Gaucher Disease. *Cell Rep.* **2016**, *16*, 2546–2553. [CrossRef]
11. Rodriguez-Gil, J.L.; Watkins-Chow, D.E.; Baxter, L.L.; Elliot, G.; Harper, U.L.; Wincovitch, S.M.; Wedel, J.C.; Incao, A.A.; Huebecker, M.; Boehm, F.J.; et al. Genetic background modifies phenotypic severity and longevity in a mouse model of Niemann-Pick disease type C1. *Dis. Model. Mech.* **2020**, *13*, dmm042614. [CrossRef]
12. Klein, A.D. Modeling diseases in multiple mouse strains for precision medicine studies. *Physiol. Genom.* **2017**, *49*, 177–179. [CrossRef] [PubMed]
13. Seok, J.; Warren, H.S.; Alex, G.C.; Michael, N.M.; Henry, V.B.; Xu, W.; Richards, D.R.; McDonald-Smith, G.P.; Gao, H.; Hennessy, L.; et al. Genomic Responses in Mouse Models Poorly Mimic Human Inflammatory Diseases. *Proc. Natl. Acad. Sci. USA* **2013**, *110*, 3507–3512. [CrossRef] [PubMed]
14. Bennett, B.J.; Farber, C.R.; Orozco, L.; Kang, H.M.; Ghazalpour, A.; Siemers, N.; Neubauer, M.; Neuhaus, I.; Yordanova, R.; Guan, B.; et al. A high-resolution association mapping panel for the dissection of complex traits in mice. *Genome Res.* **2010**, *20*, 281–290. [CrossRef] [PubMed]
15. Lusis, A.J.; Seldin, M.M.; Allayee, H.; Bennett, B.J.; Civelek, M.; Davis, R.C.; Eskin, E.; Farber, C.; Hui, S.; Mehrabian, M.; et al. The Hybrid Mouse Diversity Panel: A resource for systems genetics analyses of metabolic and cardiovascular traits. *J. Lipid Res.* **2016**, *57*, 925–942. [CrossRef] [PubMed]
16. Ghazalpour, A.; Rau, C.D.; Farber, C.R.; Bennett, B.J.; Orozco, L.D.; Van Nas, A.; Pan, C.; Allayee, H.; Beaven, S.W.; Civelek, M.; et al. Hybrid mouse diversity panel: A panel of inbred mouse strains suitable for analysis of complex genetic traits. *Mamm. Genome* **2012**, *23*, 680–692. [CrossRef] [PubMed]
17. Petkov, P.; Graber, J.; Churchill, G.A.; DiPetrillo, K.; King, B.; Paigen, K. Evidence of a Large-Scale Functional Organization of Mammalian Chromosomes. *PLoS Genet.* **2005**, *1*, e33. [CrossRef]
18. Flint, J.; Mott, R. Applying mouse complex-trait resources to behavioural genetics. *Nature* **2008**, *456*, 724–727. [CrossRef]
19. Kang, E.Y.; Han, B.; Furlotte, N.; Joo, J.W.J.; Shih, D.; Davis, R.C.; Lusis, A.J.; Eskin, E. Meta-Analysis Identifies Gene-by-Environment Interactions as Demonstrated in a Study of 4,965 Mice. *PLoS Genet.* **2014**, *10*, e1004022. [CrossRef]
20. Neuner, S.M.; Heuer, S.E.; Huentelman, M.J.; O'Connell, K.M.S.; Kaczorowski, C.C. Harnessing Genetic Complexity to Enhance Translatability of Alzheimer's Disease Mouse Models: A Path toward Precision Medicine. *Neuron* **2019**, *101*, 399–411. [CrossRef]
21. Srivastava, A.; Morgan, A.P.; Najarian, M.L.; Sarsani, V.K.; Sigmon, J.S.; Shorter, J.R.; Kashfeen, A.; McMullan, R.C.; Williams, L.H.; Giusti-Rodríguez, P.; et al. Genomes of the Mouse Collaborative Cross. *Genetics* **2017**, *206*, 537–556. [CrossRef]
22. Yang, H.; Wang, J.R.; Didion, J.; Buus, R.J.; Bell, T.A.; Welsh, C.E.; Bonhomme, F.; Yu, A.H.-T.; Nachman, M.W.; Piálek, J.; et al. Subspecific origin and haplotype diversity in the laboratory mouse. *Nat. Genet.* **2011**, *43*, 648–655. [CrossRef] [PubMed]
23. Aylor, D.L.; Valdar, W.; Foulds-Mathes, W.; Buus, R.J.; Verdugo, R.A.; Baric, R.S.; Ferris, M.T.; Frelinger, J.A.; Heise, M.; Frieman, M.B.; et al. Genetic analysis of complex traits in the emerging Collaborative Cross. *Genome Res.* **2011**, *21*, 1213–1222. [CrossRef] [PubMed]
24. Roberts, A.; de Villena, F.P.-M.; Wang, W.; McMillan, L.; Threadgill, D.W. The polymorphism architecture of mouse genetic resources elucidated using genome-wide resequencing data: Implications for QTL discovery and systems genetics. *Mamm. Genome* **2007**, *18*, 473–481. [CrossRef] [PubMed]
25. Saul, M.C.; Philip, V.M.; Reinholdt, L.G.; Chesler, E.J. High-Diversity Mouse Populations for Complex Traits. *Trends Genet.* **2019**, *35*, 501–514. [CrossRef] [PubMed]
26. Keele, G.; Zhang, T.; Pham, D.; Vincent, M.; Genomics, T.B.-C. *Undefined Regulation of Protein Abundance in Genetically Diverse Mouse Populations*; Elsevier: Amsterdam, The Netherlands, 2021.
27. Ram, R.; Morahan, G. Complex Trait Analyses of the Collaborative Cross: Tools and Databases. *Syst. Genet.* **2016**, *1488*, 121–129. [CrossRef]
28. Molenhuis, R.T.; Bruining, H.; Brandt, M.J.V.; Van Soldt, P.E.; Atamni, H.J.A.-T.; Burbach, J.P.H.; Iraqi, F.A.; Mott, R.F.; Kas, M.J.H. Modeling the quantitative nature of neurodevelopmental disorders using Collaborative Cross mice. *Mol. Autism* **2018**, *9*, 63. [CrossRef]
29. Noll, K.; Ferris, M.T.; Heise, M.T. The Collaborative Cross: A Systems Genetics Resource for Studying Host-Pathogen Interactions. *Cell Host Microbe* **2019**, *25*, 484–498. [CrossRef]
30. Rogala, A.R.; Morgan, A.P.; Christensen, A.M.; Gooch, T.J.; Bell, T.A.; Miller, D.R.; Godfrey, V.L.; De Villena, F.P.-M. The Collaborative Cross as a Resource for Modeling Human Disease: CC011/Unc, a New Mouse Model for Spontaneous Colitis. *Mamm. Genome* **2014**, *25*, 95–108. [CrossRef]
31. Mathes, W.F.; Aylor, D.L.; Miller, D.R.; Churchill, G.A.; Chesler, E.J.; de Villena, F.P.-M.; Threadgill, D.W.; Pomp, D. Architecture of energy balance traits in emerging lines of the Collaborative Cross. *Am. J. Physiol. Metab.* **2011**, *300*, E1124–E1134. [CrossRef]

32. Mao, J.-H.; Langley, S.A.; Huang, Y.; Hang, M.; Bouchard, K.E.; Celniker, S.E.; Brown, J.B.; Jansson, J.; Karpen, G.H.; Snijders, A.M. Identification of genetic factors that modify motor performance and body weight using Collaborative Cross mice. *Sci. Rep.* **2015**, *5*, 16247. [CrossRef]
33. Atamni, H.J.A.-T.; Ziner, Y.; Mott, R.; Wolf, L.; Iraqi, F.A. Glucose tolerance female-specific QTL mapped in collaborative cross mice. *Mamm. Genome* **2016**, *28*, 20–30. [CrossRef] [PubMed]
34. Lorè, N.I.; Sipione, B.; He, G.; Strug, L.J.; Atamni, H.J.; Dorman, A.; Mott, R.; Iraqi, F.A.; Bragonzi, A. Collaborative Cross Mice Yield Genetic Modifiers for Pseudomonas aeruginosa Infection in Human Lung Disease. *mBio* **2020**, *11*, e00097–e00117. [CrossRef]
35. Woods, L.C.S. QTL mapping in outbred populations: Successes and challenges. *Physiol. Genom.* **2014**, *46*, 81–90. [CrossRef] [PubMed]
36. Talbot, C.J.; Nicod, A.; Cherny, S.S.; Fulker, D.W.; Collins, A.C.; Flint, J. High-resolution mapping of quantitative trait loci in outbred mice. *Nat. Genet.* **1999**, *21*, 305–308. [CrossRef]
37. Woods, L.C.S.; Mott, R. Heterogeneous Stock Populations for Analysis of Complex Traits. *Syst. Genet.* **2016**, *1488*, 31–44. [CrossRef]
38. Gatti, D.M.; Svenson, K.L.; Shabalin, A.; Wu, L.-Y.; Valdar, W.; Simecek, P.; Goodwin, N.; Cheng, R.; Pomp, D.; Palmer, A.; et al. Quantitative Trait Locus Mapping Methods for Diversity Outbred Mice. *G3 Genes | Genomes | Genet.* **2014**, *4*, 1623–1633. [CrossRef] [PubMed]
39. Logan, R.W.; Robledo, R.F.; Recla, J.M.; Philip, V.M.; Bubier, J.A.; Jay, J.J.; Harwood, C.; Wilcox, T.; Gatti, D.M.; Bult, C.J.; et al. High-precision genetic mapping of behavioral traits in the diversity outbred mouse population. *Genes Brain Behav.* **2013**, *12*, 424–437. [CrossRef]
40. Valdar, W.; Solberg, L.C.; Gauguier, D.; Burnett, S.; Klenerman, P.; Cookson, W.O.; Taylor, M.; Rawlins, J.N.P.; Mott, R.; Flint, J. Genome-wide genetic association of complex traits in heterogeneous stock mice. *Nat. Genet.* **2006**, *38*, 879–887. [CrossRef]
41. Svenson, K.L.; Gatti, D.M.; Valdar, W.; Welsh, C.E.; Cheng, R.; Chesler, E.J.; Palmer, A.A.; McMillan, L.; Churchill, G.A. High-Resolution Genetic Mapping Using the Mouse Diversity Outbred Population. *Genetics* **2012**, *190*, 437–447. [CrossRef]
42. Keane, T.M.; Goodstadt, L.; Danecek, P.; White, M.A.; Wong, K.; Yalcin, B.; Heger, A.; Agam, A.; Slater, G.; Goodson, M.; et al. Mouse genomic variation and its effect on phenotypes and gene regulation. *Nature* **2011**, *477*, 289–294. [CrossRef]
43. Parker, C.C.; Palmer, A.A. Dark Matter: Are Mice the Solution to Missing Heritability? *Front. Genet.* **2011**, *2*, 32. [CrossRef] [PubMed]
44. Chesler, E.J. Out of the bottleneck: The Diversity Outcross and Collaborative Cross mouse populations in behavioral genetics research. *Mamm. Genome* **2013**, *25*, 3–11. [CrossRef] [PubMed]
45. Koyuncu, D.; Niazi, M.K.K.; Tavolara, T.; Abeijon, C.; Ginese, M.L.; Liao, Y.; Mark, C.; Specht, A.; Gower, A.C.; Restrepo, B.I.; et al. CXCL1: A new diagnostic biomarker for human tuberculosis discovered using Diversity Outbred mice. *PLoS Pathog.* **2021**, *17*, e1009773. [CrossRef] [PubMed]
46. Kazama, H. Systems neuroscience in Drosophila: Conceptual and technical advantages. *Neuroscience* **2015**, *296*, 3–14. [CrossRef] [PubMed]
47. Yamamoto, S.; Jaiswal, M.; Charng, W.-L.; Gambin, T.; Karaca, E.; Mirzaa, G.; Wiszniewski, W.; Sandoval, H.; Haelterman, N.A.; Xiong, B.; et al. A Drosophila Genetic Resource of Mutants to Study Mechanisms Underlying Human Genetic Diseases. *Cell* **2014**, *159*, 200–214. [CrossRef]
48. Reiter, L.T.; Potocki, L.; Chien, S.; Gribskov, M.; Bier, E. A Systematic Analysis of Human Disease-Associated Gene Sequences in *Drosophila melanogaster*. *Genome Res.* **2001**, *11*, 1114–1125. [CrossRef] [PubMed]
49. Myers, E.W.; Sutton, G.G.; Delcher, A.L.; Dew, I.M.; Fasulo, D.P.; Flanigan, M.J.; Kravitz, S.A.; Mobarry, C.M.; Reinert, K.H.J.; Remington, K.A.; et al. A Whole-Genome Assembly of *Drosophila*. *Science* **2000**, *287*, 2196–2204. [CrossRef]
50. Mackay, T.F.C.; Richards, S.; Stone, E.A.; Barbadilla, A.; Ayroles, J.F.; Zhu, D.; Casillas, S.; Han, Y.; Magwire, M.M.; Cridland, J.M.; et al. The Drosophila melanogaster Genetic Reference Panel. *Nature* **2012**, *482*, 173–178. [CrossRef]
51. Huang, W.; Massouras, A.; Inoue, Y.; Peiffer, J.; Ràmia, M.; Tarone, A.M.; Turlapati, L.; Zichner, T.; Zhu, D.; Lyman, R.F.; et al. Natural variation in genome architecture among 205 *Drosophila melanogaster* Genetic Reference Panel lines. *Genome Res.* **2014**, *24*, 1193–1208. [CrossRef]
52. Anholt, R.R.H.; Mackay, T.F.C. The road less traveled: From genotype to phenotype in flies and humans. *Mamm. Genome* **2017**, *29*, 5–23. [CrossRef]
53. Ober, U.; Huang, W.; Magwire, M.; Schlather, M.; Simianer, H.; Mackay, T.F.C. Correction: Accounting for Genetic Architecture Improves Sequence Based Genomic Prediction for a Drosophila Fitness Trait. *PLoS ONE* **2015**, *10*, e0132980. [CrossRef]
54. Edwards, S.M.; Sørensen, I.F.; Sarup, P.; Mackay, T.F.; Sørensen, P. Genomic Prediction for Quantitative Traits Is Improved by Mapping Variants to Gene Ontology Categories in *Drosophila melanogaster*. *Genetics* **2016**, *203*, 1871–1883. [CrossRef]
55. Garlapow, M.E.; Huang, W.; Yarboro, M.T.; Peterson, K.R.; Mackay, T.F.C. Quantitative Genetics of Food Intake in Drosophila melanogaster. *PLoS ONE* **2015**, *10*, e0138129. [CrossRef]
56. Negron, Y.L.S.; Hansen, N.F.; Harbison, S.T. The Sleep Inbred Panel, a Collection of Inbred *Drosophila melanogaster* with Extreme Long and Short Sleep Duration. *G3 Genes | Genomes | Genet.* **2018**, *8*, 2865–2873. [CrossRef] [PubMed]
57. Bevers, R.P.J.; Litovchenko, M.; Kapopoulou, A.; Braman, V.S.; Robinson, M.R.; Auwerx, J.; Hollis, B.; Deplancke, B. Mitochondrial haplotypes affect metabolic phenotypes in the Drosophila Genetic Reference Panel. *Nat. Metab.* **2019**, *1*, 1226–1242. [CrossRef]

58. Harbison, S.T.; Negron, Y.L.S.; Hansen, N.F.; Lobell, A.S. Selection for long and short sleep duration in Drosophila melanogaster reveals the complex genetic network underlying natural variation in sleep. *PLoS Genet.* **2017**, *13*, e1007098. [CrossRef] [PubMed]
59. Unckless, R.L.; Rottschaefer, S.M.; Lazzaro, B.P. A Genome-Wide Association Study for Nutritional Indices in *Drosophila*. *G3 Genes | Genomes | Genet.* **2015**, *5*, 417–425. [CrossRef]
60. Lafuente, E.; Duneau, D.; Beldade, P. Genetic basis of thermal plasticity variation in Drosophila melanogaster body size. *PLoS Genet.* **2018**, *14*, e1007686. [CrossRef] [PubMed]
61. Harbison, S.T.; Kumar, S.; Huang, W.; McCoy, L.J.; Smith, K.R.; Mackay, T.F.C. Genome-Wide Association Study of Circadian Behavior in Drosophila melanogaster. *Behav. Genet.* **2018**, *49*, 60–82. [CrossRef]
62. Chow, C.Y.; Kelsey, K.J.; Wolfner, M.F.; Clark, A.G. Candidate genetic modifiers of retinitis pigmentosa identified by exploiting natural variation in *Drosophila*. *Hum. Mol. Genet.* **2015**, *25*, 651–659. [CrossRef]
63. Lavoy, S.; Chittoor-Vinod, V.G.; Chow, C.Y.; Martin, I. Genetic Modifiers of Neurodegeneration in a *Drosophila* Model of Parkinson's Disease. *Genetics* **2018**, *209*, 1345–1356. [CrossRef]
64. Klein, A.D.; Mazzulli, J.R. Is Parkinson's disease a lysosomal disorder? *Brain* **2018**, *141*, 2255–2262. [CrossRef]
65. Marder, K.; Wang, Y.; Alcalay, R.N.; Mejia-Santana, H.; Tang, M.-X.; Lee, A.; Raymond, D.; Mirelman, A.; Saunders-Pullman, R.; Clark, L.; et al. Age-specific penetrance of *LRRK2* G2019S in the Michael J. Fox Ashkenazi Jewish LRRK2 Consortium. *Neurology* **2015**, *85*, 89–95. [CrossRef] [PubMed]
66. Olivares, G.H.; Olguín, P.; Klein, A.D. Modeling Parkinson's Disease Heterogeneity to Accelerate Precision Medicine. *Trends Mol. Med.* **2019**, *25*, 1052–1055. [CrossRef] [PubMed]
67. Mackay, T.F.; Huang, W. Charting the genotype–phenotype map: Lessons from the *Drosophila melanogaster* Genetic Reference Panel. *Wiley Interdiscip. Rev. Dev. Biol.* **2017**, *7*, e289. [CrossRef] [PubMed]
68. Swarup, S.; Huang, W.; Mackay, T.F.C.; Anholt, R.R.H. Analysis of natural variation reveals neurogenetic networks for *Drosophila* olfactory behavior. *Proc. Natl. Acad. Sci. USA* **2012**, *110*, 1017–1022. [CrossRef] [PubMed]
69. Shorter, J.; Couch, C.; Huang, W.; Carbone, M.A.; Peiffer, J.; Anholt, R.R.H.; Mackay, T.F.C. Genetic architecture of natural variation in *Drosophila melanogaster* aggressive behavior. *Proc. Natl. Acad. Sci. USA* **2015**, *112*, E3555–E3563. [CrossRef] [PubMed]
70. Long, A.D.; Macdonald, S.J.; King, E.G. Dissecting complex traits using the Drosophila Synthetic Population Resource. *Trends Genet.* **2014**, *30*, 488–495. [CrossRef]
71. Duina, A.A.; Miller, M.E.; Keeney, J.B. Budding Yeast for Budding Geneticists: A Primer on the *Saccharomyces cerevisiae* Model System. *Genetics* **2014**, *197*, 33–48. [CrossRef]
72. Walberg, M.W. Applicability of Yeast Genetics to Neurologic Disease. *Arch. Neurol.* **2000**, *57*, 1129–1134. [CrossRef]
73. Mancera, E.; Bourgon, R.; Brozzi, A.; Huber, W.; Steinmetz, L.M. High-resolution mapping of meiotic crossovers and non-crossovers in yeast. *Nature* **2008**, *454*, 479–485. [CrossRef] [PubMed]
74. Sanchez, A.; Borde, V. Methods to Map Meiotic Recombination Proteins in *Saccharomyces cerevisiae*. In *Homologous Recombination*; Humana: New York, NY, USA, 2020; pp. 295–306. [CrossRef]
75. Botstein, D.; Fink, G.R. Yeast: An Experimental Organism for Modern Biology. *Science* **1988**, *240*, 1439–1443. [CrossRef] [PubMed]
76. Giaever, G.; Nislow, C. The Yeast Deletion Collection: A Decade of Functional Genomics. *Genetics* **2014**, *197*, 451–465. [CrossRef] [PubMed]
77. Galardini, M.; Busby, B.P.; Vieitez, C.; Dunham, A.S.; Typas, A.; Beltrao, P. The impact of the genetic background on gene deletion phenotypes in *Saccharomyces cerevisiae*. *Mol. Syst. Biol.* **2019**, *15*, e8831. [CrossRef] [PubMed]
78. Parts, L.; Batté, A.; Lopes, M.; Yuen, M.W.; Laver, M.; Luis, B.S.; Yue, J.; Pons, C.; Eray, E.; Aloy, P.; et al. Natural variants suppress mutations in hundreds of essential genes. *Mol. Syst. Biol.* **2021**, *17*, e10138. [CrossRef] [PubMed]
79. Khurana, V.; Lindquist, S. Modelling neurodegeneration in Saccharomyces cerevisiae: Why cook with baker's yeast? *Nat. Rev. Neurosci.* **2010**, *11*, 436–449. [CrossRef]
80. Ehrenreich, I.M.; Magwene, P.M. Genetic Dissection of Heritable Traits in Yeast Using Bulk Segregant Analysis. *Cold Spring Harb. Protoc.* **2017**, *2017*, pdb.prot088989. [CrossRef] [PubMed]
81. Bloom, J.S.; Boocock, J.; Treusch, S.; Sadhu, M.J.; Day, L.; Oates-Barker, H.; Kruglyak, L. Rare variants contribute disproportionately to quantitative trait variation in yeast. *eLife* **2019**, *8*, e49212. [CrossRef]
82. Lander, E.S.; Botstein, D. Mapping mendelian factors underlying quantitative traits using RFLP linkage maps. *Genetics* **1989**, *121*, 185–199. [CrossRef] [PubMed]
83. Michelmore, R.W.; Paran, I.; Kesseli, R.V. Identification of markers linked to disease-resistance genes by bulked segregant analysis: A rapid method to detect markers in specific genomic regions by using segregating populations. *Proc. Natl. Acad. Sci. USA* **1991**, *88*, 9828–9832. [CrossRef]
84. Liti, G.; Carter, D.M.; Moses, A.M.; Warringer, J.; Parts, L.; James, S.A.; Davey, R.P.; Roberts, I.N.; Burt, A.; Koufopanou, V.; et al. Population genomics of domestic and wild yeasts. *Nature* **2009**, *458*, 337–341. [CrossRef]
85. Swinnen, S.; Thevelein, J.M.; Nevoigt, E. Genetic mapping of quantitative phenotypic traits in Saccharomyces cerevisiae. *FEMS Yeast Res.* **2012**, *12*, 215–227. [CrossRef] [PubMed]
86. Kessi-Pérez, E.I.; Molinet, J.; Martínez, C. Disentangling the genetic bases of Saccharomyces cerevisiae nitrogen consumption and adaptation to low nitrogen environments in wine fermentation. *Biol. Res.* **2020**, *53*, 2. [CrossRef] [PubMed]
87. Haas, R.; Horev, G.; Lipkin, E.; Kesten, I.; Portnoy, M.; Buhnik-Rosenblau, K.; Soller, M.; Kashi, Y. Mapping Ethanol Tolerance in Budding Yeast Reveals High Genetic Variation in a Wild Isolate. *Front. Genet.* **2019**, *10*, 998. [CrossRef] [PubMed]

88. Wang, Z.; Qi, Q.; Lin, Y.; Guo, Y.; Liu, Y.; Wang, Q. QTL Analysis Reveals Genomic Variants Linked to High-Temperature Fermentation Performance in the Industrial Yeast. *Biotechnol. Biofuels* **2019**, *12*, 59. [CrossRef]
89. Liti, G.; Louis, E.J. Yeast Evolution and Comparative Genomics. *Annu. Rev. Microbiol.* **2005**, *59*, 135–153. [CrossRef]
90. Warringer, J.; Zörgö, E.; Cubillos, F.A.; Zia, A.; Gjuvsland, A.; Simpson, J.T.; Forsmark, A.; Durbin, R.; Omholt, S.W.; Louis, E.J.; et al. Trait Variation in Yeast Is Defined by Population History. *PLoS Genet.* **2011**, *7*, e1002111. [CrossRef]
91. Perlstein, E.; Ruderfer, D.; Roberts, D.C.; Schreiber, S.L.; Kruglyak, L. Genetic basis of individual differences in the response to small-molecule drugs in yeast. *Nat. Genet.* **2007**, *39*, 496–502. [CrossRef]
92. Cubillos, F.A.; Louis, E.J.; Liti, G. Generation of a large set of genetically tractable haploid and diploid *Saccharomyces strains*. *FEMS Yeast Res.* **2009**, *9*, 1217–1225. [CrossRef]
93. Linder, R.A.; Majumder, A.; Chakraborty, M.; Long, A. Two Synthetic 18-Way Outcrossed Populations of Diploid Budding Yeast with Utility for Complex Trait Dissection. *Genetics* **2020**, *215*, 323–342. [CrossRef]
94. Cubillos, F.; Parts, L.; Salinas, F.; Bergström, A.; Scovacricchi, E.; Zia, A.; Illingworth, C.J.R.; Mustonen, V.; Ibstedt, S.; Warringer, J.; et al. High-Resolution Mapping of Complex Traits with a Four-Parent Advanced Intercross Yeast Population. *Genetics* **2013**, *195*, 1141–1155. [CrossRef] [PubMed]
95. Diouf, I.; Pascual, L. Multiparental Population in Crops: Methods of Development and Dissection of Genetic Traits. In *Crop Breeding*; Tripodi, P., Ed.; Humana: New York, NY, USA, 2020; Volume 2264, pp. 13–32. [CrossRef]
96. Peter, J.; Schacherer, J. Population genomics of yeasts: Towards a comprehensive view across a broad evolutionary scale. *Yeast* **2015**, *33*, 73–81. [CrossRef] [PubMed]
97. Bendixsen, D.P.; Frazão, J.G.; Stelkens, R. *Saccharomyces* yeast hybrids on the rise. *Yeast* **2021**, *39*, 40–54. [CrossRef] [PubMed]
98. Schacherer, J.; Shapiro, J.A.; Ruderfer, D.M.; Kruglyak, L. Comprehensive polymorphism survey elucidates population structure of Saccharomyces cerevisiae. *Nature* **2009**, *458*, 342–345. [CrossRef]
99. Peter, J.; De Chiara, M.; Friedrich, A.; Yue, J.-X.; Pflieger, D.; Bergström, A.; Sigwalt, A.; Barre, B.; Freel, K.; Llored, A.; et al. Genome evolution across 1,011 Saccharomyces cerevisiae isolates. *Nature* **2018**, *556*, 339–344. [CrossRef]
100. Khurana, V.; Peng, J.; Chung, C.Y.; Auluck, P.K.; Fanning, S.; Tardiff, D.F.; Bartels, T.; Koeva, M.; Eichhorn, S.W.; Benyamini, H.; et al. Genome-Scale Networks Link Neurodegenerative Disease Genes to alpha-Synuclein through Specific Molecular Pathways. *Cell Syst.* **2017**, *4*, 157–170. [CrossRef]
101. Jung, P.P.; Zhang, Z.; Paczia, N.; Jaeger, C.; Ignac, T.; May, P.; Linster, C.L. Natural variation of chronological aging in the Saccharomyces cerevisiae species reveals diet-dependent mechanisms of life span control. *npj Aging Mech. Dis.* **2018**, *4*, 3. [CrossRef]
102. Breschi, A.; Gingeras, T.R.; Guigó, A.B.R. Comparative transcriptomics in human and mouse. *Nat. Rev. Genet.* **2017**, *18*, 425–440. [CrossRef]
103. Adams, M.D.; Celniker, S.E.; Holt, R.A.; Evans, C.A.; Gocayne, J.D.; Amanatides, P.G.; Scherer, S.E.; Li, P.W.; Hoskins, R.A.; Galle, R.F.; et al. The Genome Sequence of *Drosophila melanogaster*. *Science* **2000**, *287*, 2185–2195. [CrossRef]
104. Belda, I.; Ruiz, J.; Santos, A.; Van Wyk, N.; Pretorius, I.S. Saccharomyces cerevisiae. *Trends Genet.* **2019**, *35*, 956–957. [CrossRef]
105. Zhu, F.; Nair, R.R.; Fisher, E.M.C.; Cunningham, T.J. Humanising the mouse genome piece by piece. *Nat. Commun.* **2019**, *10*, 1845. [CrossRef] [PubMed]
106. Ugur, B.; Chen, K.; Bellen, H.J. Drosophila tools and assays for the study of human diseases. *Dis. Models Mech.* **2016**, *9*, 235–244. [CrossRef] [PubMed]
107. Smith, M.G.; Snyder, M. Yeast as a Model for Human Disease. *Curr. Protoc. Hum. Genet.* **2006**, *48*, 15–21. [CrossRef] [PubMed]